Study on flux propagation and complex impedance in NiZn and MnZn ferrites

Marcin Kącki, dr. Marek S. Ryłko
Marcin.Kacki@sma-magnetics.com, Marek.Rylko@sma-magnetics.com
SMA Magnetics Sp. z o.o.

Edward Herbert
psma-ed@fmtt.com
http://fmtt.com/

Sponsored by
The Power Sources Manufacturers Association
e-mail: power@psma.com
http://www.psma.com/
P.O. Box 418
Mendham, NJ 07945-0418

1. Contents

2. Table of figures

3. Abstract

This report presents result of the research work on the magnetic flux distribution in the ferrite core for various materials. Obtained data compares and contrasts various effects such as dimensional resonance, eddy current and core geometry. Obtained results reveals the need to introduce the standardized test for magnetic materials required by a detail design analysis. Magnetic materials permeability, resistivity and permittivity characteristics are missing in the data published by ferrite manufacturers.

4. Acknowledgements

We would like to express our deep gratitude to Professor Charles R. Sullivan and Professor John G. Hayes for their valuable, constructive suggestions and research supervision during the planning and developing this research work.

We would like to offer special thanks to the R&D team of the Ferroxcube Polska Eastern Europe for their support, open discussion and providing samples for research.

Finally, we wish to thank Fair-Rite Products Corporation for frame core machining and precise drilling.

Furthermore, we would like to acknowledge SMA Magnetics R&D staff for the support.

5. Introduction

The magnetic core size and magnetic field amplitude and frequency has a strong impact on the magnetic flux distribution in the core. In general, the flux distribution in the core is a function of the core size for given frequency. In most cases the main contributor to the non-uniform flux distribution are eddy currents. Although eddy currents are known for decades in iron based cores that are mitigated by laminations, the ferrite materials exhibit eddy current of capacitive character that is considered by Glenn's Skutt while not experimentally validated [1]-[5].

The ferrites are of primary interests of the presented research due to advancements in wide bandgap semiconductors that sets the power electronic frontier beyond frequencies achievable up until date. This challenges design procedures since the high frequency switched converters may develop non-uniform flux density in the core that will reduce overall system performance. This requires design procedures to be redefined that will include much wider range of the materials' parameters to be considered.

As an example, the toroidal core with external diameter of approx. 25 mm is large enough to exhibit non-uniform flux distribution due to skin effects at frequencies up to 30 MHz, albeit eddy current effect is usually considered insignificant in the ferrite core. In a ferrite core at high frequency, the magnetic field produced by eddy current and displacement current displaces the magnetic flux from the inner portion of the core cross-section. This results in a flux skin effect analogous to the electric current skin effect in the winding [3]. Figure 1 shows magnetic flux density change in the core. For analysis at 10 kHz the magnetic field intensity is stronger at the

inner side of the core while reduced at the outer surface that is the effect of the reluctance path distribution with the radius. While eddy current is developed in an analysis at 1 MHz that looks similar to classical current distribution in a conductor where flux is concentrated in the outer circumference of the core while the core centre exhibits flux density weakening. Non-uniform flux distribution can lead to local magnetic saturation that will reduce core equivalent permeability and may increase core losses.

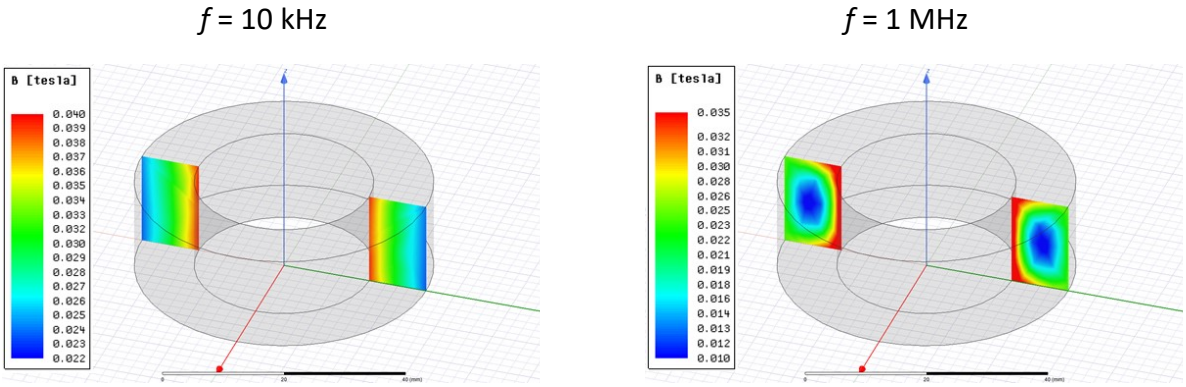

Figure 1. FEA modeling of field distribution in the core.

6. Tested cores

In order to examine the flux distribution in the core two ferrite material groups are investigated first is based on MnZn with 7 selected materials while other is based on NiZn with 4 selected materials.

In order to isolate core shape effect three core shapes are tested that two are based on 50 mm and 105 mm ring cores. Third test is based on the frame core and it is designed to separate the reluctance effect from the skin effect as ring core reluctance increases with the radius.

Detailed test plan is shown in Table 1 while description of the experiments are presented in the next section.

Table 1. Measurements TEST PLAN.

Material	Core shape	Experiment I (flux density test)	Experiment II (impedance test)
3E10	TX50	✓	✓
3E15	TX50	✓	✓
3E6	TX50	✓	✓
3E27	TX50	✓	✓
3C11	TX50	✓	✓

4S60	TX50	✓	✓
4A11	TX50	✓	✓
FR78	TX105 & Frame core	✓	✓
FR79	TX105 & Frame core	✓	✓
FR61	TX105 & Frame core	✓	✓
FR67	TX105 & Frame core	✓	✓

Tested cores has two vertical and one horizontal bores. Bore diameter is 0.75 mm. In toroidal cores reluctance increases with core radius, therefore the frame core is to provide homogenous flux distribution. Frame core separate the reluctance effect from the skin effect. Tested cores have similar cross-section areas. Detailed dimensions and materials are provided in Figure 2 and Table 2, Figure 3 and Table 3, Figure 4 and Table 4 for TX50, TX105 and frame core, respectively [7]-[8].

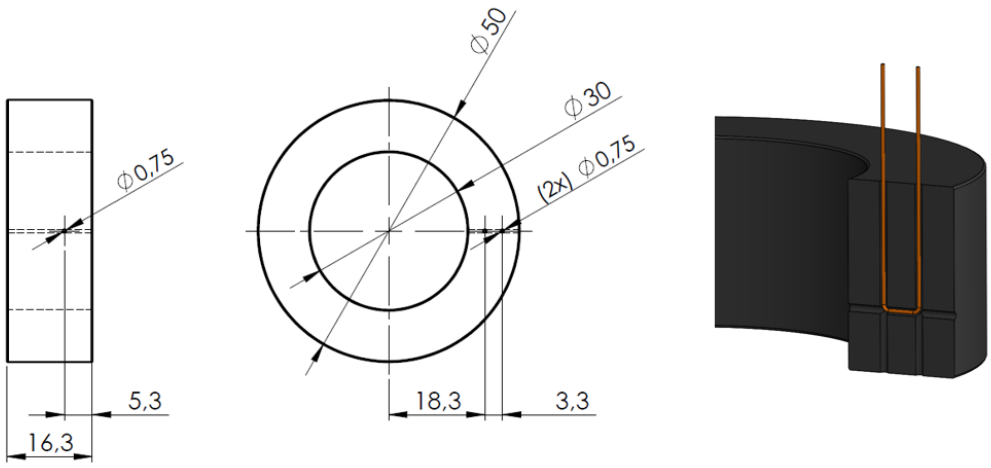

Figure 2. TX50 ring core dimensions.

Table 2. Tx50 Cores Material Properties – Manufacturer Specification.

Material	Type	Permeability	Resistivity (Ωm)
3E15	MnZn	15 000	0.5
3E10	MnZn	10 000	0.5
3E6	MnZn	10 000	0.1
3E27	MnZn	6000	0.5
3C11	MnZn	4300	1
4S60	NiZn	2000	10^5
4A11	NiZn	850	10^5

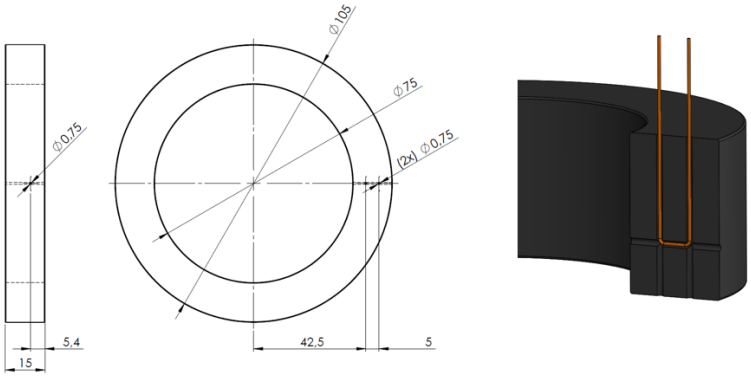

Figure 3. TX105 ring core dimension.

Table 3. Tx105 Cores Material Properties – Manufacturer Specification.

Material	Type	Permeability	Resistivity (Ωm)
FR78	MnZn	2 300	200
FR79	MnZn	1 400	200
FR61	NiZn	120	10^9
FR67	NiZn	40	10^7

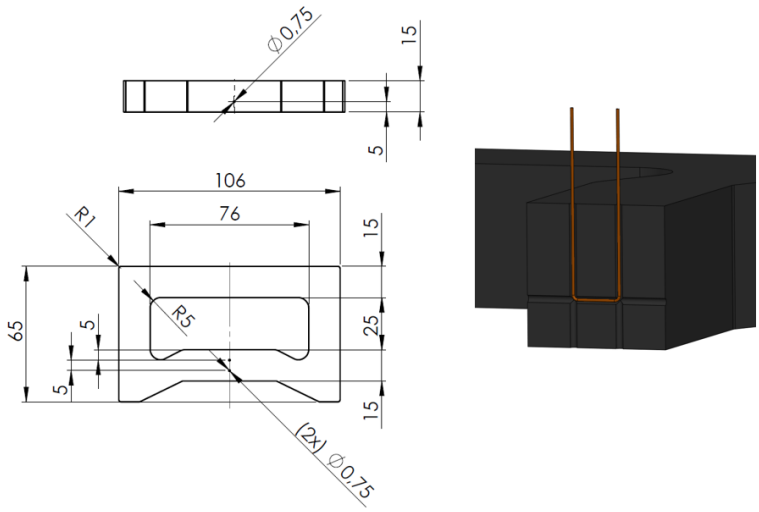

Figure 4. Frame core dimensions.

Table 4. FRAME CORES MATERIAL PROPERTIES – MANUFACTURER SPECIFICATION.

Material	Type	Permeability	Resistivity [Ωm]
FR78	MnZn	2 300	200
FR79	MnZn	1 400	200
FR61	NiZn	120	10^9
FR67	NiZn	40	10^7

7. Experimental setup

7.1. Experiment I – flux density test

This experiment is aimed to determine the voltage of each inner ferrite segment. The measurement setup and sense winding arrangement are presented in Figure 5. An Agilent 33220A arbitrary waveform generator controls amplifier AG 1017 L which supply single turn excitation winding. Oscilloscope DPD 3034 allows acquiring data for a single excitation point. This test setup allows to test cores with frequencies up to 1.5 MHz. The vertical and horizontal bores divides core into nine areas. Since the anticipated flux distribution is symmetrical where symmetry axes crosses in the middle of the core cross-section, the sectioned areas are combined as the middle Section A that comprises section X and outer Section B that comprises sections 1-5. The core cross-section is shown in Figure 6.

The flux is a function of the sinusoidal voltage and frequency as follows for N=1:

$$\Phi = A_C \cdot B = A_C \frac{V_{RMS}\sqrt{2}}{2\pi f A_C N} = \frac{V_{RMS}}{\sqrt{2}\,\pi f}$$

where:

Φ – magnetic flux in Wb
V_{RMS} – measured voltage in V
f – frequency in Hz
N – turns number
A_C - core cross section in m^2

The flux density ratio frequency characteristics are normalised by main flux density for each frequency.

$$\text{Magnetic flux density ratio}(f) = \frac{B_A(f)}{B_E(f)}$$

where:

$B_A(f)$ – flux density in section A
$B_E(f)$ – flux density in the entire area of the core

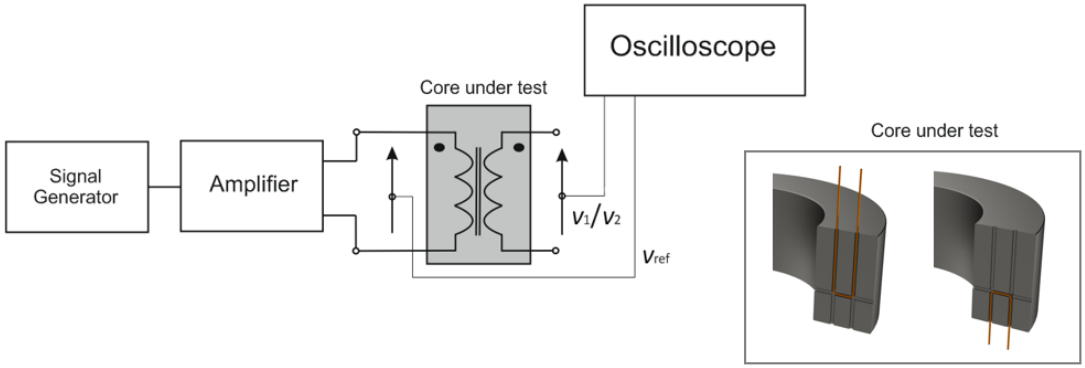

Figure 5. Experiment I – measurement system.

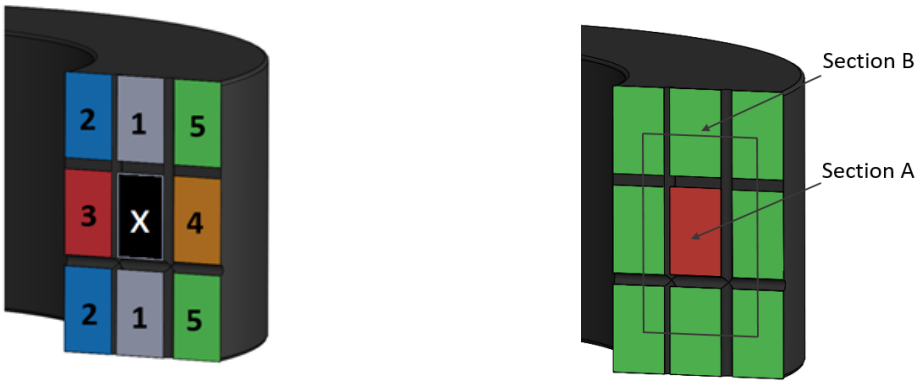

Figure 6. Tested core cross section.

7.2. Experiment II – impedance test

This experiment is to determine impedance and phase shift measured on each inner ferrite segment. The measurement setup and winding arrangement are presented in Figure 7. The impedance characteristics were measured with a Wayne Kerr 6550B analyzer. Test setup with an impedance analyzer allows for tests up to 10 MHz.

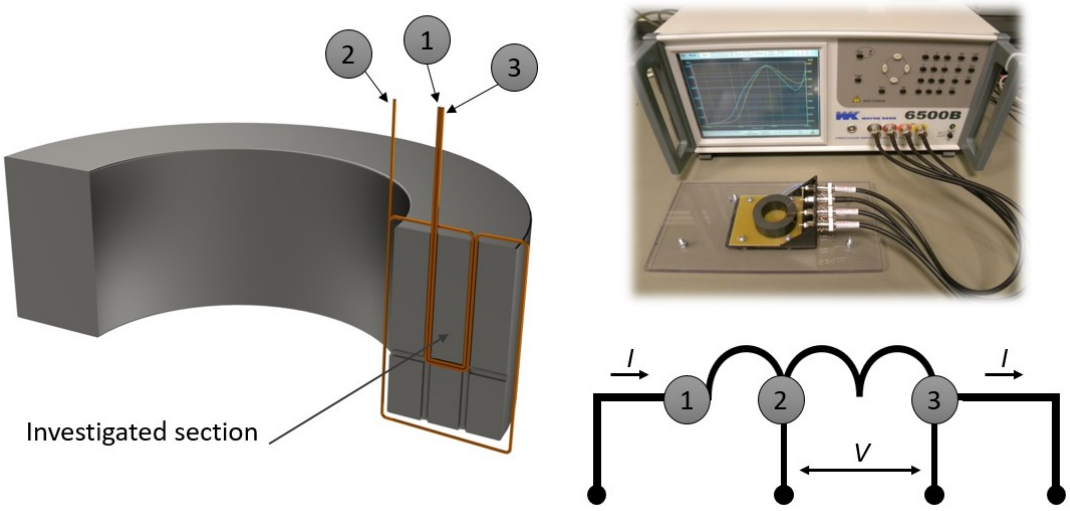

Figure 7. Experiment II – impedance measurement setup.

Measured impedance for Section A and Section B is compared by use of scaling by the area ratio:

$$Z_{NA} = Z_A * \frac{S_E}{S_A};\ Z_{NB} = Z_B * \frac{S_E}{S_B}$$

where:

Z_{NA} – Scaled impedance for Section A
Z_{NB} – Scaled impedance for Section B
Z_A – Impedance for Section A in Ω
Z_B – Impedance for Section B in Ω
S_A – Section A cross section in mm^2
S_B – Section B cross section in mm^2
S_E – Entire core cross section after drilling in mm^2

8. Experimental investigation

8.1. Experiment I – flux density test

8.1.1. TX50 core with 3E10 material

Flux distribution in the each segment of TX50 core made from 3E10 material are shown in Figure 8. Magnetic flux density for Section A and B are shown in Figure 9. As can be seen, flux in the inner core part start decreasing above 300 kHz. Corresponding voltage waveforms for Excitation, Segment A and Segment B at each frequency are presented in Table 5.

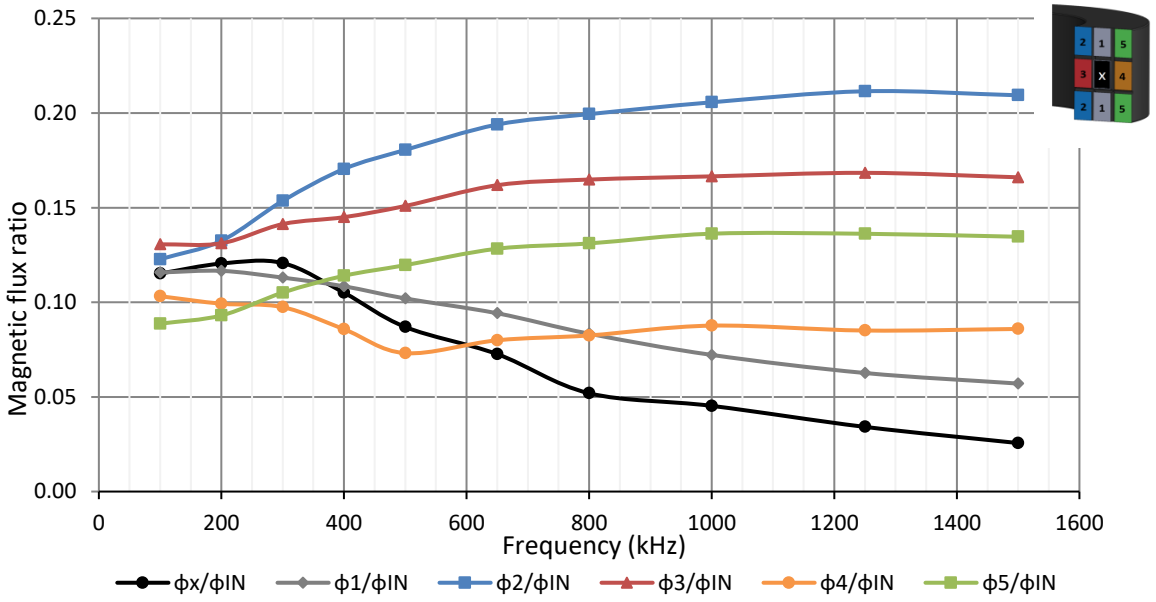

Figure 8. Magnetic flux distribution in the each area of 3E10 TX50 ring core.

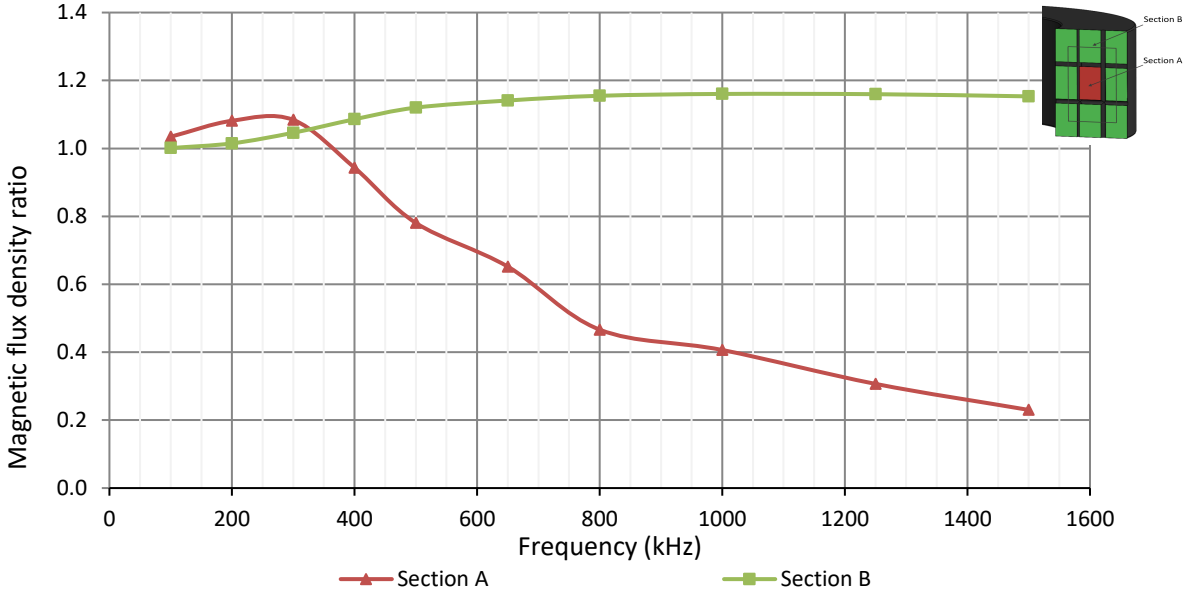

Figure 9. Magnetic flux distribution in the each section of 3E10 TX50 ring core.

Table 5. MEASURED VOLTAGES FOR TX50 3E10 RING CORE.

f = 100 kHz Blue – Excitation voltage, Red – Section A, Green – Section B 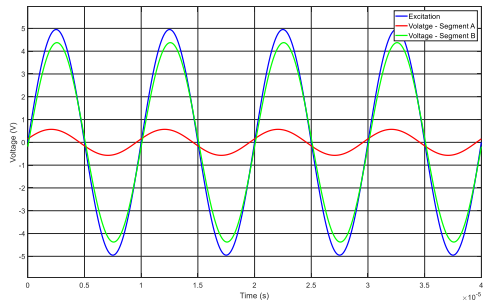	f = 200 kHz Blue – Excitation voltage, Red – Section A, Green – Section B 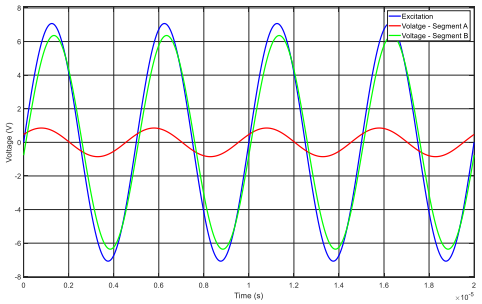
f = 300 kHz Blue – Excitation voltage, Red – Section A, Green – Section B 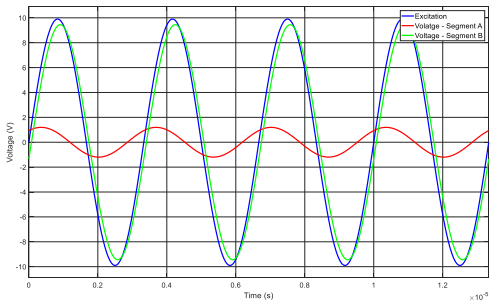	f = 400 kHz Blue – Excitation voltage, Red – Section A, Green – Section B 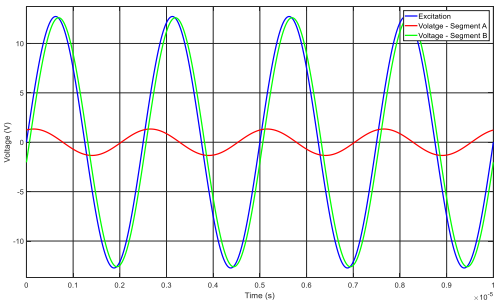
f = 500 kHz Blue – Excitation voltage, Red – Section A, Green – Section B 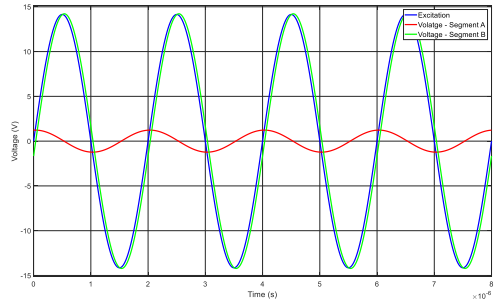	f = 650 kHz Blue – Excitation voltage, Red – Section A, Green – Section B 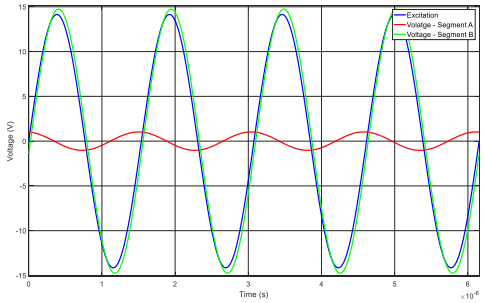

f = 800 kHz

Blue – Excitation voltage, Red – Section A, Green – Section B

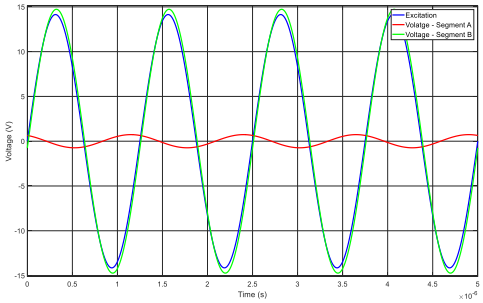

f = 1000 kHz

Blue – Excitation voltage, Red – Section A, Green – Section B

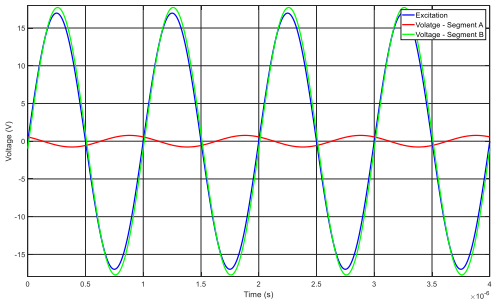

f = 1250 kHz

Blue – Excitation voltage, Red – Section A, Green – Section B

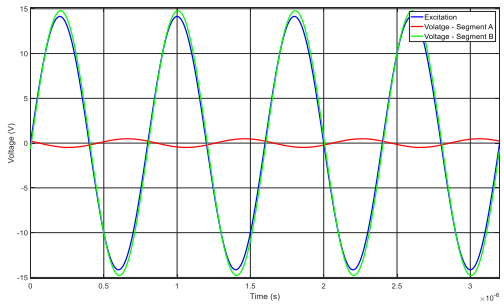

f = 1500 kHz

Blue – Excitation voltage, Red – Section A, Green – Section B

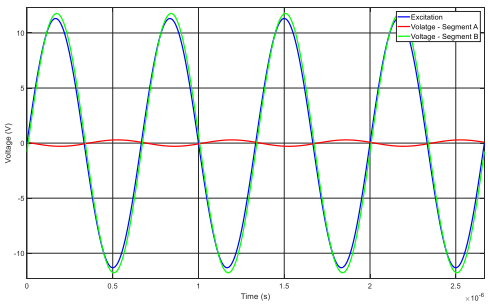

8.1.2. TX50 core with 3E15 material

Flux distributions in the each segment of TX50 core made from 3E15 material are shown in Figure 10, while magnetic flux density for Section A and B is shown in Figure 11. Corresponding voltage waveforms for Excitation, Segment A and Segment B at each frequency are presented in Table 6.

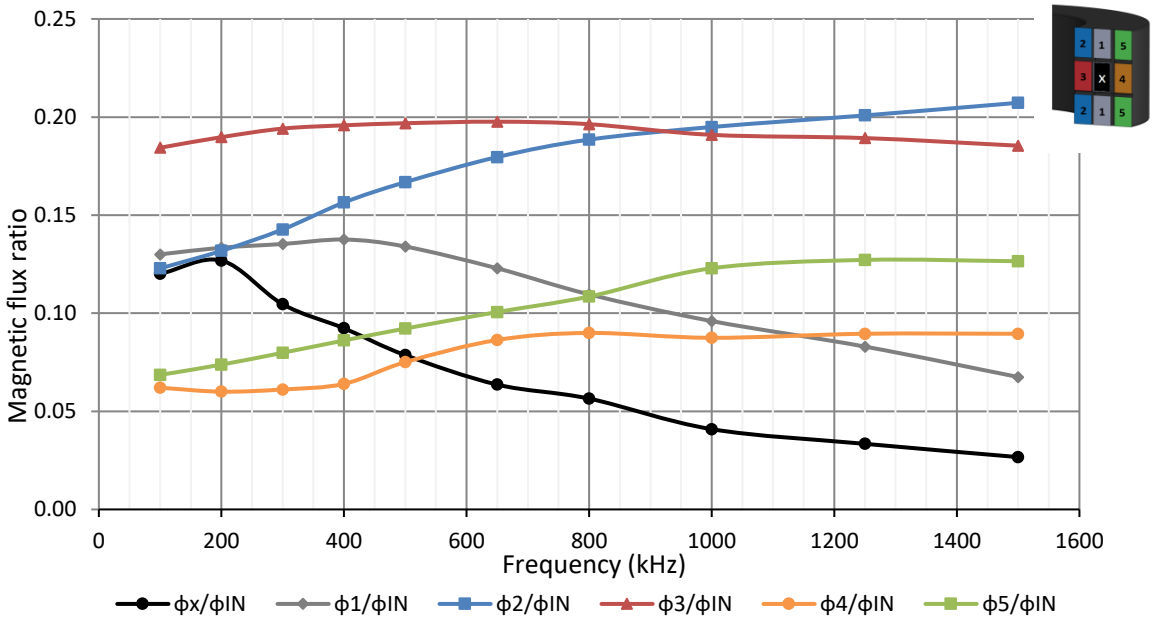

Figure 10. Magnetic flux distribution in the each area of 3E15 TX50 ring core.

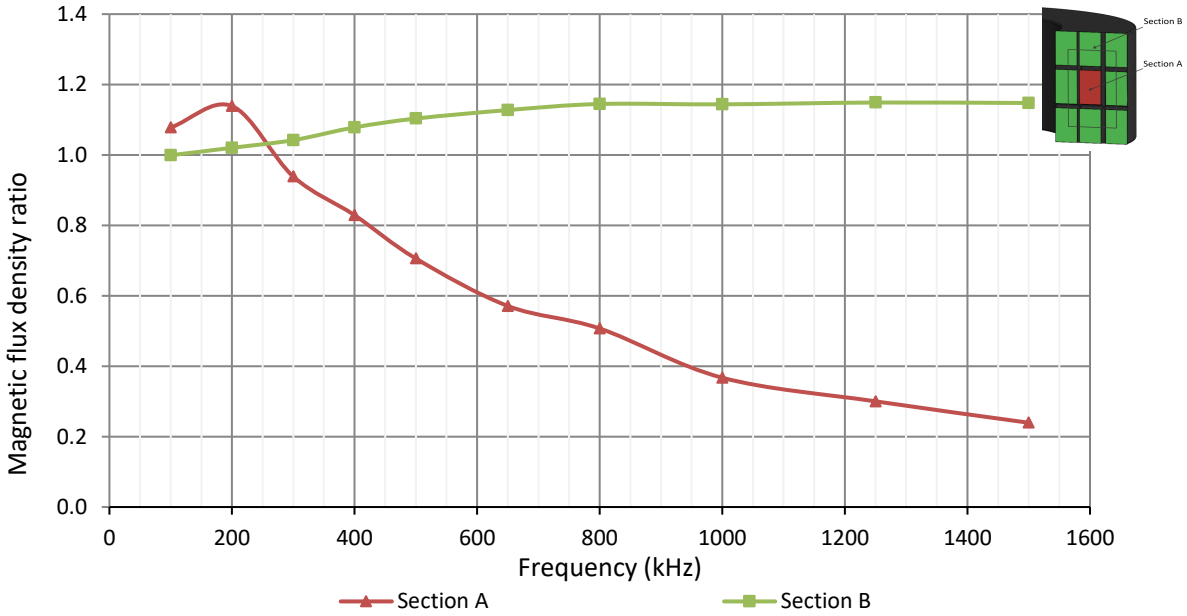

Figure 11. Magnetic flux distribution in the each section of 3E15 TX50 ring core.

Table 6. MEASURED VOLTAGES FOR TX50 3E15 RING CORE.

f = 100 kHz Blue – Excitation voltage, Red – Section A, Green – Section B 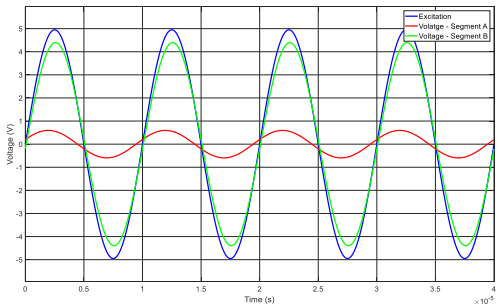	f = 200 kHz Blue – Excitation voltage, Red – Section A, Green – Section B 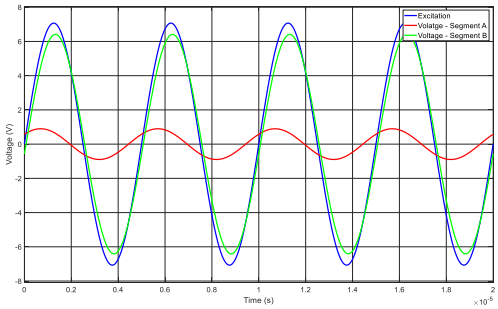
f = 300 kHz Blue – Excitation voltage, Red – Section A, Green – Section B 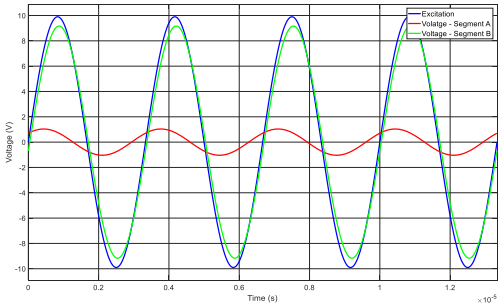	f = 400 kHz Blue – Excitation voltage, Red – Section A, Green – Section B 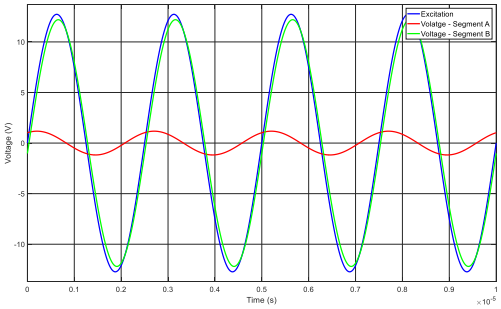
f = 500 kHz Blue – Excitation voltage, Red – Section A, Green – Section B 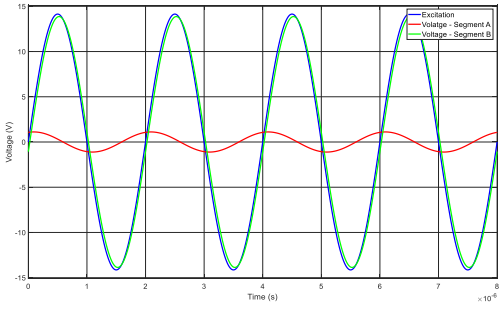	f = 650 kHz Blue – Excitation voltage, Red – Section A, Green – Section B 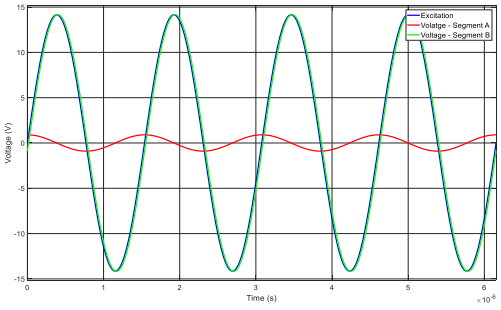

f = 800 kHz

Blue – Excitation voltage, Red – Section A, Green – Section B

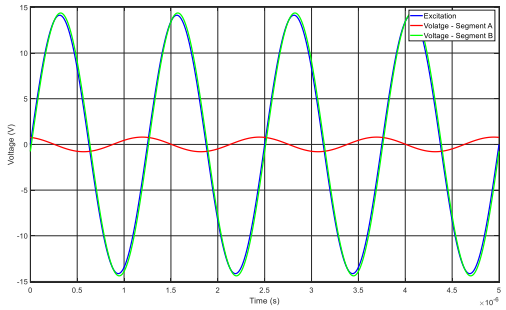

f = 1000 kHz

Blue – Excitation voltage, Red – Section A, Green – Section B

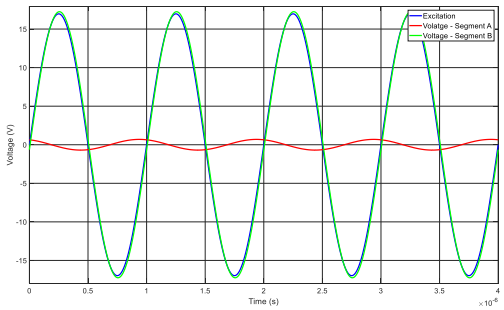

f = 1250 kHz

Blue – Excitation voltage, Red – Section A, Green – Section B

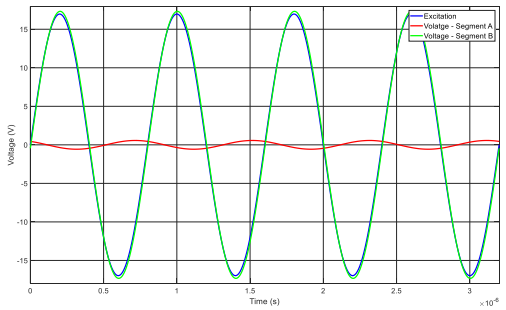

f = 1500 kHz

Blue – Excitation voltage, Red – Section A, Green – Section B

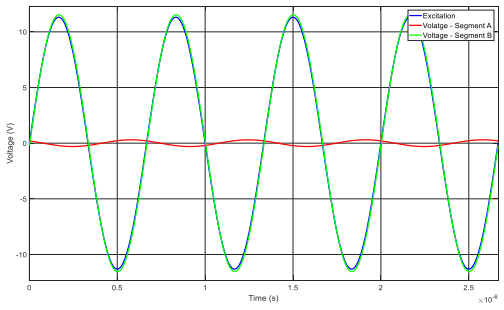

8.1.3. TX50 core with 3E6 material

Flux distributions in the each segment of TX50 core made from 3E6 material are shown in Figure 12, while magnetic flux density for Section A and B is shown in Figure 13. Corresponding voltage waveforms for Excitation, Segment A and Segment B at each frequency are presented in Table 7.

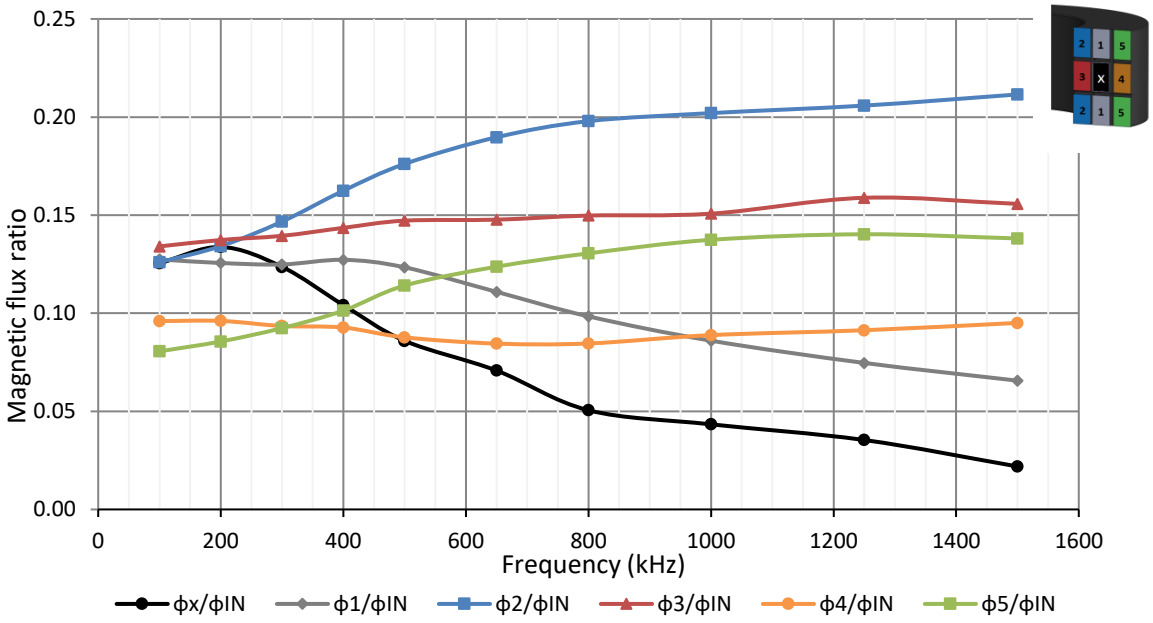

Figure 12. Magnetic flux distribution in the each area of 3E6 TX50 ring core.

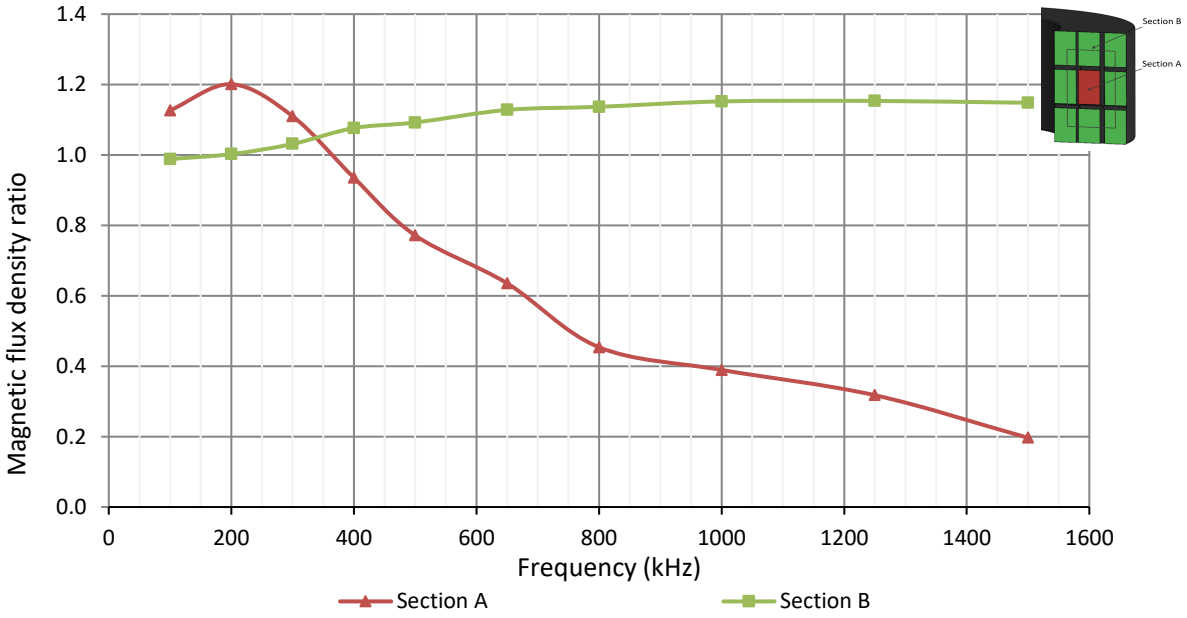

Figure 13. Magnetic flux distribution in the each section of 3E6 TX50 ring core.

Table 7. MEASURED VOLTAGES FOR TX50 3E6 RING CORE.

f = 100 kHz Blue – Excitation voltage, Red – Section A, Green – Section B 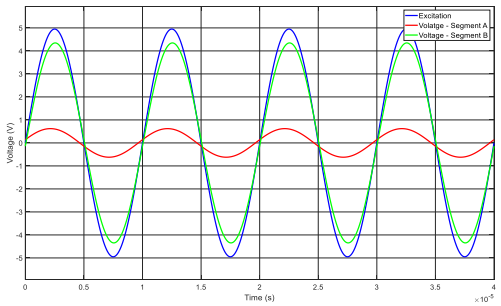	f = 200 kHz Blue – Excitation voltage, Red – Section A, Green – Section B 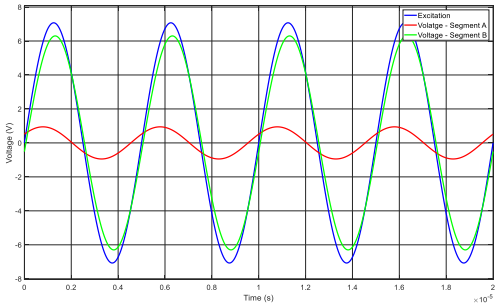
f = 300 kHz Blue – Excitation voltage, Red – Section A, Green – Section B 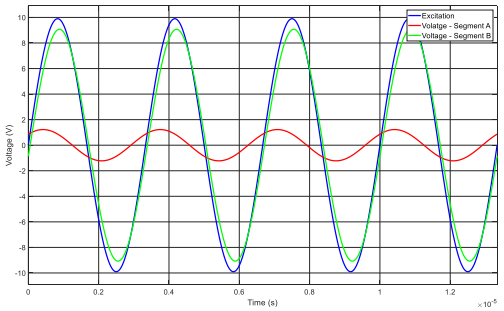	f = 400 kHz Blue – Excitation voltage, Red – Section A, Green – Section B 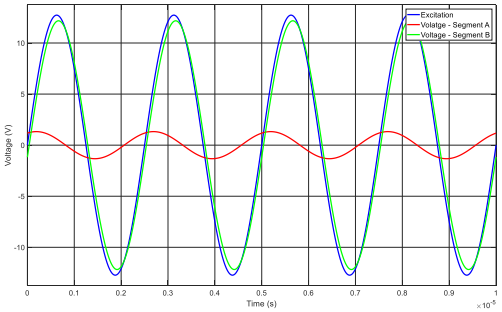
f = 500 kHz Blue – Excitation voltage, Red – Section A, Green – Section B 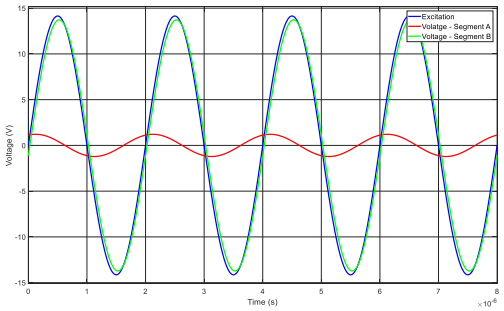	f = 650 kHz Blue – Excitation voltage, Red – Section A, Green – Section B 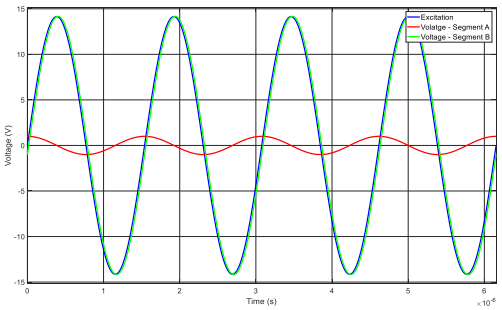

f = 800 kHz

Blue – Excitation voltage, Red – Section A, Green – Section B

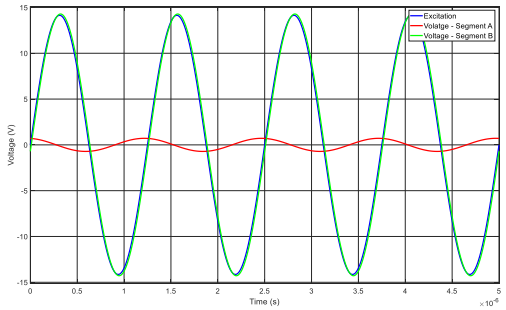

f = 1000 kHz

Blue – Excitation voltage, Red – Section A, Green – Section B

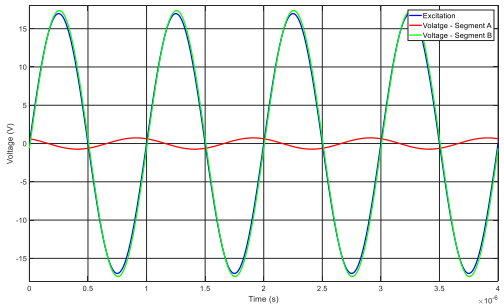

f = 1250 kHz

Blue – Excitation voltage, Red – Section A, Green – Section B

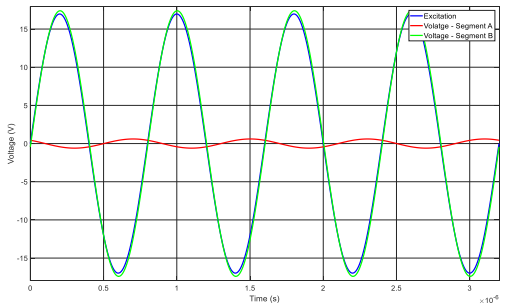

f = 1500 kHz

Blue – Excitation voltage, Red – Section A, Green – Section B

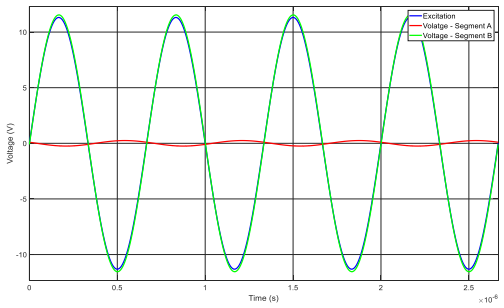

8.1.4. TX50 core with 3E27 material

Flux distributions in the each segment of TX50 core made from 3E27 material are shown in Figure 14, while magnetic flux density for Section A and B is shown in Figure 15 Corresponding voltage waveforms for Excitation, Segment A and Segment B at each frequency are presented in Table 8.

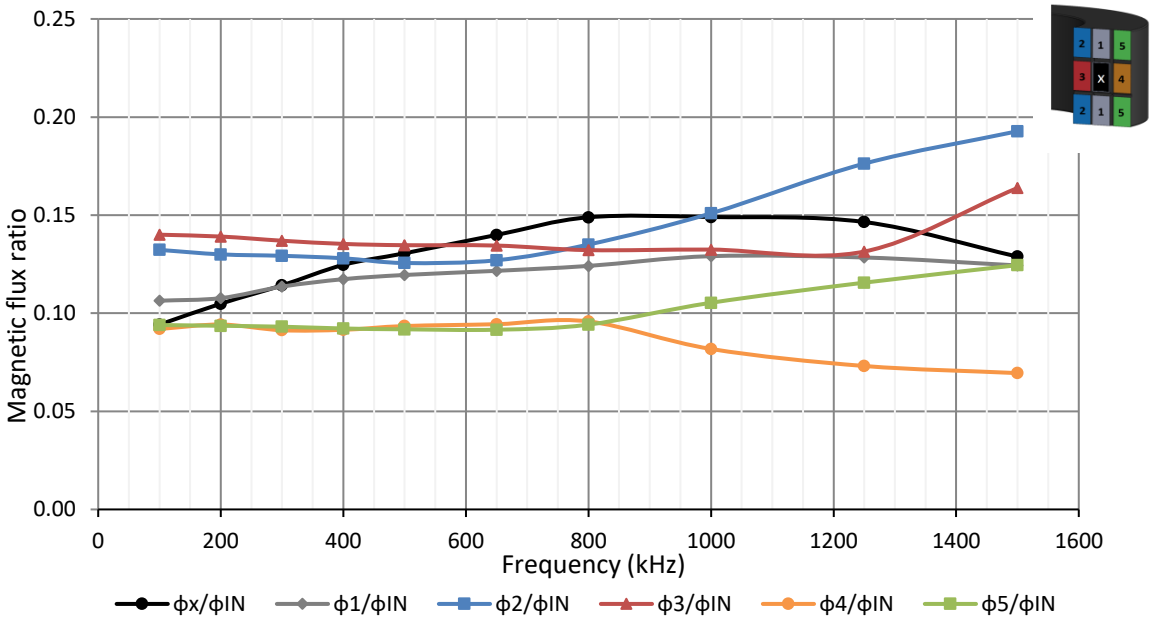

Figure 14. Magnetic flux distribution in the each area of 3E27 TX50 ring core.

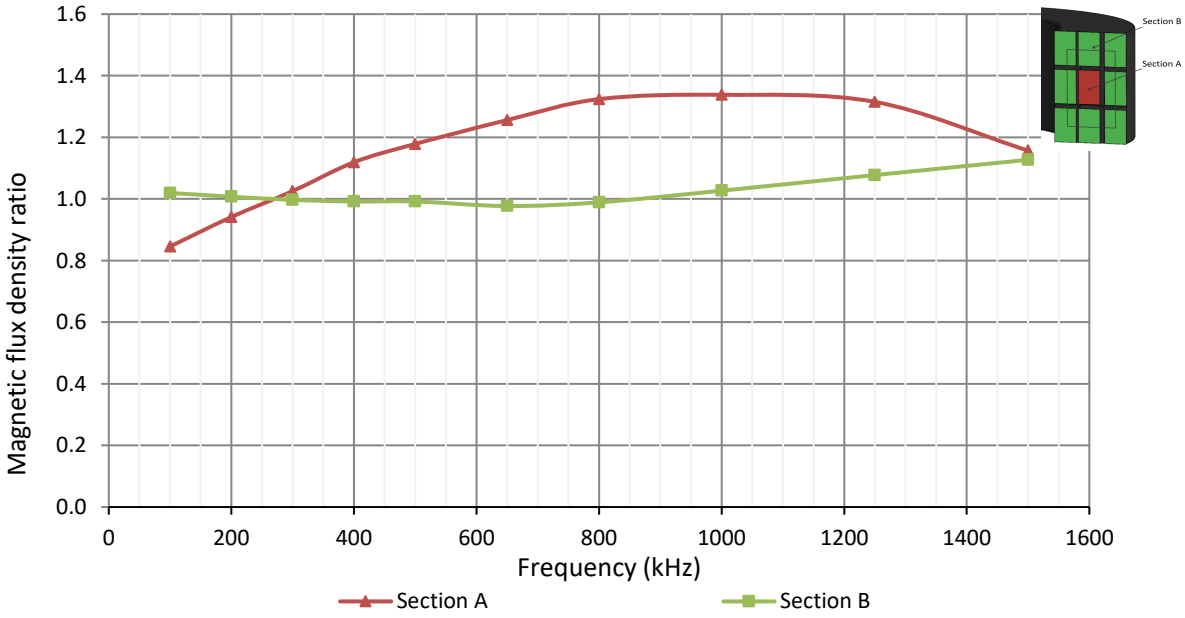

Figure 15. Magnetic flux distribution in the each section of 3E27 TX50 ring core.

Table 8. MEASURED VOLTAGES FOR TX50 3E27 RING CORE.

f = 100 kHz Blue – Excitation voltage, Red – Section A, Green – Section B 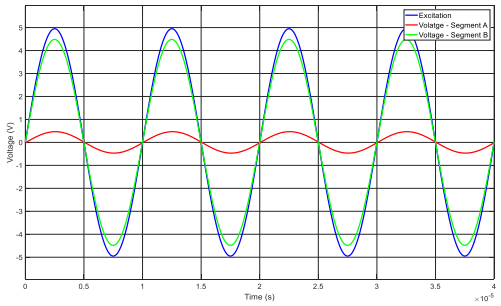	f = 200 kHz Blue – Excitation voltage, Red – Section A, Green – Section B 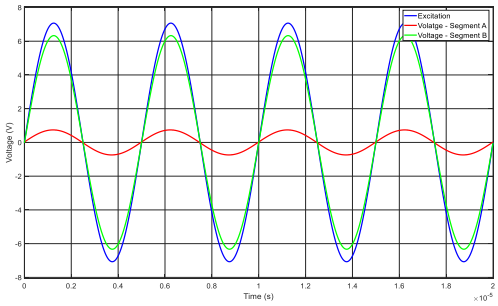
f = 300 kHz Blue – Excitation voltage, Red – Section A, Green – Section B 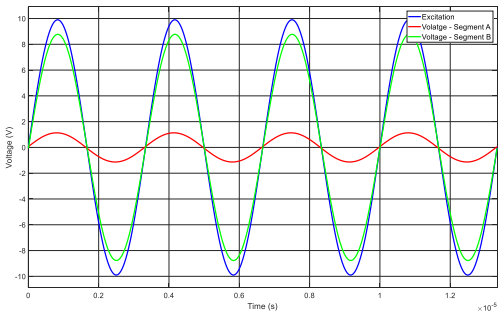	f = 400 kHz Blue – Excitation voltage, Red – Section A, Green – Section B 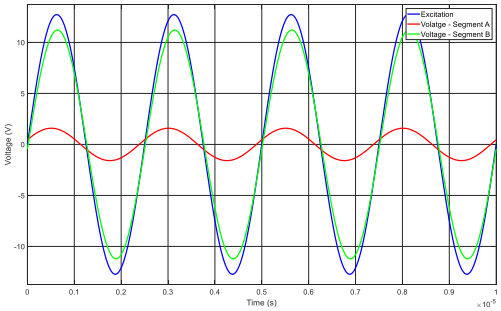
f = 500 kHz Blue – Excitation voltage, Red – Section A, Green – Section B 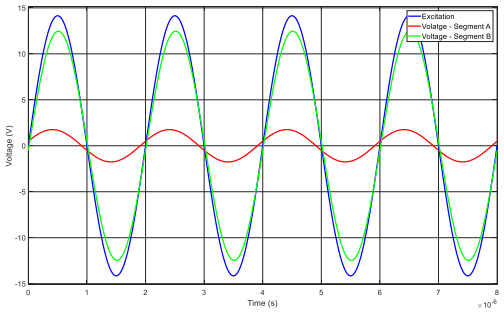	f = 650 kHz Blue – Excitation voltage, Red – Section A, Green – Section B 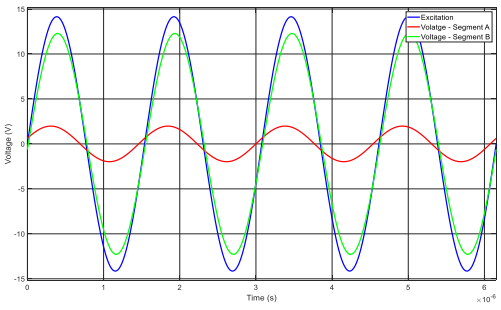

f = 800 kHz

Blue – Excitation voltage, Red – Section A, Green – Section B

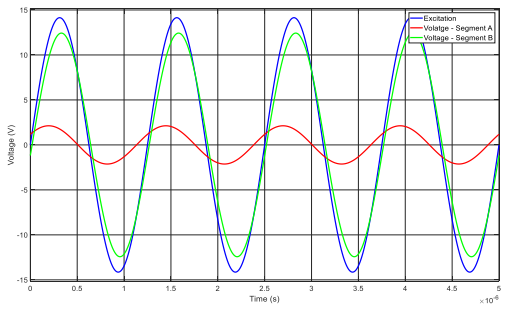

f = 1000 kHz

Blue – Excitation voltage, Red – Section A, Green – Section B

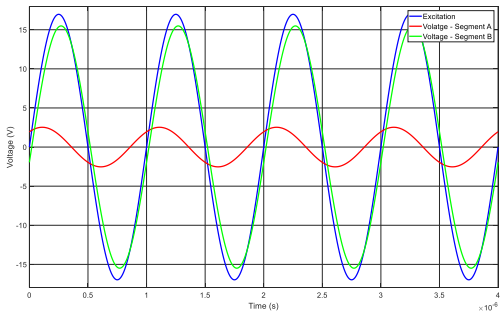

f = 1250 kHz

Blue – Excitation voltage, Red – Section A, Green – Section B

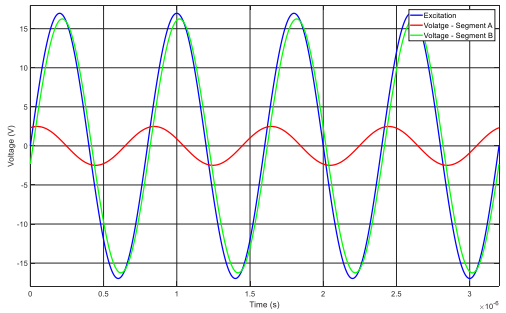

f = 1500 kHz

Blue – Excitation voltage, Red – Section A, Green – Section B

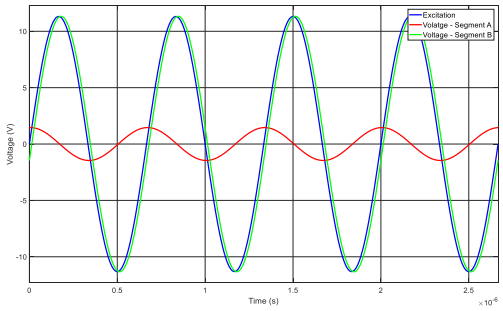

8.1.5. TX50 core with 3C11 material

Flux distributions in the each segment of TX50 core made from 3C11 material are shown in Figure 16, while magnetic flux density for Section A and B is shown in Figure 17. Corresponding voltage waveforms for Excitation, Segment A and Segment B at each frequency are presented in Table 9.

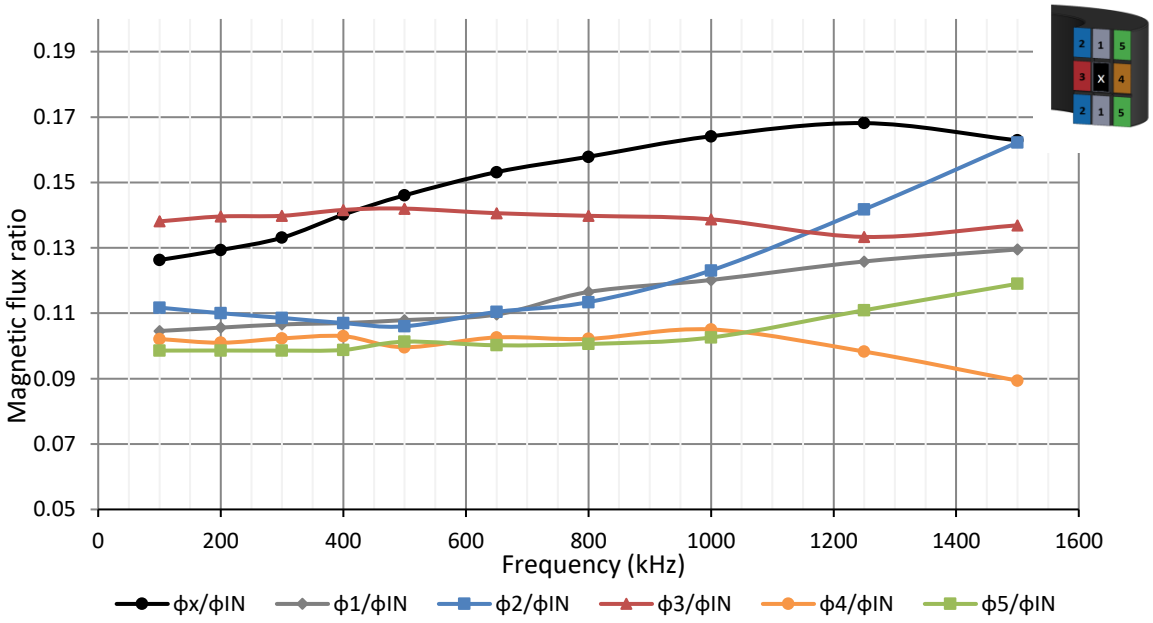

Figure 16. Magnetic flux distribution in the each area of 3C11 TX50 ring core.

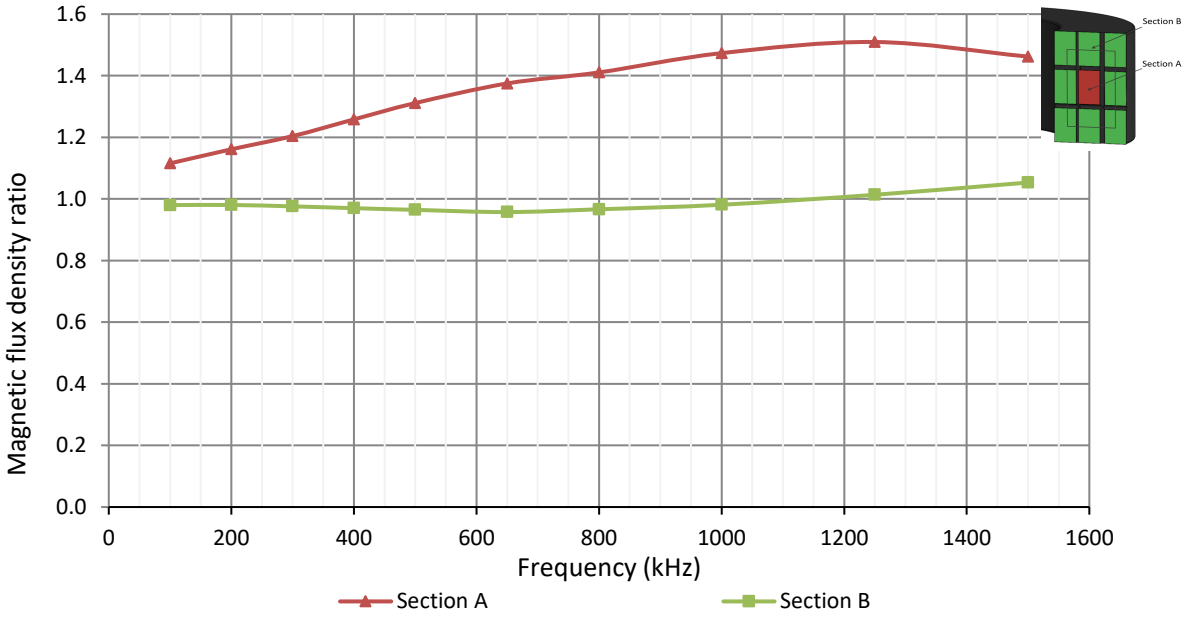

Figure 17. Magnetic flux distribution in the each section of 3C11 TX50 ring core.

Table 9. MEASURED VOLTAGES FOR TX50 3C11 RING CORE.

f = 100 kHz Blue – Excitation voltage, Red – Section A, Green – Section B 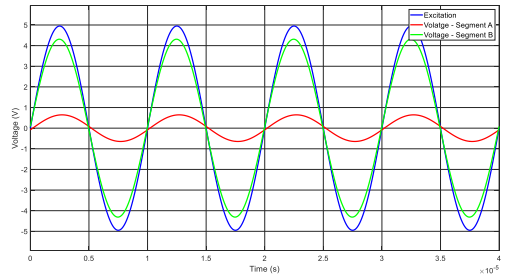	f = 200 kHz Blue – Excitation voltage, Red – Section A, Green – Section B 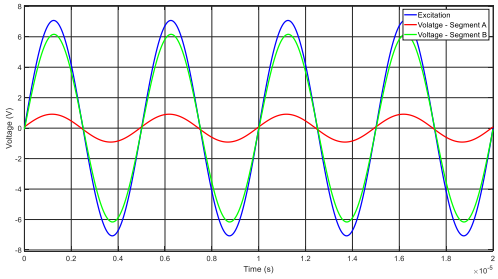
f = 300 kHz Blue – Excitation voltage, Red – Section A, Green – Section B 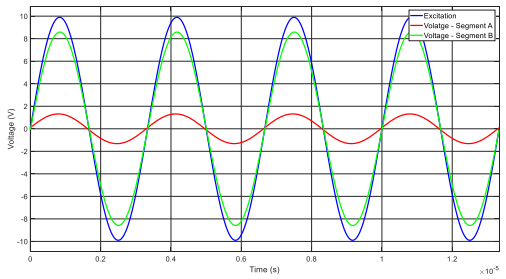	f = 400 kHz Blue – Excitation voltage, Red – Section A, Green – Section B 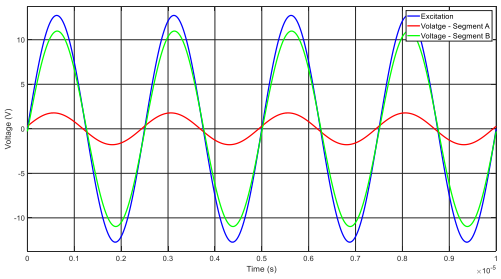
f = 500 kHz Blue – Excitation voltage, Red – Section A, Green – Section B 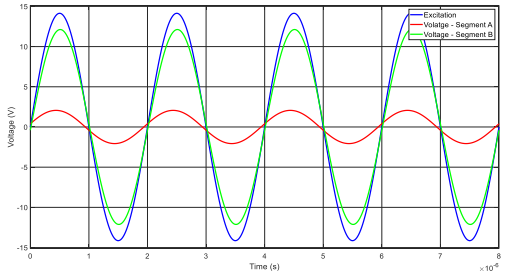	f = 650 kHz Blue – Excitation voltage, Red – Section A, Green – Section B 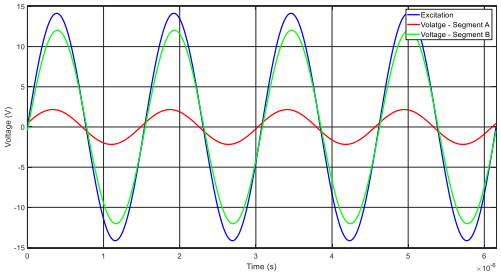

f = 800 kHz

Blue – Excitation voltage, Red – Section A, Green – Section B

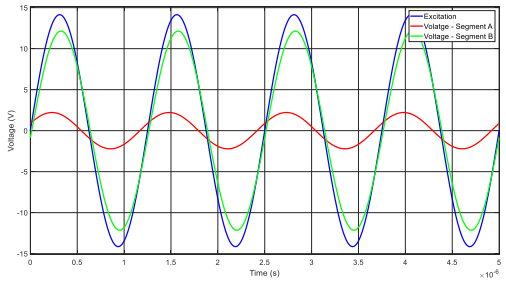

f = 1000 kHz

Blue – Excitation voltage, Red – Section A, Green – Section B

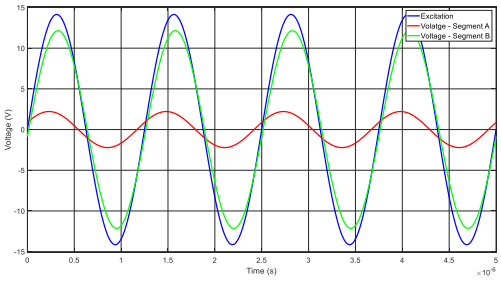

f = 1250 kHz

Blue – Excitation voltage, Red – Section A, Green – Section B

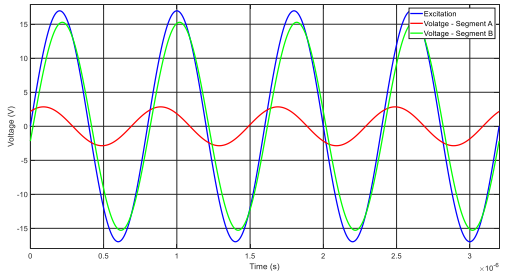

f = 1500 kHz

Blue – Excitation voltage, Red – Section A, Green – Section B

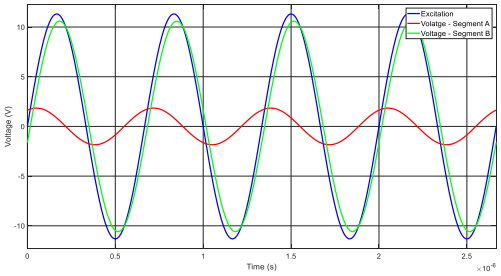

8.1.6. TX50 core with 4S60 material

Flux distributions in the each segment of TX50 core made from 4S60 material are shown in Figure 18, while magnetic flux density for Section A and B is shown in Figure 19. Corresponding voltage waveforms for Excitation, Segment A and Segment B at each frequency are presented in Table 10.

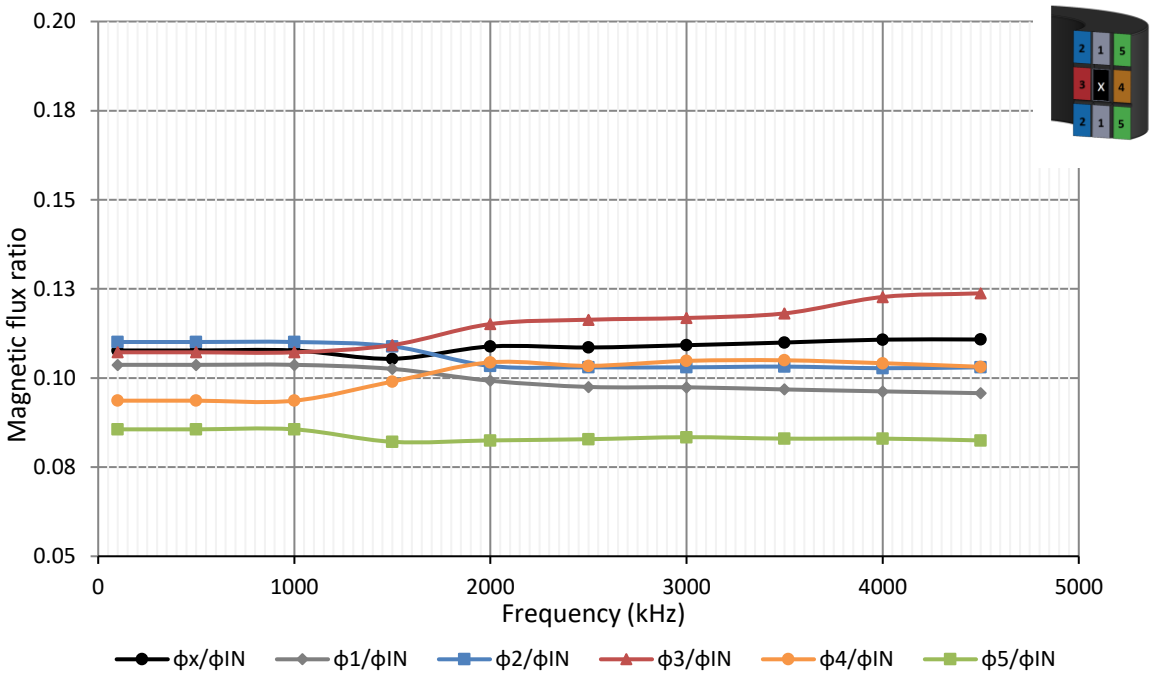

Figure 18. Magnetic flux distribution in the each area of 4S60 TX50 ring core.

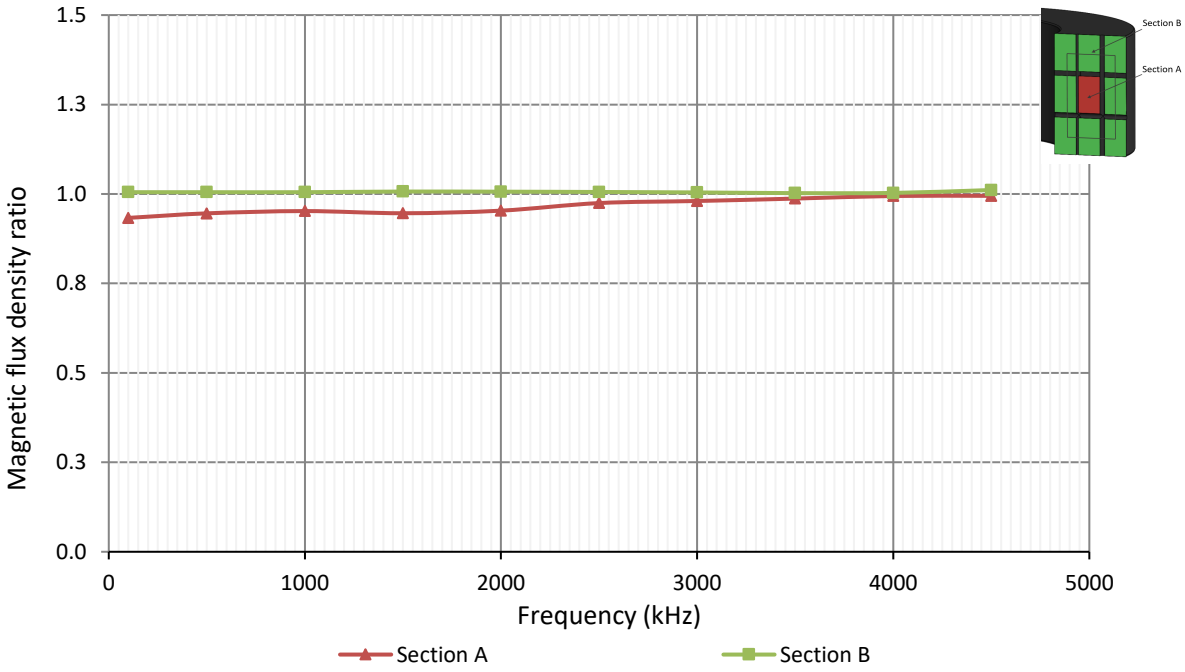

Figure 19. Magnetic flux distribution in the each section of 4S60 TX50 ring core.

Table 10. MEASURED VOLTAGES FOR TX50 4S60 RING CORE.

f = 100 kHz Blue – Excitation voltage, Red – Section A, Green – Section B 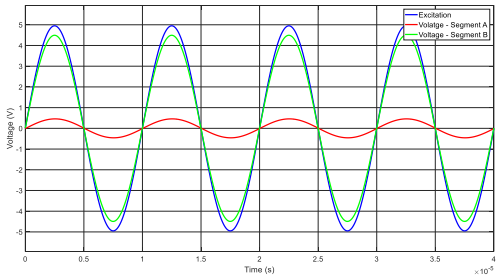	f = 500 kHz Blue – Excitation voltage, Red – Section A, Green – Section B 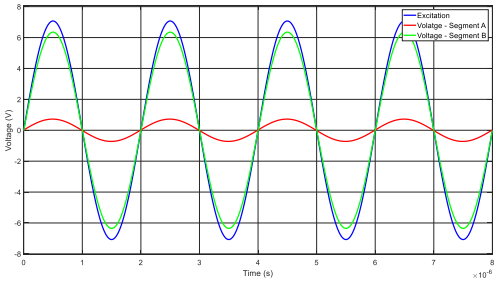
f = 1 000 kHz Blue – Excitation voltage, Red – Section A, Green – Section B 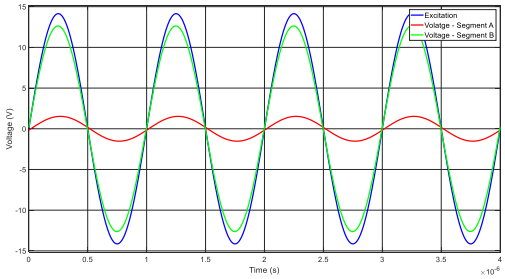	f = 1 500 kHz Blue – Excitation voltage, Red – Section A, Green – Section B 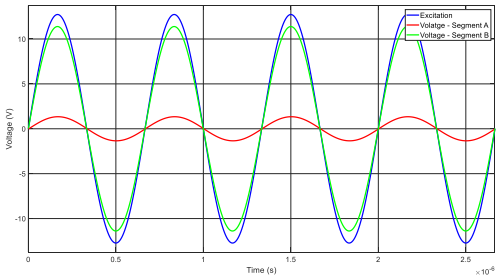
f = 2 000 kHz Blue – Excitation voltage, Red – Section A, Green – Section B 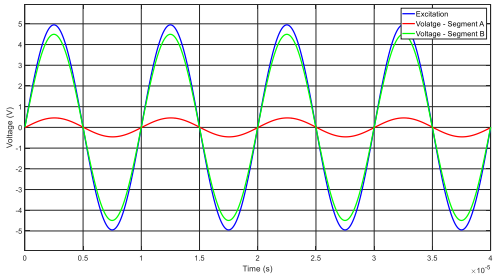	f = 2 500 kHz Blue – Excitation voltage, Red – Section A, Green – Section B 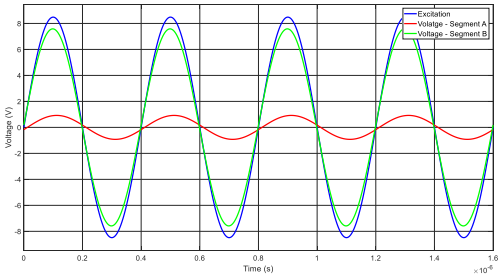

f = 3 000 kHz

Blue – Excitation voltage, Red – Section A, Green – Section B

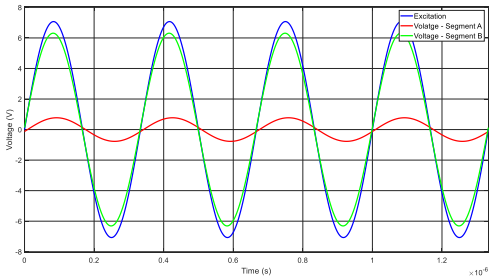

f = 3 500 kHz

Blue – Excitation voltage, Red – Section A, Green – Section B

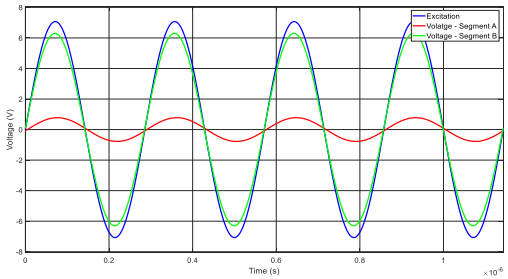

f = 4 000 kHz

Blue – Excitation voltage, Red – Section A, Green – Section B

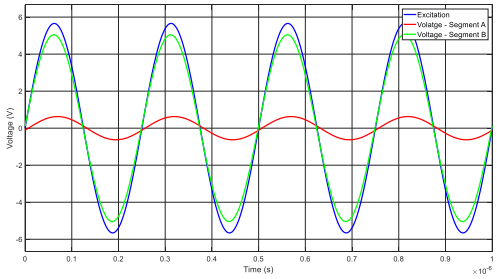

f = 4 500 kHz

Blue – Excitation voltage, Red – Section A, Green – Section B

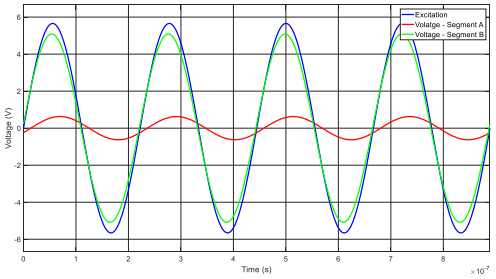

8.1.7. TX50 core with 4A11 material

Flux distributions in the each segment of TX50 core made from 4S60 material are shown in Figure 20, while magnetic flux density for Section A and B is shown in Figure 21. Corresponding voltage waveforms for Excitation, Segment A and Segment B at each frequency are presented in Table 11.

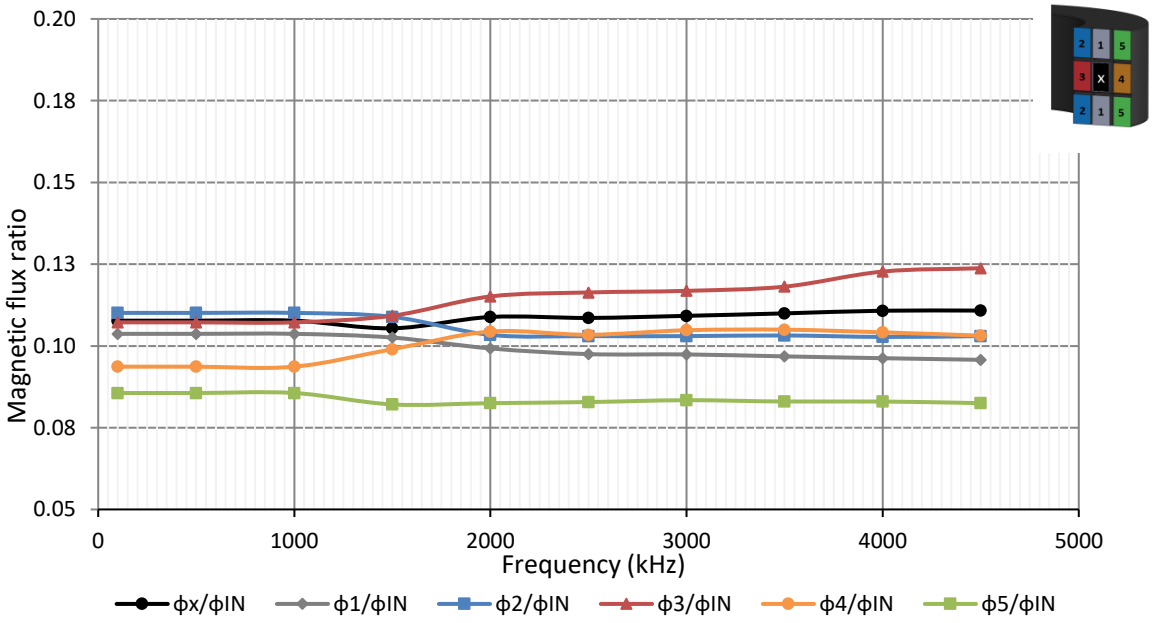

Figure 20. Magnetic flux distribution in the each area of 4A11 TX50 ring core.

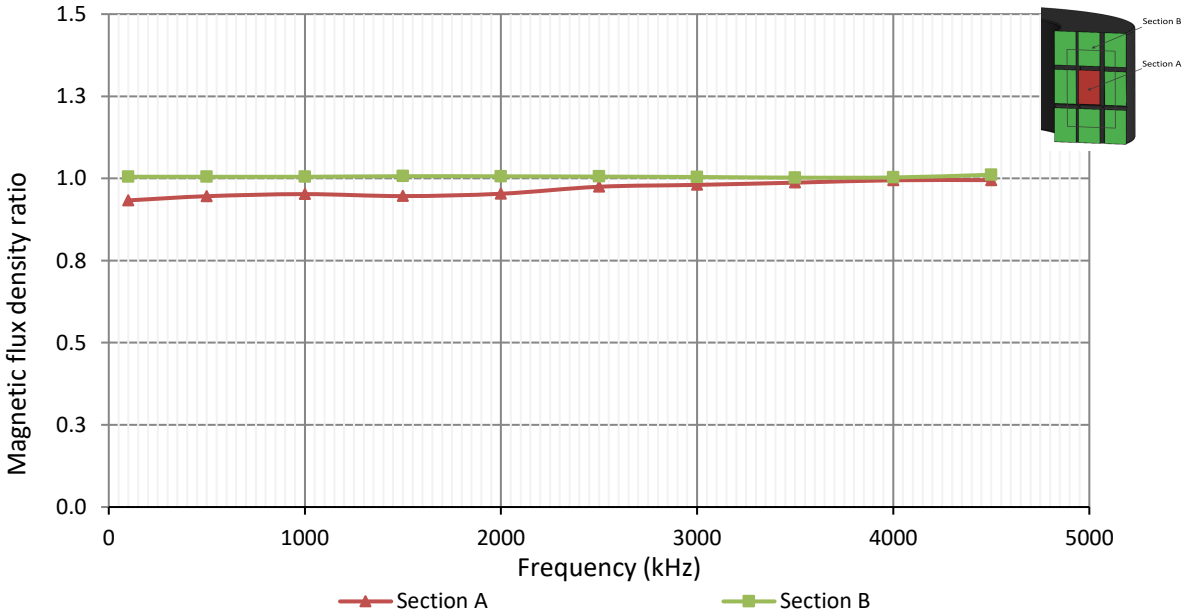

Figure 21. Magnetic flux distribution in the each section of 4A11 TX50 ring core.

Table 11. MEASURED VOLTAGES FOR TX50 4A11 RING CORE.

f = 100 kHz Blue – Excitation voltage, Red – Section A, Green – Section B 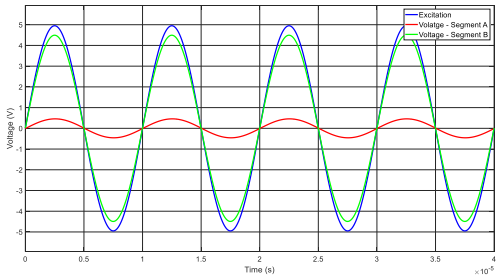	f = 500 kHz Blue – Excitation voltage, Red – Section A, Green – Section B 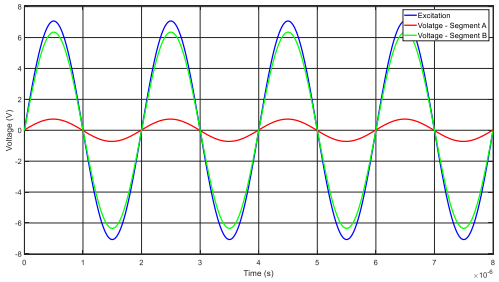
f = 1 000 kHz Blue – Excitation voltage, Red – Section A, Green – Section B 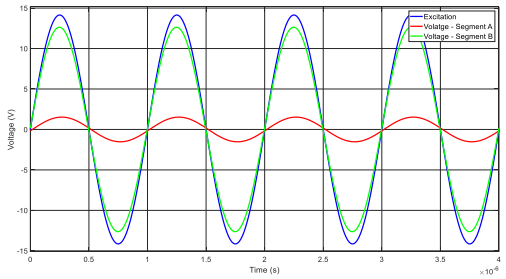	f = 1 500 kHz Blue – Excitation voltage, Red – Section A, Green – Section B 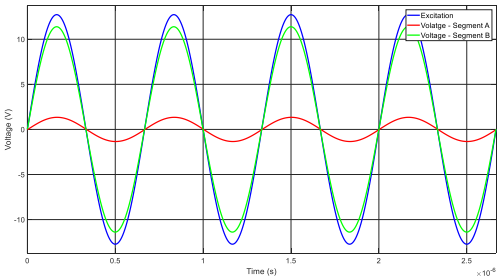
f = 2 000 kHz Blue – Excitation voltage, Red – Section A, Green – Section B 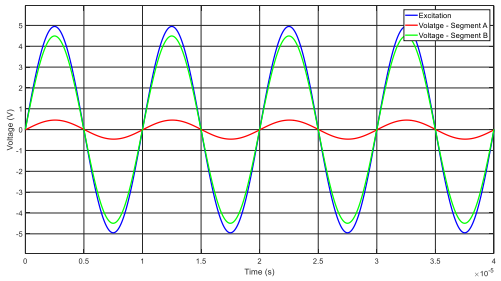	f = 2 500 kHz Blue – Excitation voltage, Red – Section A, Green – Section B 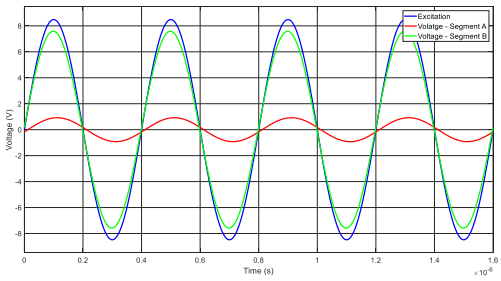

f = 3 000 kHz

Blue – Excitation voltage, Red – Section A, Green – Section B

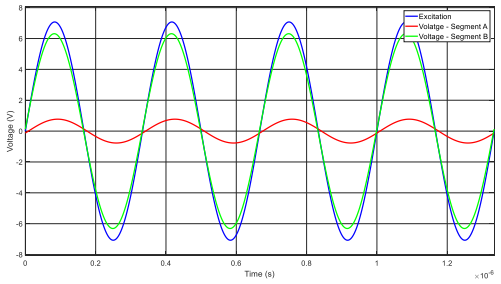

f = 3 500 kHz

Blue – Excitation voltage, Red – Section A, Green – Section B

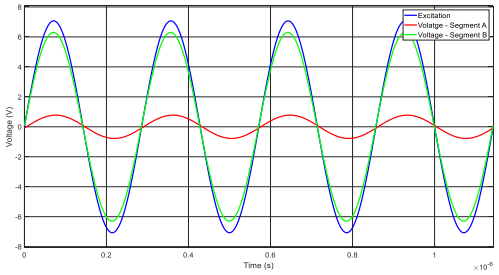

f = 4 000 kHz

Blue – Excitation voltage, Red – Section A, Green – Section B

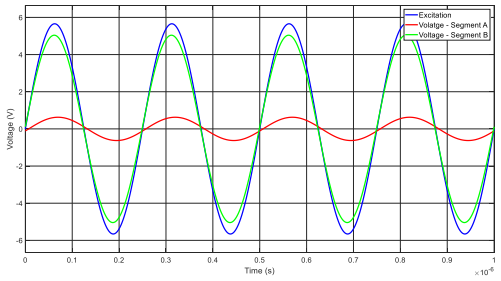

f = 4 500 kHz

Blue – Excitation voltage, Red – Section A, Green – Section B

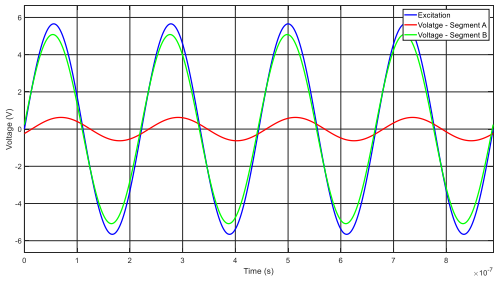

8.1.8. TX105 core with FR78 material

Flux distributions in the each segment of TX105 core made from FR78 material are shown in Figure 22, while magnetic flux density for Section A and B is shown in Figure 23. Corresponding voltage waveforms for Excitation, Segment A and Segment B at each frequency are presented in Table 12.

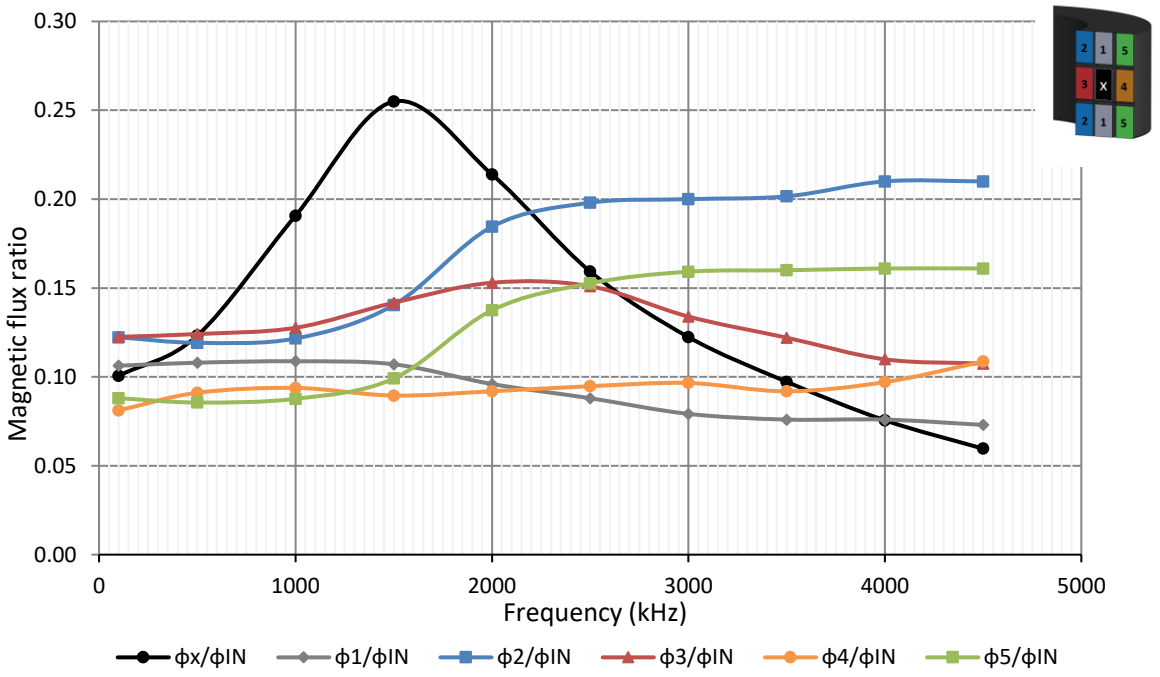

Figure 22. Magnetic flux distribution in the each area of FR78 TX105 ring core.

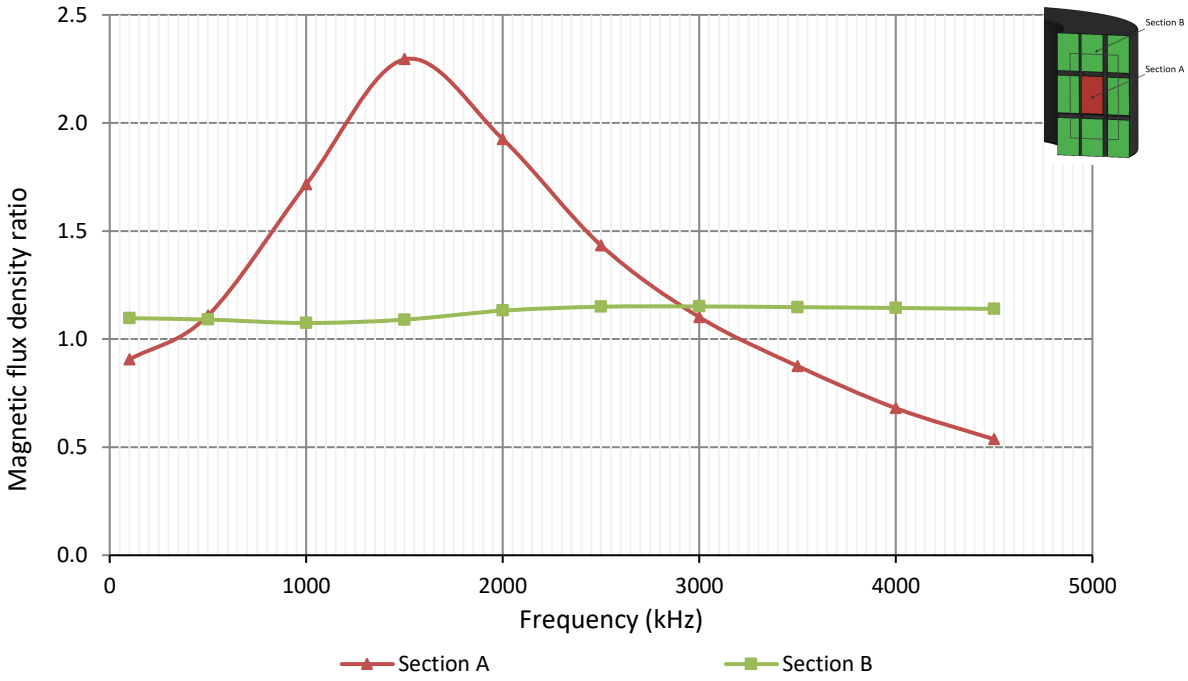

Figure 23. Magnetic flux distribution in the each section of FR78 TX105 ring core.

Table 12. MEASURED VOLTAGES FOR TX105 FR78 RING CORE.

f = 100 kHz Blue – Excitation voltage, Red – Section A, Green – Section B 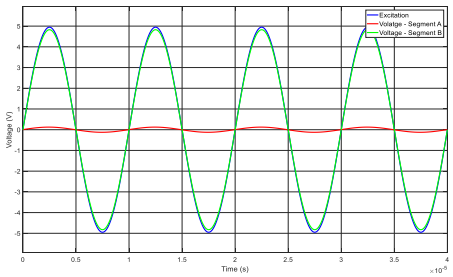	f = 500 kHz Blue – Excitation voltage, Red – Section A, Green – Section B 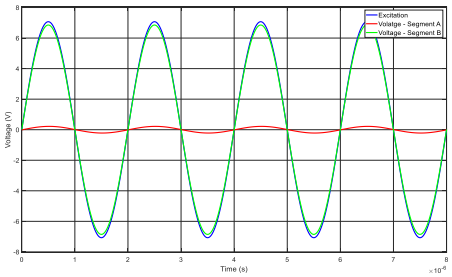
f = 1 000 kHz Blue – Excitation voltage, Red – Section A, Green – Section B 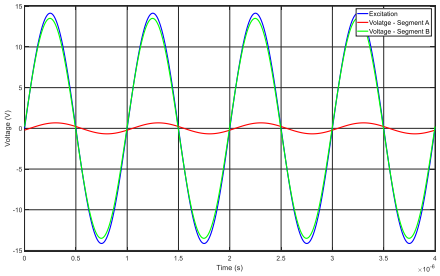	f = 1 500 kHz Blue – Excitation voltage, Red – Section A, Green – Section B 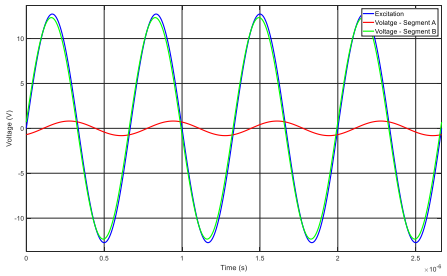
f = 2 000 kHz Blue – Excitation voltage, Red – Section A, Green – Section B 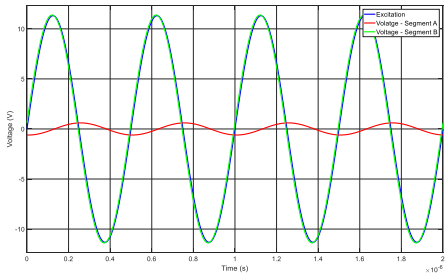	f = 2 500 kHz Blue – Excitation voltage, Red – Section A, Green – Section B 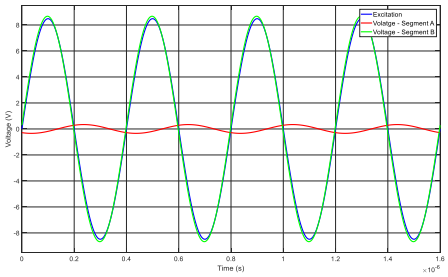

f = 3 000 kHz

Blue – Excitation voltage, Red – Section A, Green – Section B

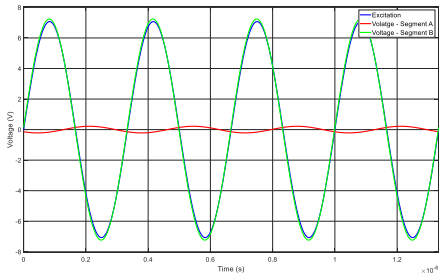

f = 3 500 kHz

Blue – Excitation voltage, Red – Section A, Green – Section B

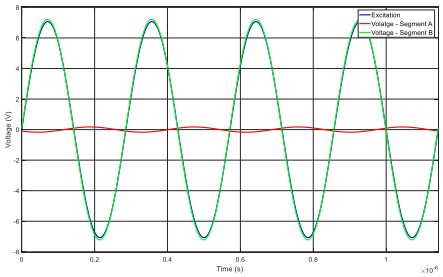

f = 4 000 kHz

Blue – Excitation voltage, Red – Section A, Green – Section B

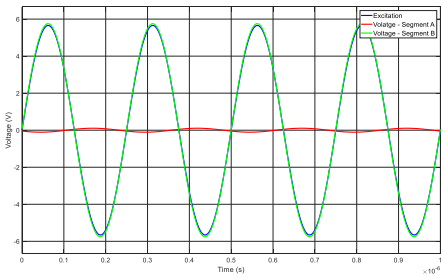

f = 4 500 kHz

Blue – Excitation voltage, Red – Section A, Green – Section B

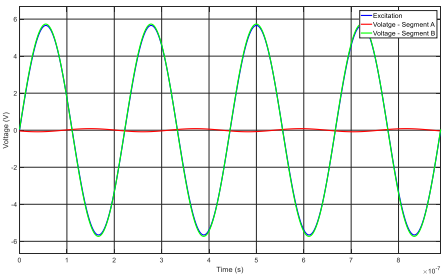

8.1.9. TX105 core with FR79 material

Flux distributions in the each segment of TX105 core made from FR79 material are shown in Figure 24, while magnetic flux density for Section A and B is shown in Figure 25. Corresponding voltage waveforms for Excitation, Segment A and Segment B at each frequency are presented in Table 13.

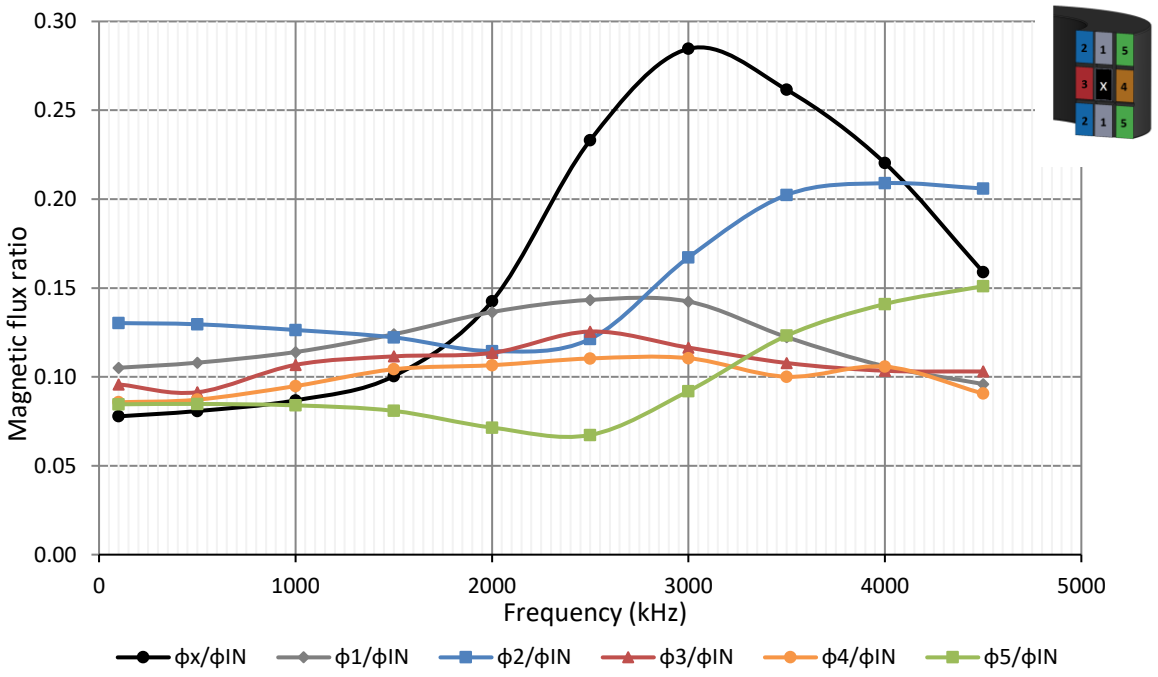

Figure 24. Magnetic flux distribution in the each area of FR79 TX105 ring core.

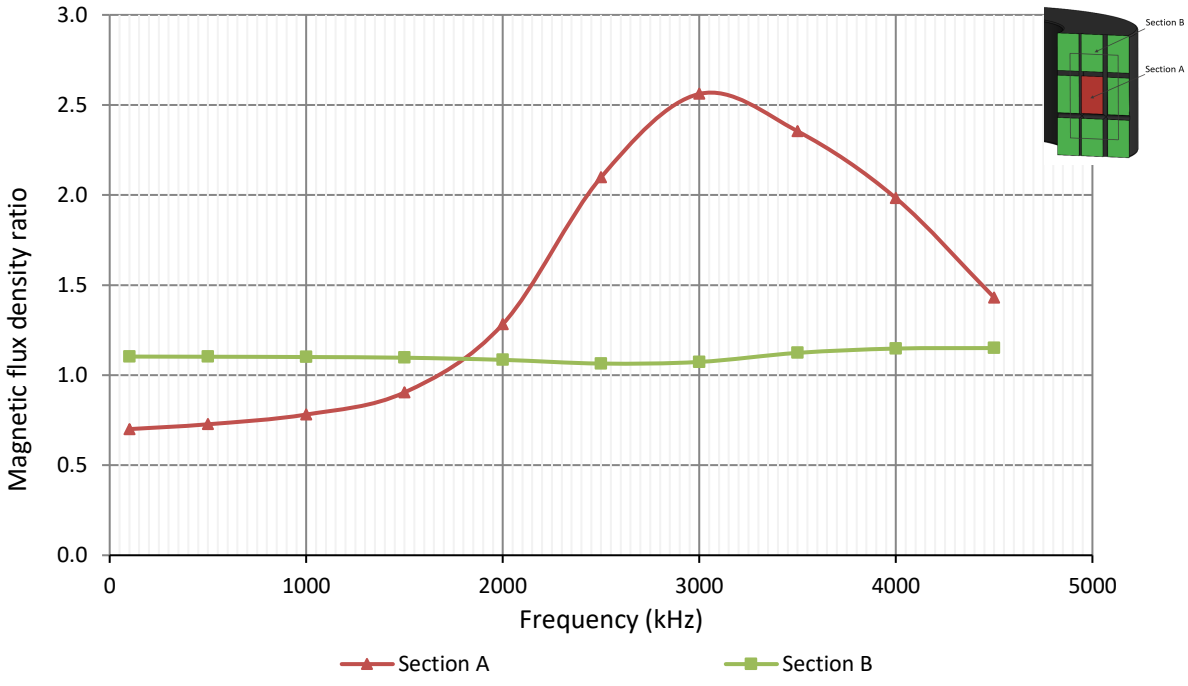

Figure 25. Magnetic flux distribution in the each section of FR79 TX105 ring core.

TABLE 13. MEASURED VOLTAGES FOR TX105 FR79 RING CORE.

f = 100 kHz Blue – Excitation voltage, Red – Section A, Green – Section B 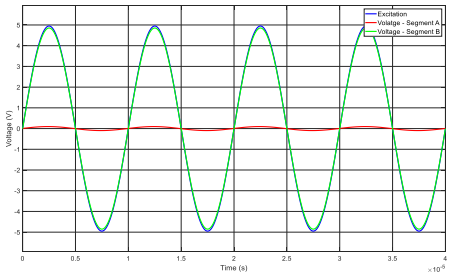	f = 500 kHz Blue – Excitation voltage, Red – Section A, Green – Section B 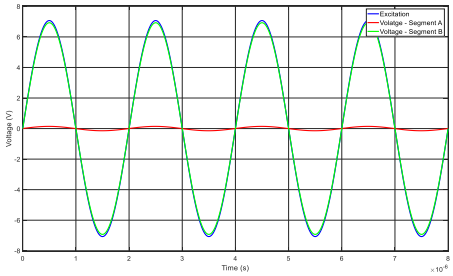
f = 1 000 kHz Blue – Excitation voltage, Red – Section A, Green – Section B 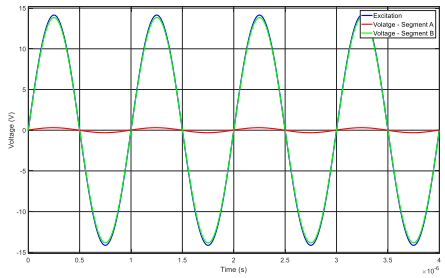	f = 1 500 kHz Blue – Excitation voltage, Red – Section A, Green – Section B 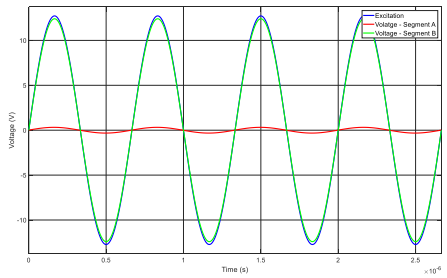
f = 2 000 kHz Blue – Excitation voltage, Red – Section A, Green – Section B 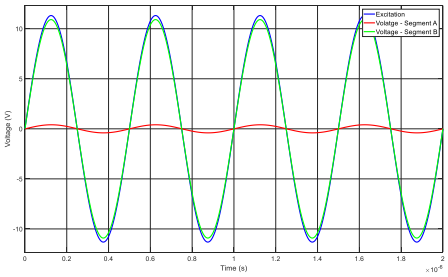	f = 2 500 kHz Blue – Excitation voltage, Red – Section A, Green – Section B 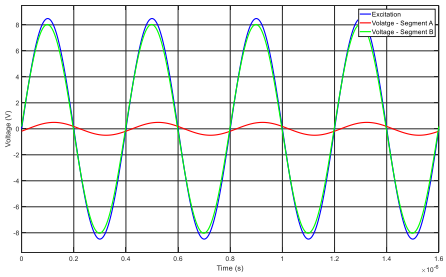

f = 3 000 kHz

Blue – Excitation voltage, Red – Section A, Green – Section B

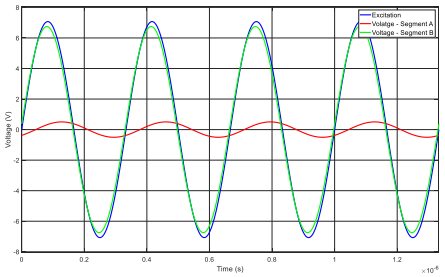

f = 3 500 kHz

Blue – Excitation voltage, Red – Section A, Green – Section B

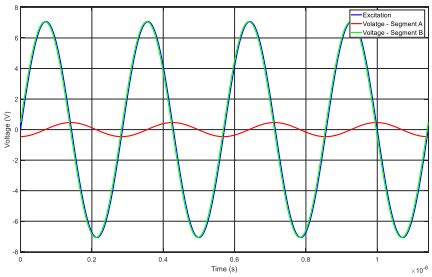

f = 4 000 kHz

Blue – Excitation voltage, Red – Section A, Green – Section B

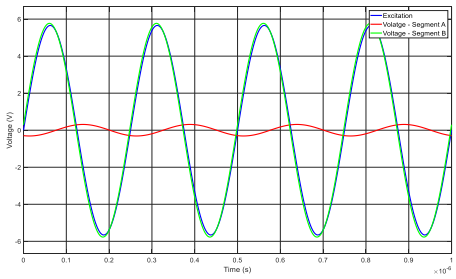

f = 4 500 kHz

Blue – Excitation voltage, Red – Section A, Green – Section B

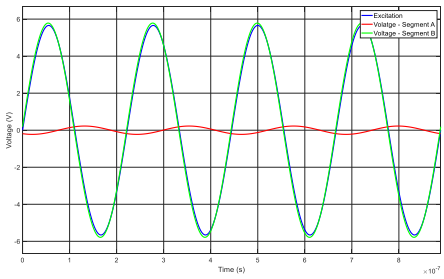

8.1.10. TX105 core with FR61 material

Flux distributions in the each segment of TX105 core made from FR61 material are shown in Figure 26, while magnetic flux density for Section A and B is shown in Figure 27. Corresponding voltage waveforms for Excitation, Segment A and Segment B at each frequency are presented in Table 14.

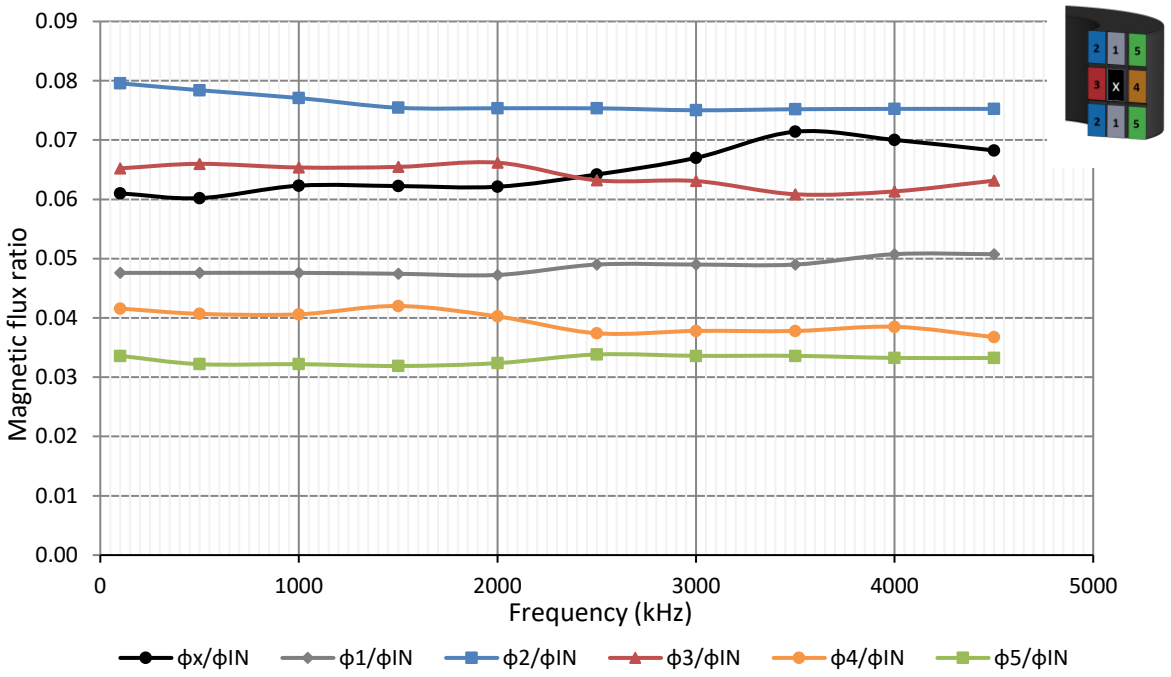

Figure 26. Magnetic flux distribution in the each area of FR61 TX105 ring core.

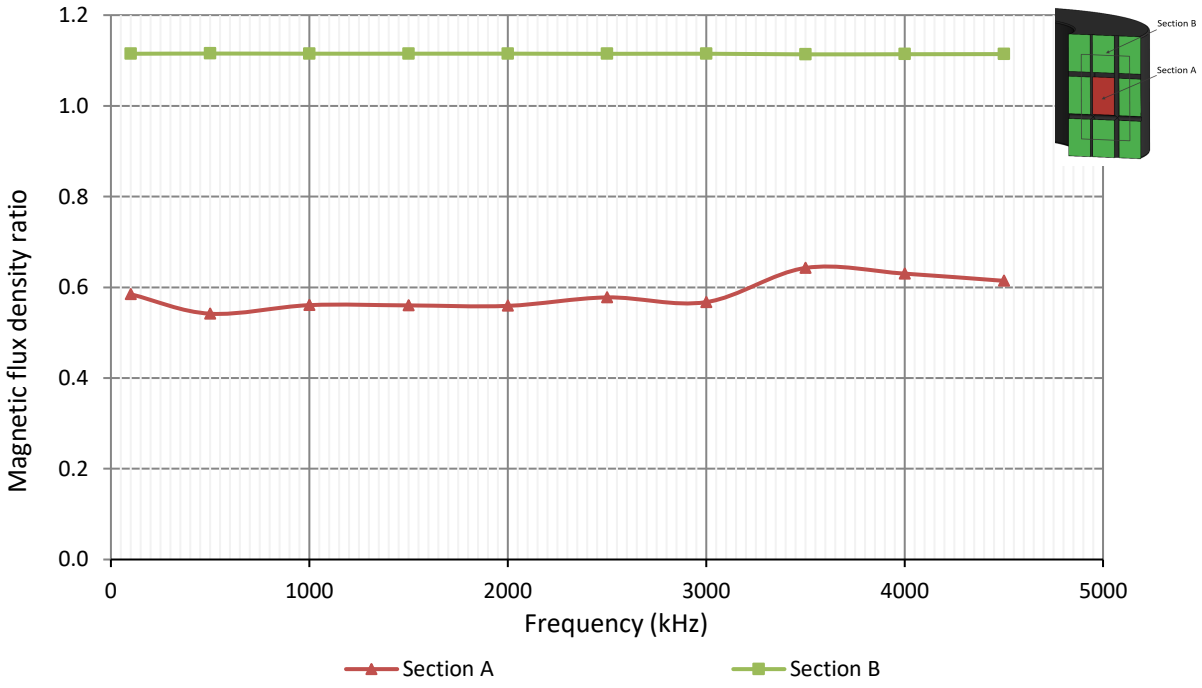

Figure 27. Magnetic flux distribution in the each section of FR61 TX105 ring core.

Table 14. MEASURED VOLTAGES FOR TX105 FR61 RING CORE.

f = 100 kHz Blue – Excitation voltage, Red – Section A, Green – Section B 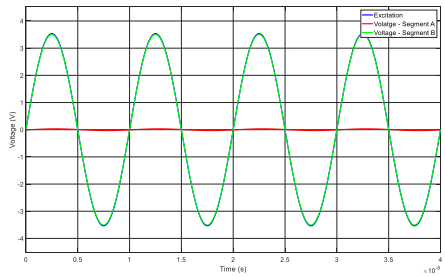	f = 500 kHz Blue – Excitation voltage, Red – Section A, Green – Section B 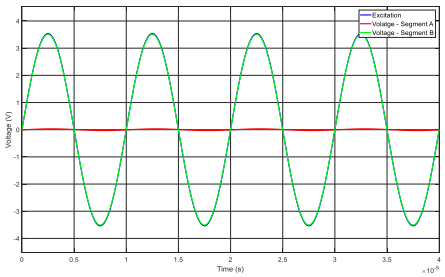
f = 1 000 kHz Blue – Excitation voltage, Red – Section A, Green – Section B 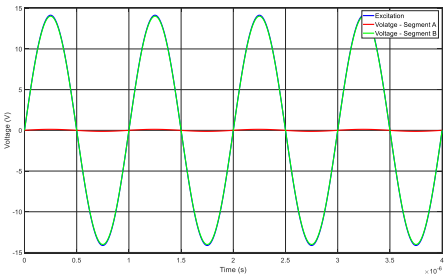	f = 1 500 kHz Blue – Excitation voltage, Red – Section A, Green – Section B 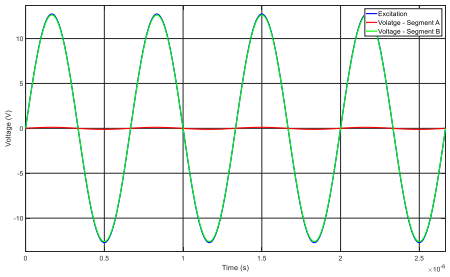
f = 2 000 kHz Blue – Excitation voltage, Red – Section A, Green – Section B 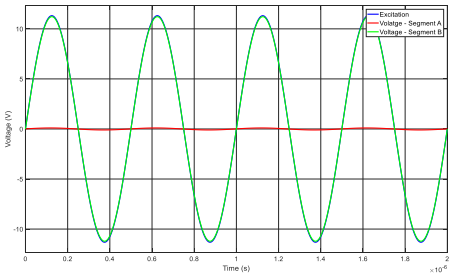	f = 2 500 kHz Blue – Excitation voltage, Red – Section A, Green – Section B 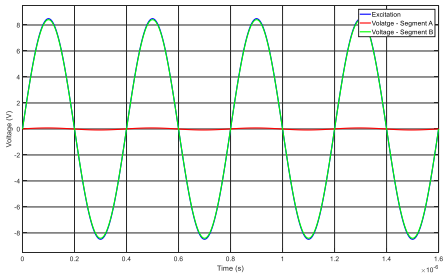

f = 3 000 kHz

Blue – Excitation voltage, Red – Section A, Green – Section B

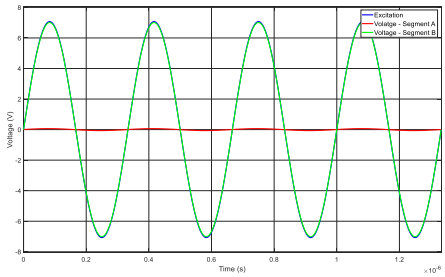

f = 3 500 kHz

Blue – Excitation voltage, Red – Section A, Green – Section B

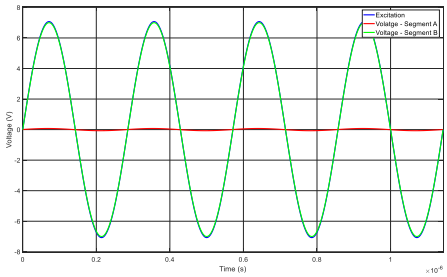

f = 4 000 kHz

Blue – Excitation voltage, Red – Section A, Green – Section B

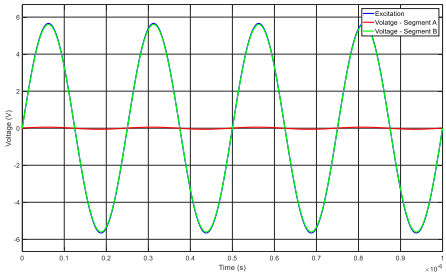

f = 4 500 kHz

Blue – Excitation voltage, Red – Section A, Green – Section B

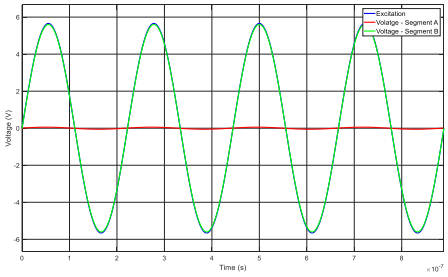

8.1.11. TX105 core with FR67 material

Flux distributions in the each segment of TX105 core made from FR67 material are shown in Figure 28, while magnetic flux density for Section A and B is shown in Figure 29. Corresponding voltage waveforms for Excitation, Segment A and Segment B at each frequency are presented in Table 15.

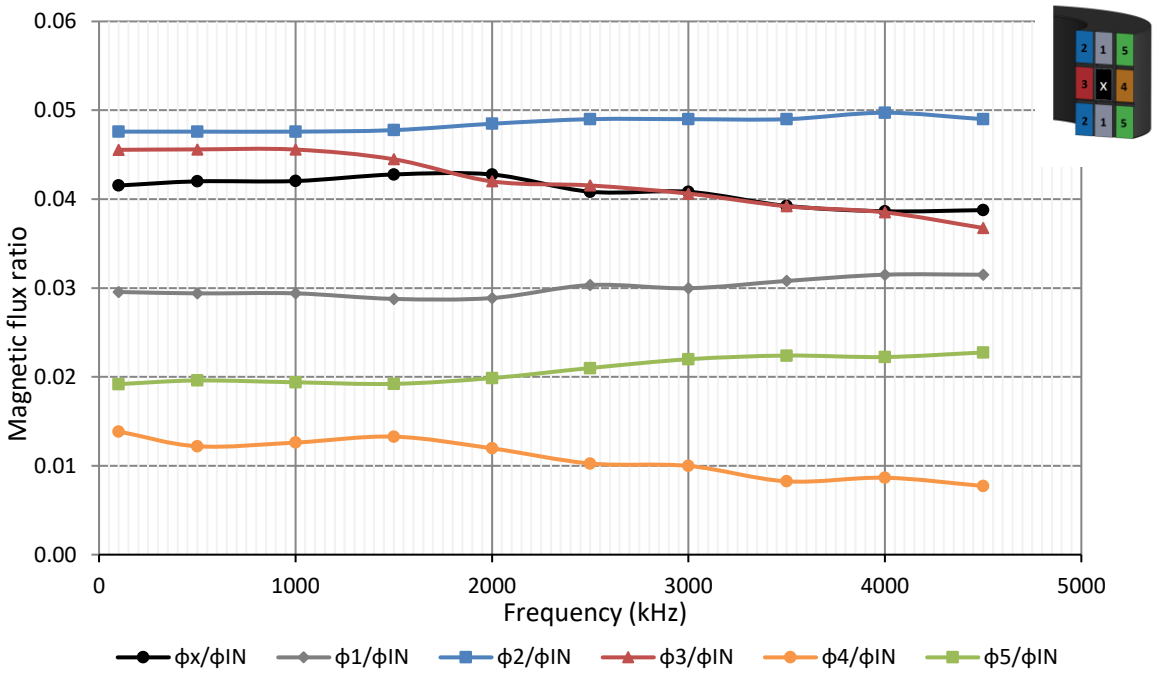

Figure 28. Magnetic flux distribution in the each area of FR67 TX105 ring core.

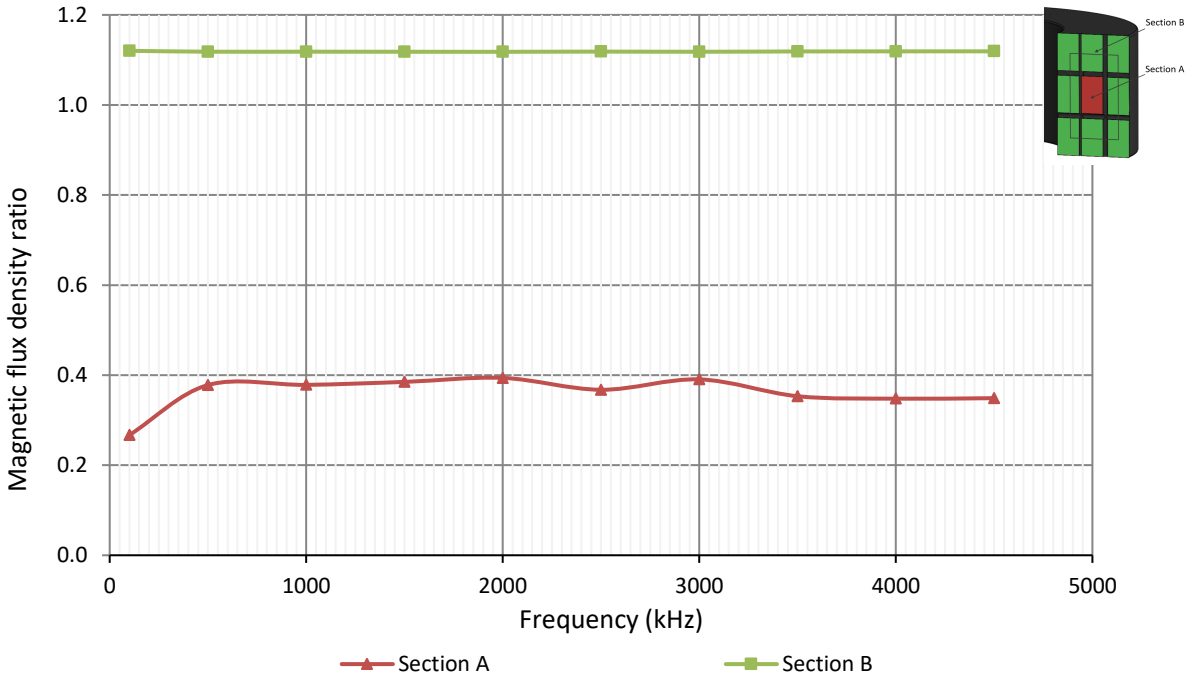

Figure 29. Magnetic flux distribution in the each section of FR67 TX105 ring core.

Table 15. MEASURED VOLTAGES FOR TX105 FR67 RING CORE.

f = 100 kHz Blue – Excitation voltage, Red – Section A, Green – Section B 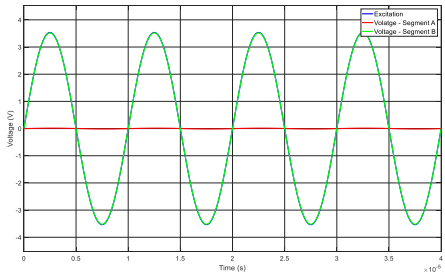	f = 500 kHz Blue – Excitation voltage, Red – Section A, Green – Section B 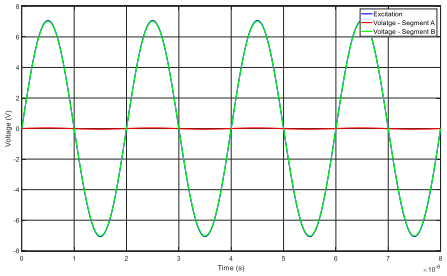
f = 1 000 kHz Blue – Excitation voltage, Red – Section A, Green – Section B 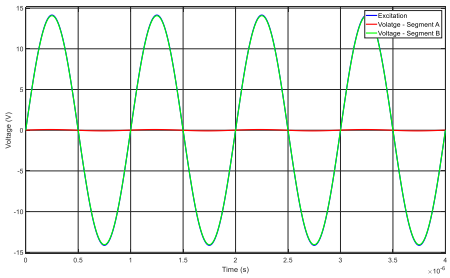	f = 1 500 kHz Blue – Excitation voltage, Red – Section A, Green – Section B 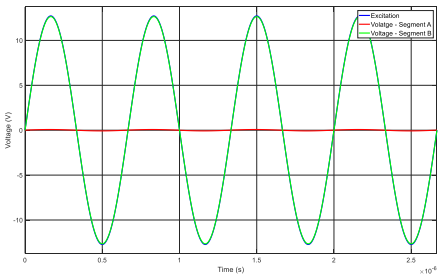
f = 2 000 kHz Blue – Excitation voltage, Red – Section A, Green – Section B 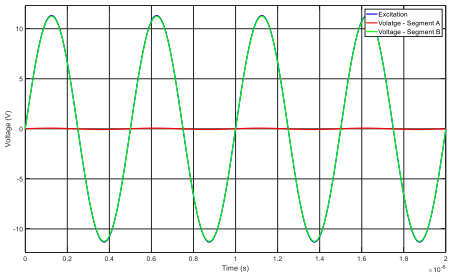	f = 2 500 kHz Blue – Excitation voltage, Red – Section A, Green – Section B 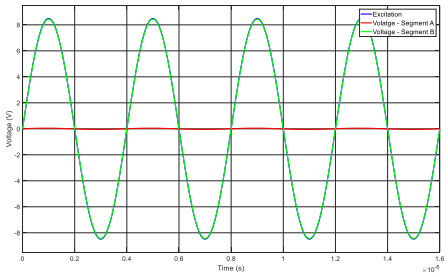

f = 3 000 kHz

Blue – Excitation voltage, Red – Section A, Green – Section B

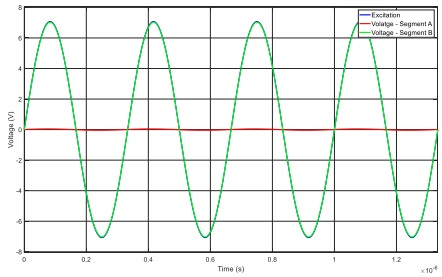

f = 3 500 kHz

Blue – Excitation voltage, Red – Section A, Green – Section B

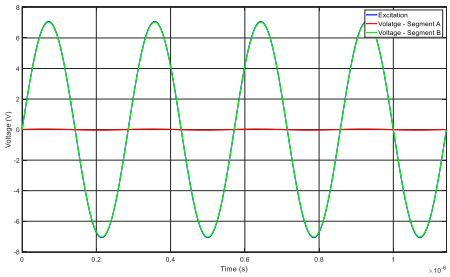

f = 4 000 kHz

Blue – Excitation voltage, Red – Section A, Green – Section B

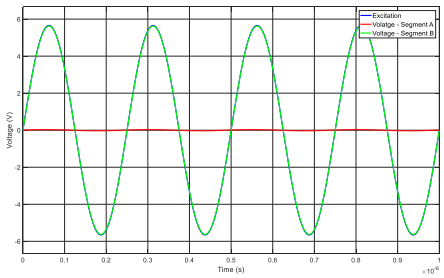

f = 4 500 kHz

Blue – Excitation voltage, Red – Section A, Green – Section B

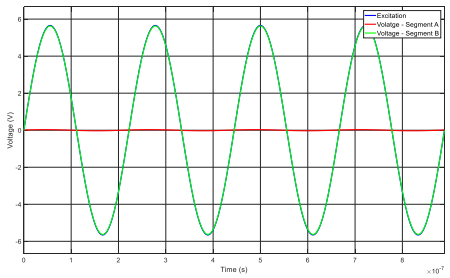

8.1.12. Frame core with FR78 material

Flux distributions in the each segment of Frame core made from FR78 material are shown in Figure 30, while magnetic flux density for Section A and B is shown in Figure 31. Corresponding voltage waveforms for Excitation, Segment A and Segment B at each frequency are presented in Table 16.

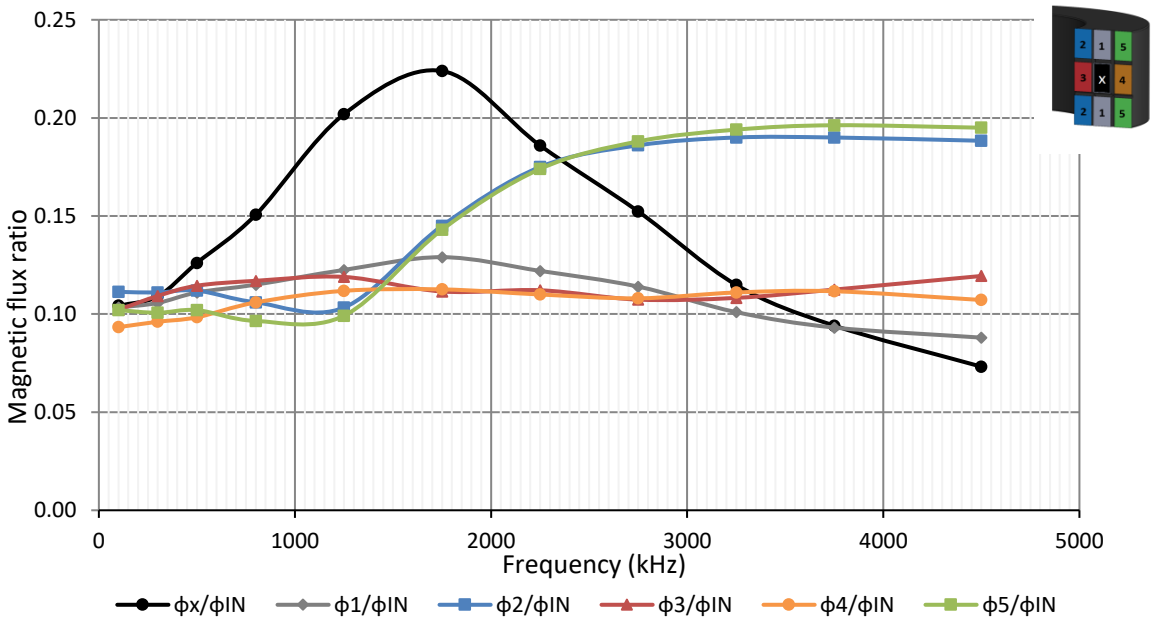

Figure 30. Magnetic flux distribution in the each area of FR78 frame core.

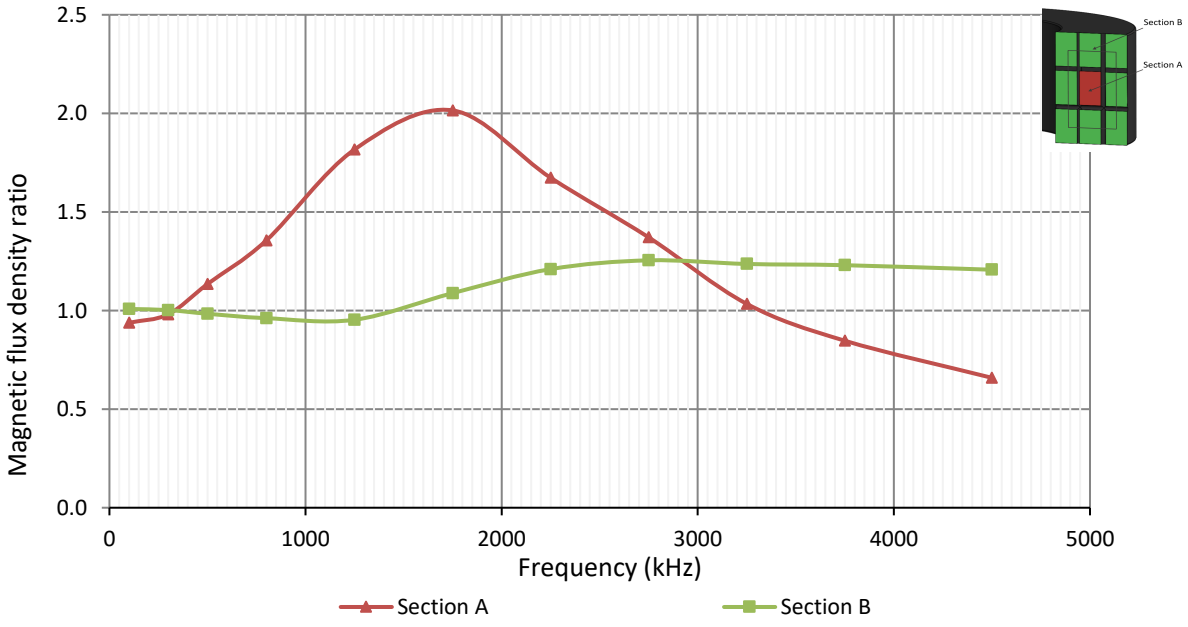

Figure 31. Magnetic flux distribution in the each section of FR78 frame core.

Table 16. MEASURED VOLTAGES FOR FR78 FRAME CORE.

f = 100 kHz Blue – Excitation voltage, Red – Section A, Green – Section B 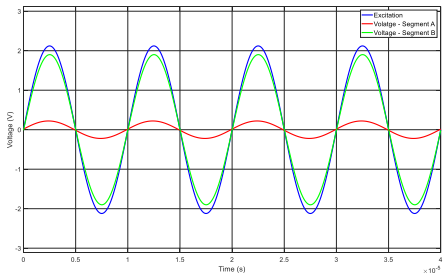	f = 500 kHz Blue – Excitation voltage, Red – Section A, Green – Section B 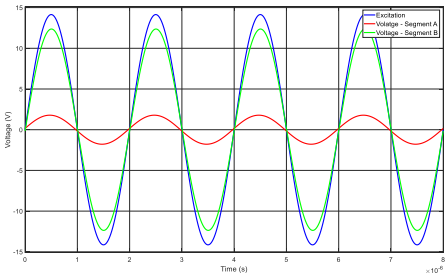
f = 800 kHz Blue – Excitation voltage, Red – Section A, Green – Section B 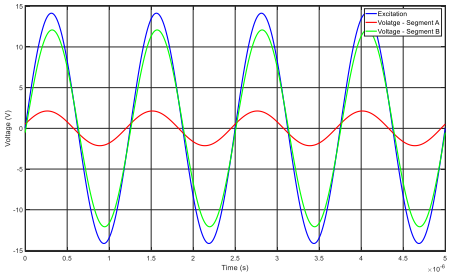	f = 1 250 kHz Blue – Excitation voltage, Red – Section A, Green – Section B 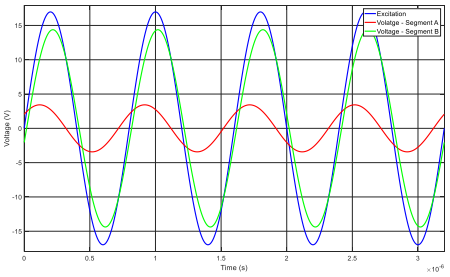
f = 1 750 kHz Blue – Excitation voltage, Red – Section A, Green – Section B 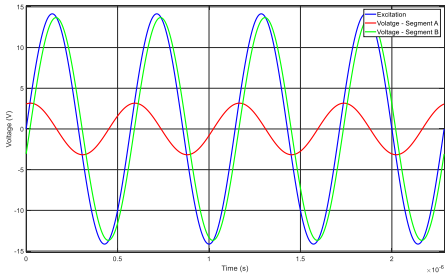	f = 2 250 kHz Blue – Excitation voltage, Red – Section A, Green – Section B 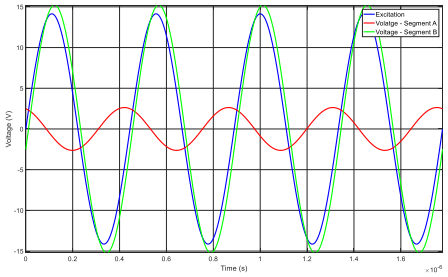

f = 2 750 kHz

Blue – Excitation voltage, Red – Section A, Green – Section B

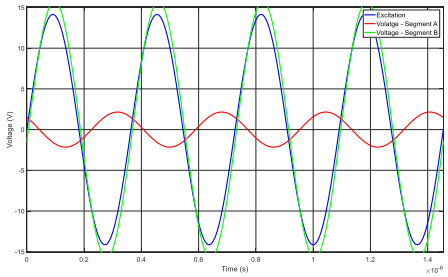

f = 3 250 kHz

Blue – Excitation voltage, Red – Section A, Green – Section B

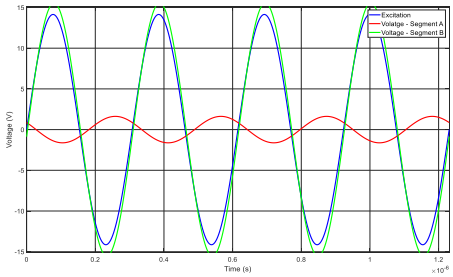

f = 3 750 kHz

Blue – Excitation voltage, Red – Section A, Green – Section B

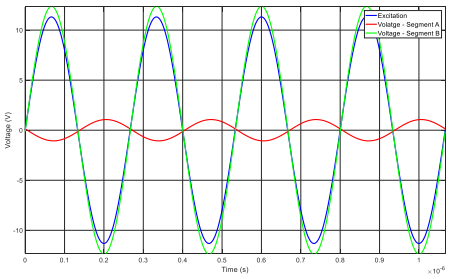

f = 4 500 kHz

Blue – Excitation voltage, Red – Section A, Green – Section B

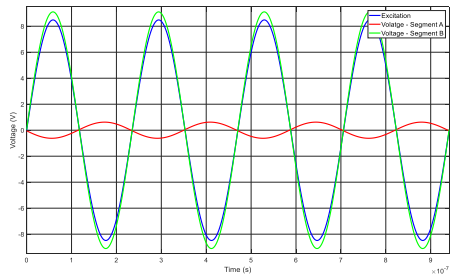

8.1.13. Frame core with FR79 material

Flux distributions in the each segment of Frame core made from FR79 material are shown in Figure 32, while magnetic flux density for Section A and B is shown in Figure 33. Corresponding voltage waveforms for Excitation, Segment A and Segment B at each frequency are presented in Table 17.

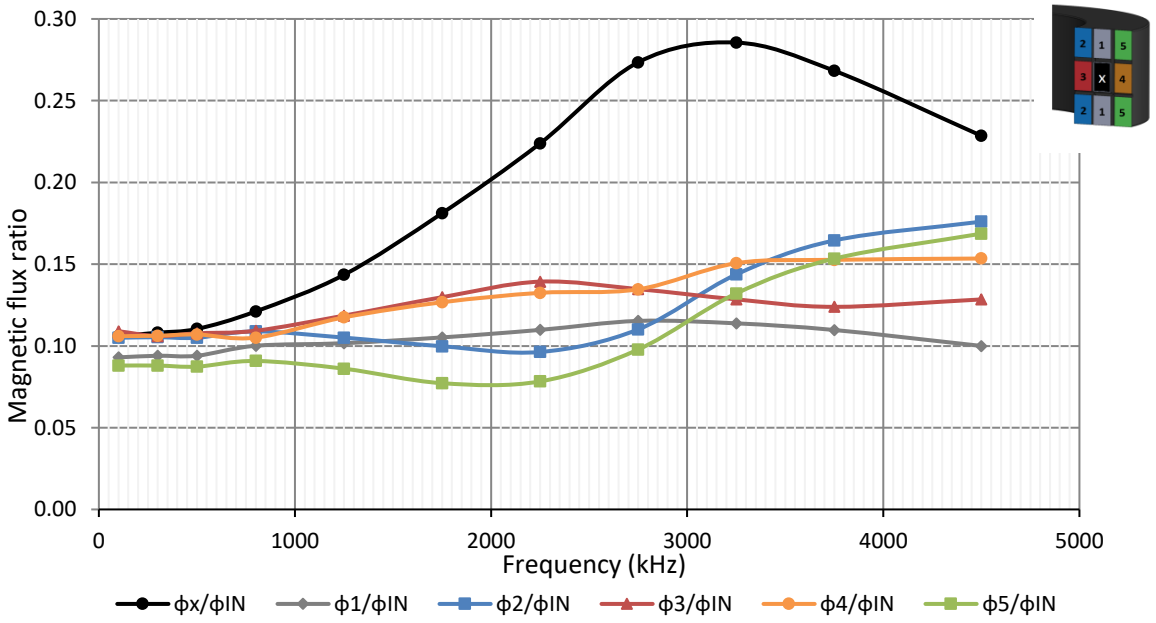

Figure 32. Magnetic flux distribution in the each area of FR79 frame core.

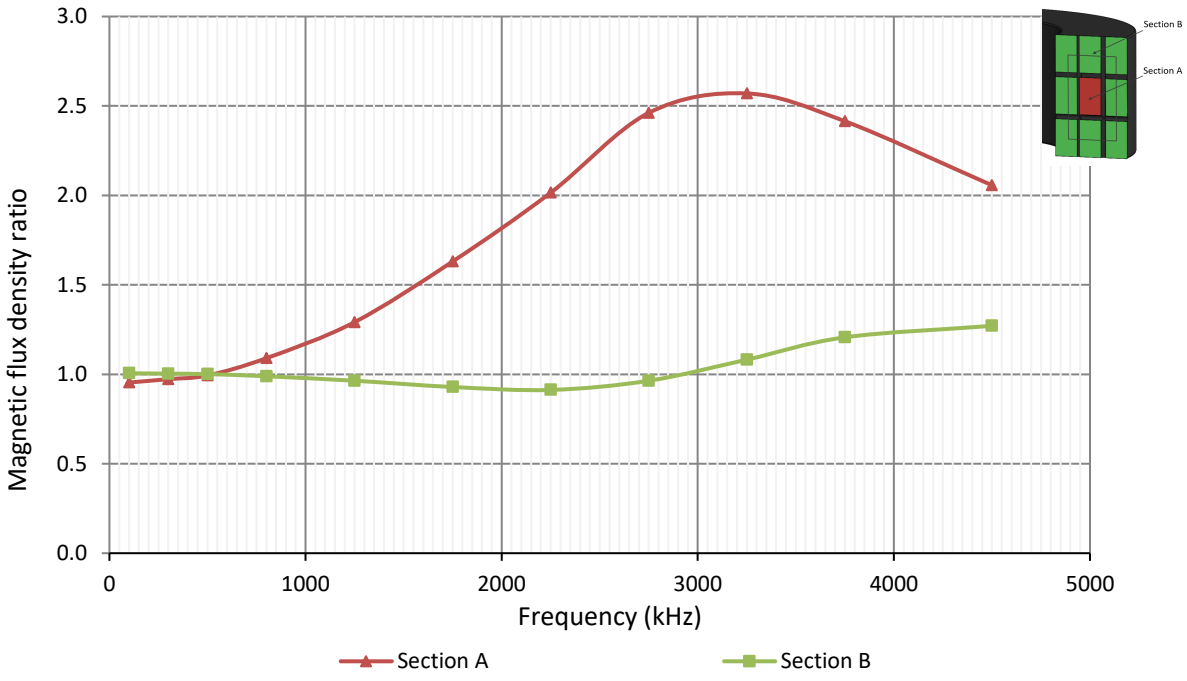

Figure 33. Magnetic flux distribution in the each section of FR79 frame core.

Table 17. MEASURED VOLTAGES FOR FR79 FRAME CORE.

f = 100 kHz Blue – Excitation voltage, Red – Section A, Green – Section B 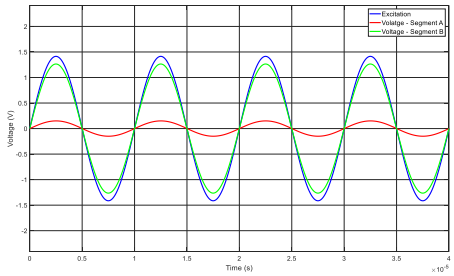	f = 500 kHz Blue – Excitation voltage, Red – Section A, Green – Section B 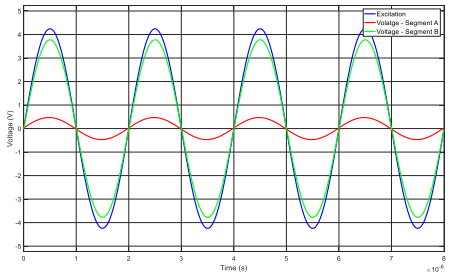
f = 800 kHz Blue – Excitation voltage, Red – Section A, Green – Section B 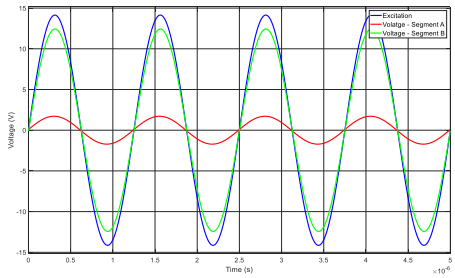	f = 1 250 kHz Blue – Excitation voltage, Red – Section A, Green – Section B 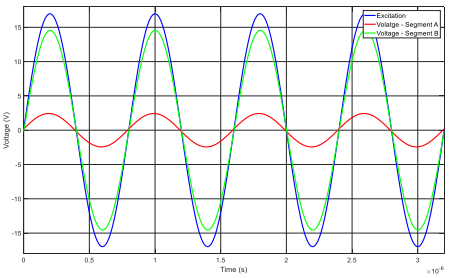
f = 1 750 kHz Blue – Excitation voltage, Red – Section A, Green – Section B 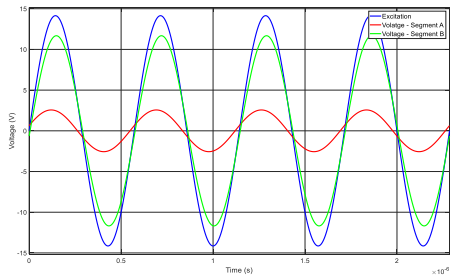	f = 2 250 kHz Blue – Excitation voltage, Red – Section A, Green – Section B 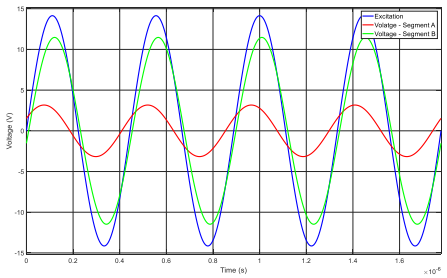

f = 2 750 kHz

Blue – Excitation voltage, Red – Section A, Green – Section B

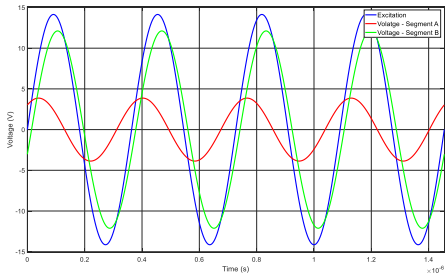

f = 3 250 kHz

Blue – Excitation voltage, Red – Section A, Green – Section B

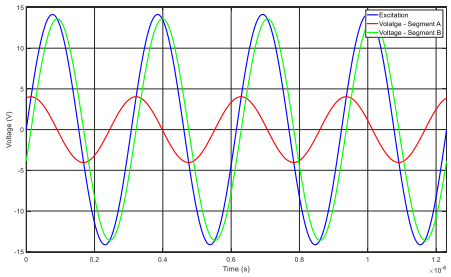

f = 3 750 kHz

Blue – Excitation voltage, Red – Section A, Green – Section B

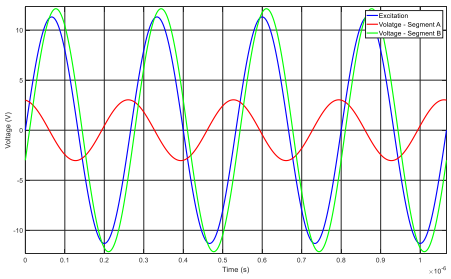

f = 4 500 kHz

Blue – Excitation voltage, Red – Section A, Green – Section B

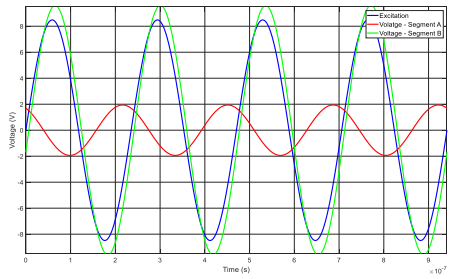

8.1.14. Frame core with FR61 material

Flux distribution in the each segment of Frame core made from FR61 material are shown in Figure 34, while magnetic flux density for Section A and B is shown in Figure 35. Corresponding voltage waveforms for Excitation, Segment A and Segment B at each frequency are presented in Table 18.

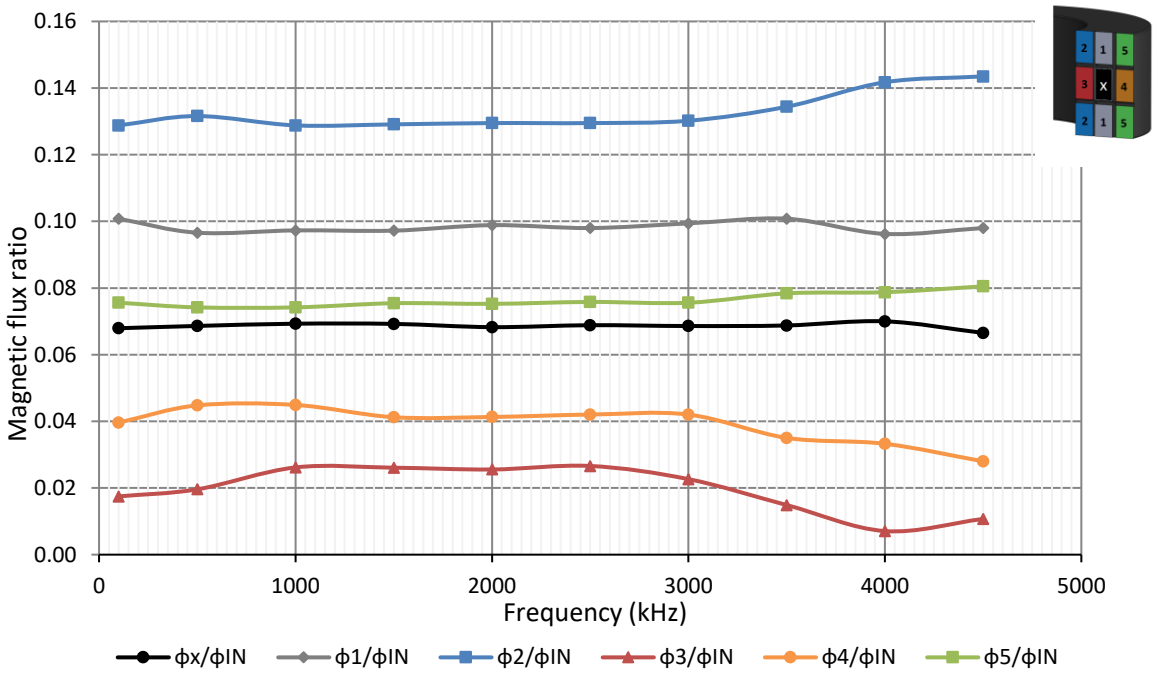

Figure 34. Magnetic flux distribution in the each area of FR61 frame core.

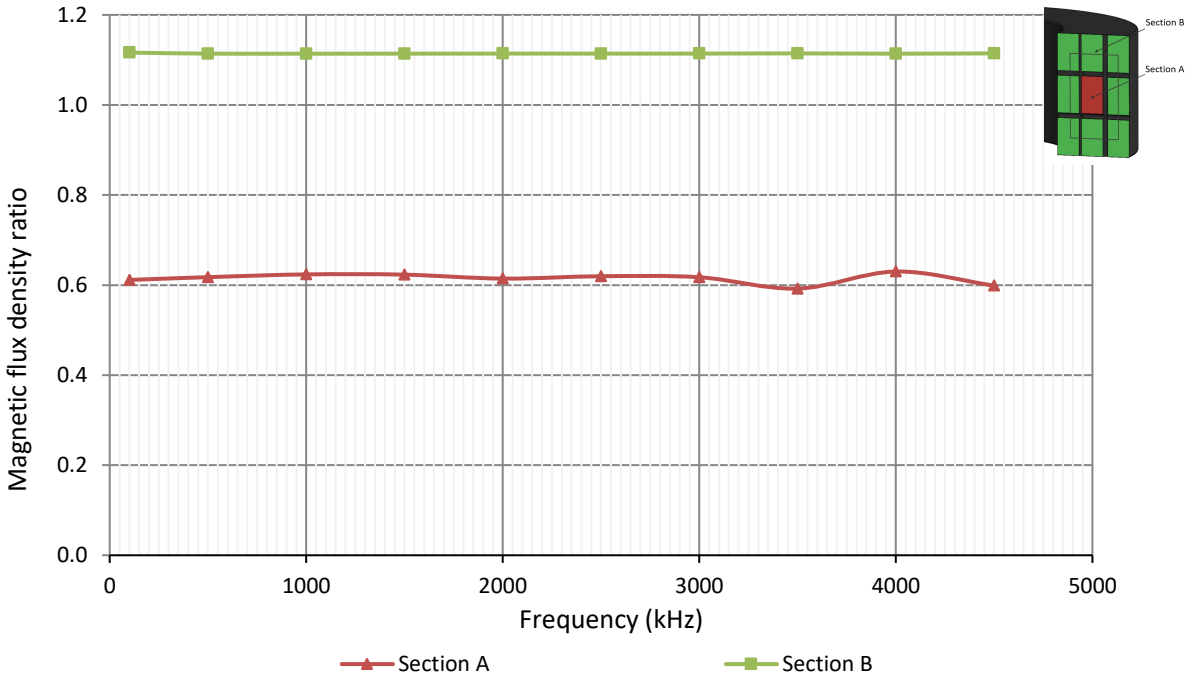

Figure 35. Magnetic flux distribution in the each section of FR61 frame core.

Table 18 . MEASURED VOLTAGES FOR FR61 FRAME CORE.

f = 100 kHz Blue – Excitation voltage, Red – Section A, Green – Section B 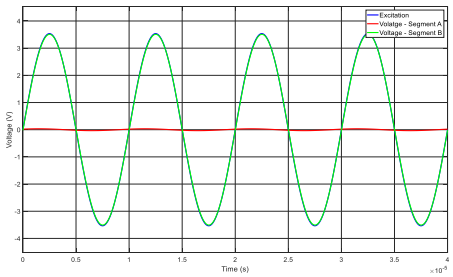	f = 500 kHz Blue – Excitation voltage, Red – Section A, Green – Section B 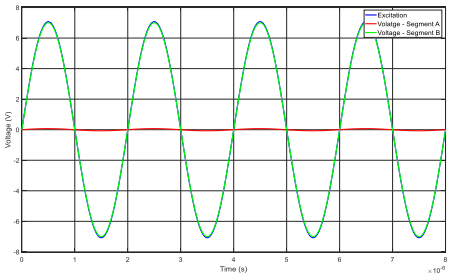
f = 1 000 kHz Blue – Excitation voltage, Red – Section A, Green – Section B 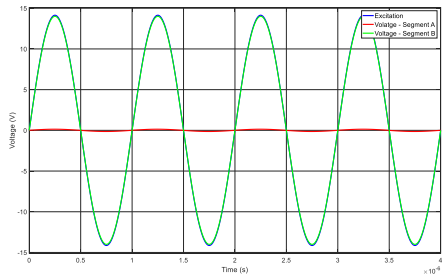	f = 1 500 kHz Blue – Excitation voltage, Red – Section A, Green – Section B 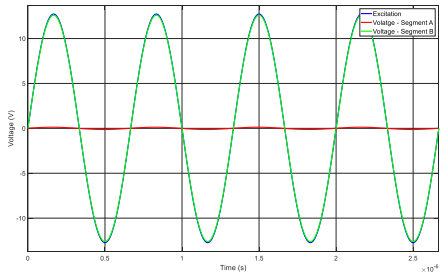
f = 2 000 kHz Blue – Excitation voltage, Red – Section A, Green – Section B 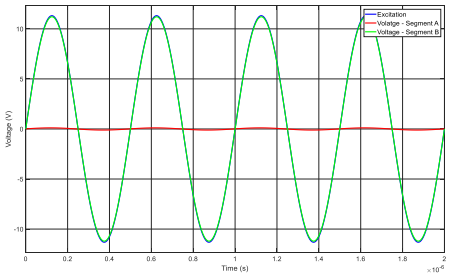	f = 2 500 kHz Blue – Excitation voltage, Red – Section A, Green – Section B 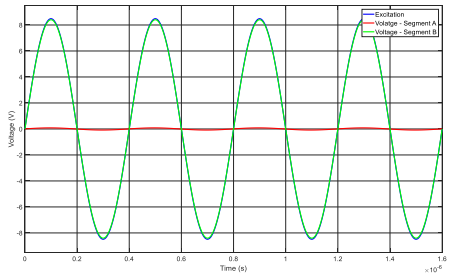

f = 3 000 kHz

Blue – Excitation voltage, Red – Section A, Green – Section B

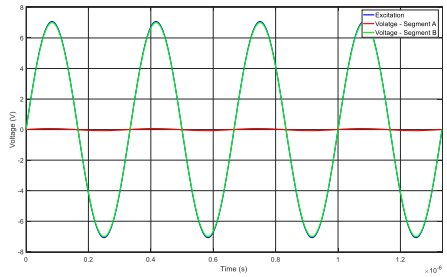

f = 3 500 kHz

Blue – Excitation voltage, Red – Section A, Green – Section B

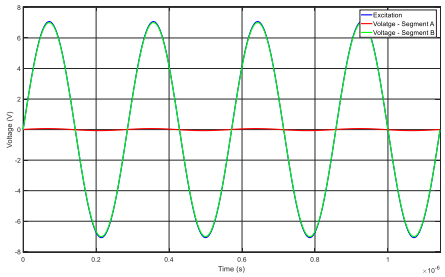

f = 4 000 kHz

Blue – Excitation voltage, Red – Section A, Green – Section B

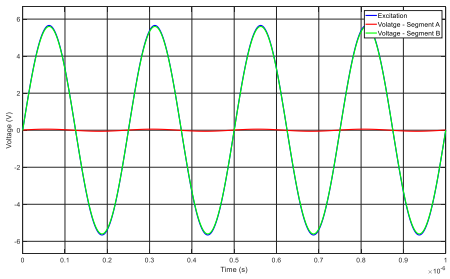

f = 4 500 kHz

Blue – Excitation voltage, Red – Section A, Green – Section B

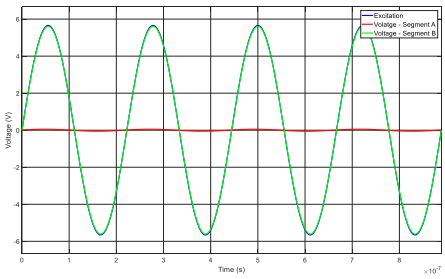

8.1.15. Frame core with FR67 material

Flux distributions in the each segment of Frame core made from FR67 material are shown in Figure 36 , while magnetic flux density for Section A and B is shown in Figure 37. Corresponding voltage waveforms for Excitation, Segment A and Segment B at each frequency are presented in Table 19 .

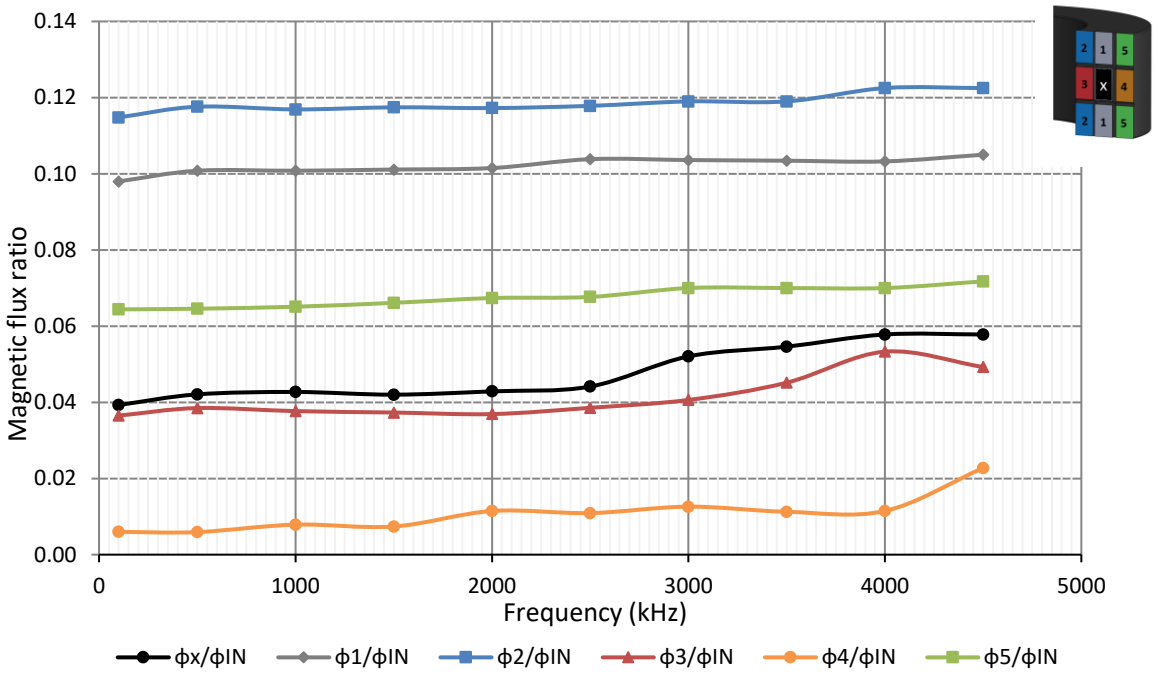

Figure 36. Magnetic flux distribution in the each area of FR67 frame core.

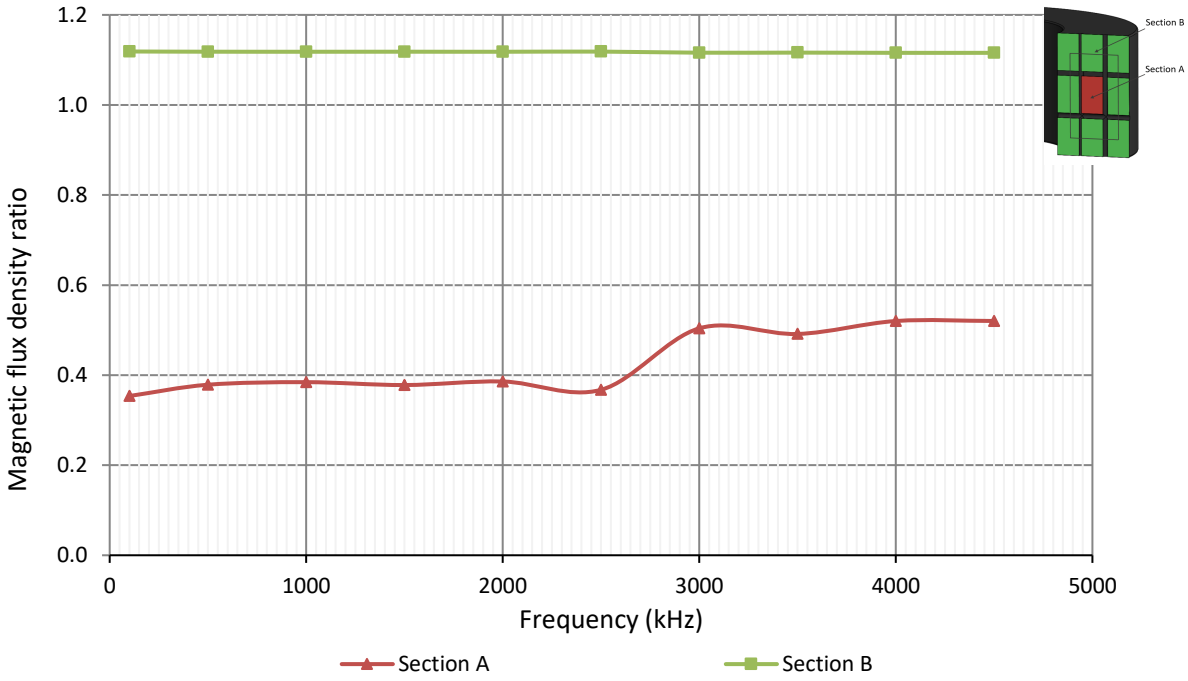

Figure 37. Magnetic flux distribution in the each section of FR67 frame core.

Table 19. MEASURED VOLTAGES FOR FR67 FRAME CORE.

f = 100 kHz Blue – Excitation voltage, Red – Section A, Green – Section B 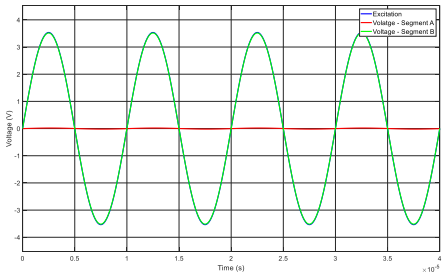	f = 500 kHz Blue – Excitation voltage, Red – Section A, Green – Section B 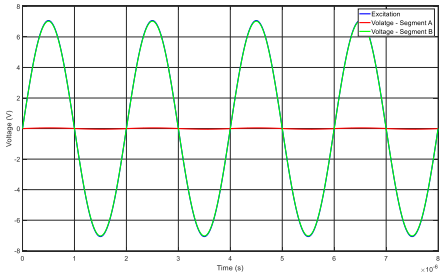
f = 1 000 kHz Blue – Excitation voltage, Red – Section A, Green – Section B 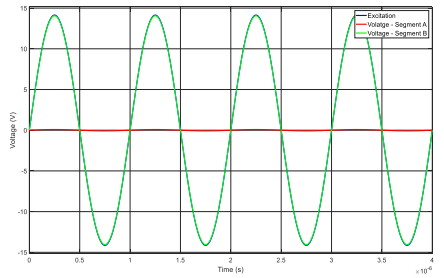	f = 1 500 kHz Blue – Excitation voltage, Red – Section A, Green – Section B 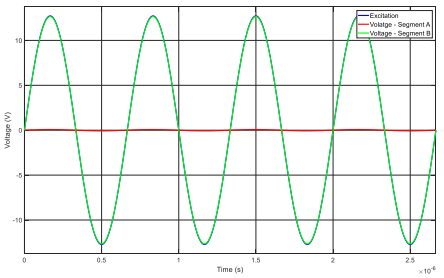
f = 2 000 kHz Blue – Excitation voltage, Red – Section A, Green – Section B 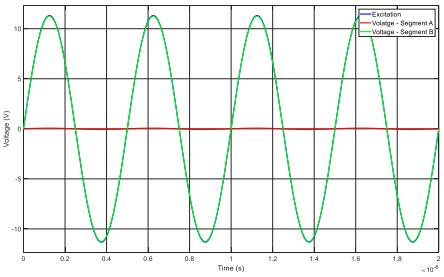	f = 2 500 kHz Blue – Excitation voltage, Red – Section A, Green – Section B 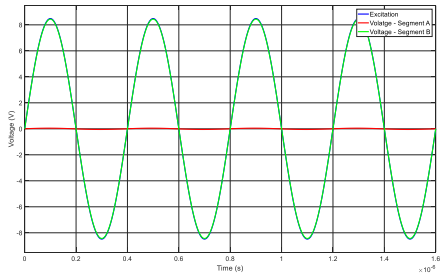

f = 3 000 kHz

Blue – Excitation voltage, Red – Section A, Green – Section B

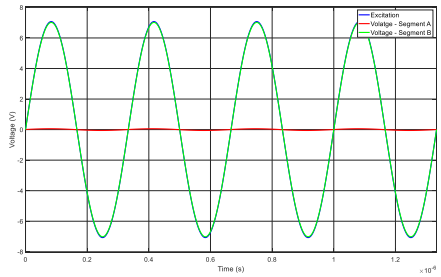

f = 3 500 kHz

Blue – Excitation voltage, Red – Section A, Green – Section B

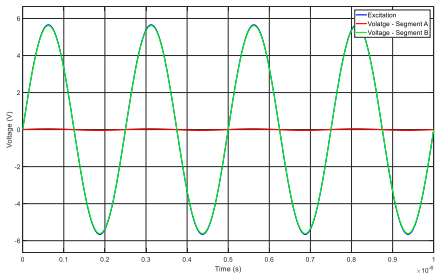

f = 4 000 kHz

Blue – Excitation voltage, Red – Section A, Green – Section B

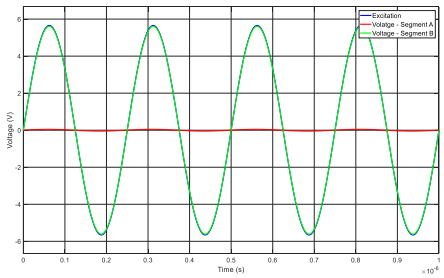

f = 4 500 kHz

Blue – Excitation voltage, Red – Section A, Green – Section B

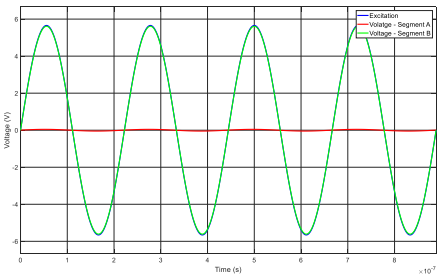

8.2. Experiment II – Impedance test

Measured impedance and phase shift of each inner ferrite segment has been used to calculate normalized impedance and phase shift for section A and B, respectively for each tested core. Results are shown in Figure 38 - Figure 67.

8.2.1. TX50 core with 3E10 material

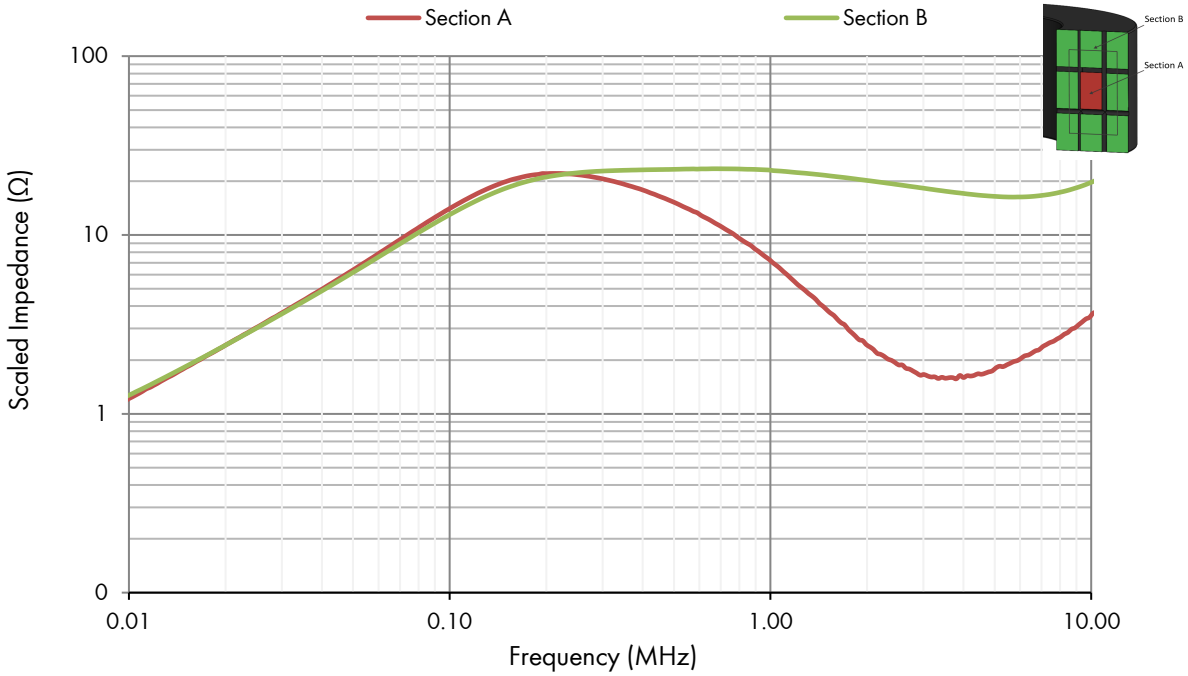

Figure 38. Section A and B scaled impedance vs. frequency for TX50 3E10 ring core.

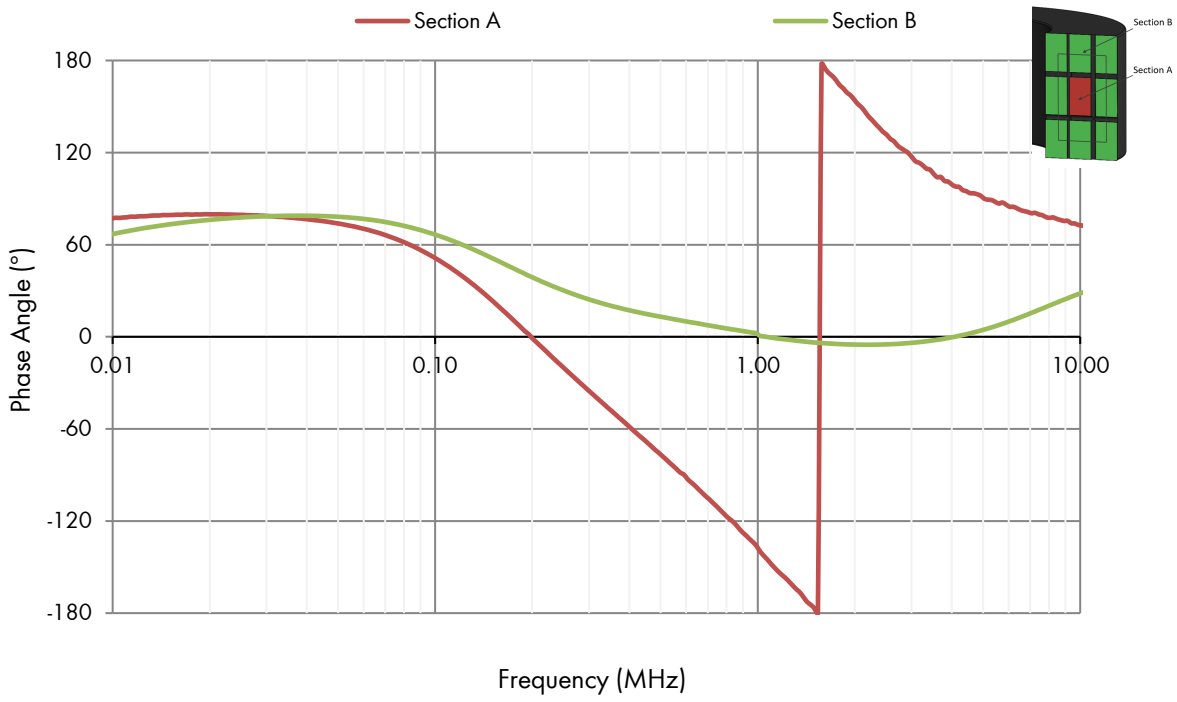

Figure 39. Section A and B phase vs. frequency for TX50 3E10 ring core.

8.2.2. TX50 core with 3E15 material

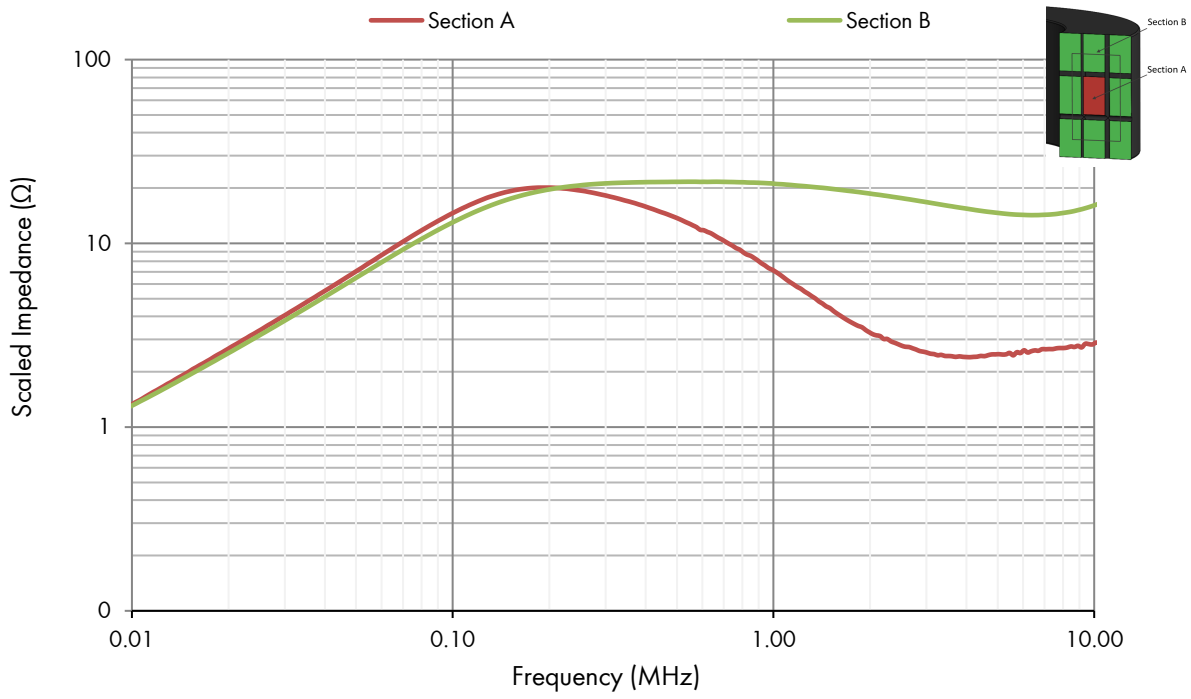

Figure 40. Section A and B scaled impedance vs. frequency for TX50 3E15 ring core.

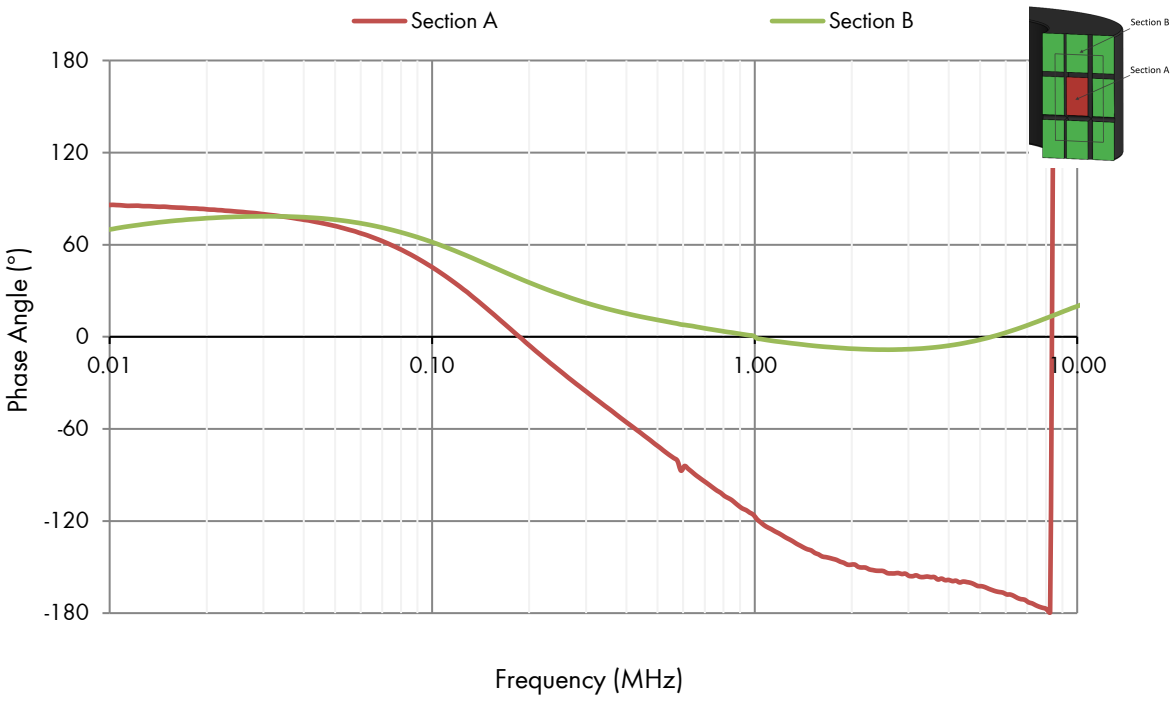

Figure 41. Section A and B phase vs. frequency for TX50 3E15 ring core.

8.2.3. TX50 core with 3E6 material

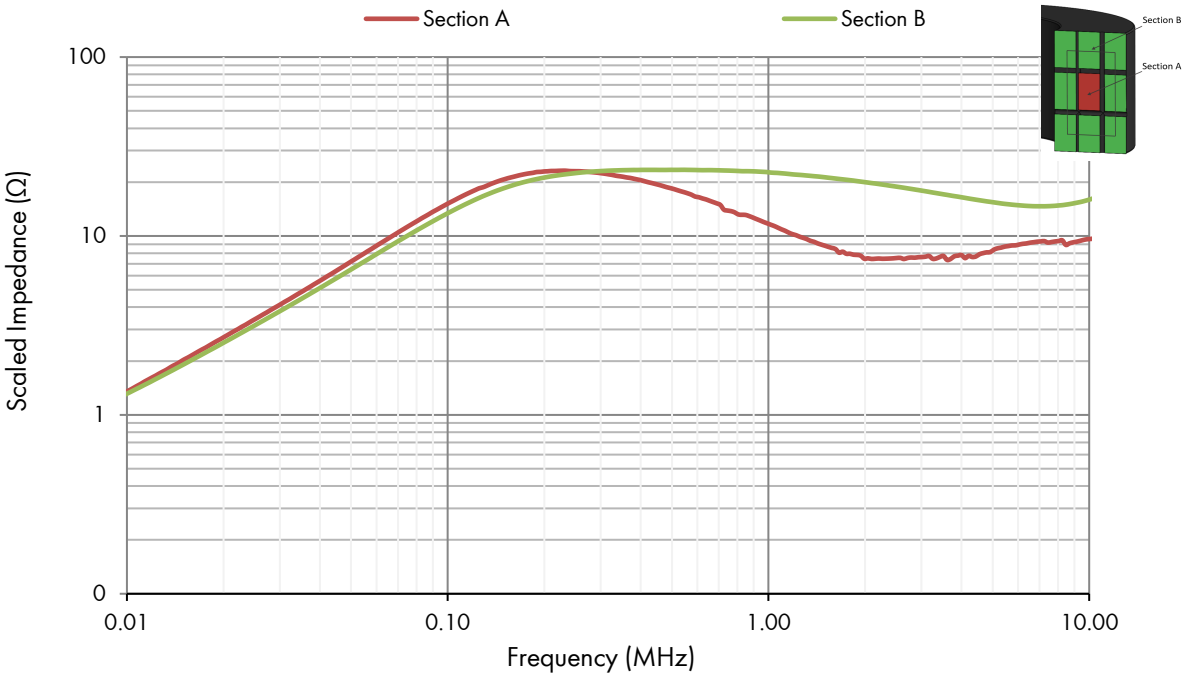

Figure 42. Section A and B scaled impedance vs. frequency for TX50 3E6 ring core.

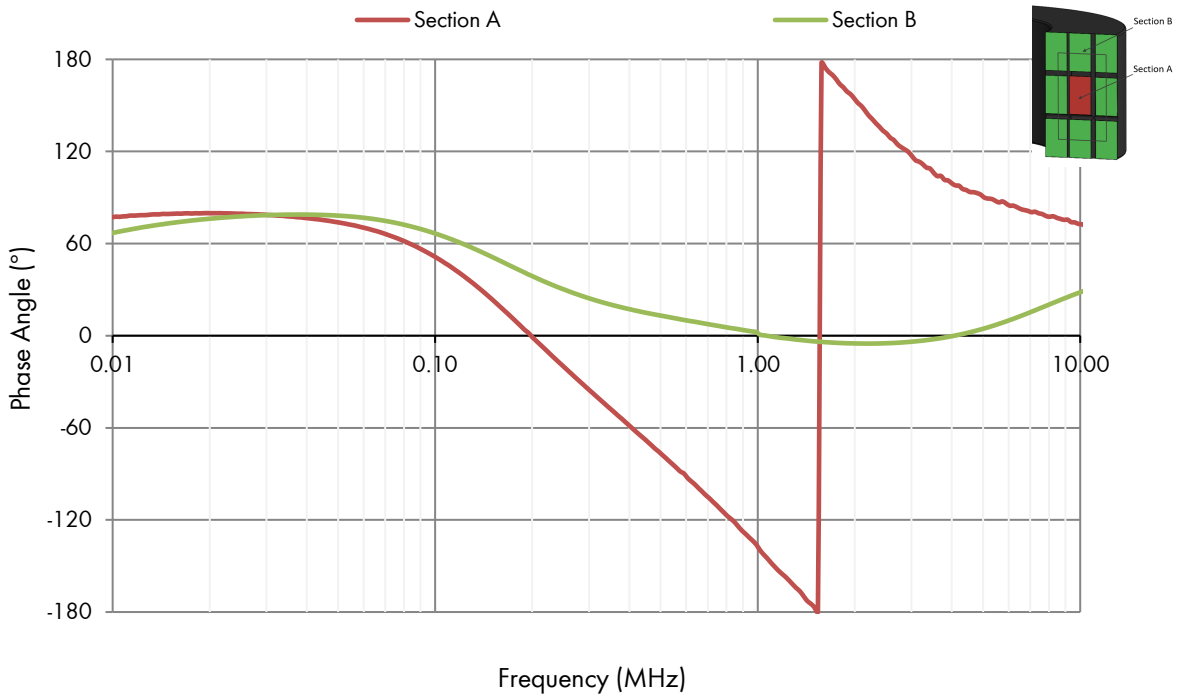

Figure 43. Section A and B phase vs. frequency for TX50 3E6 ring core.

8.2.4. TX50 core with 3E27 material

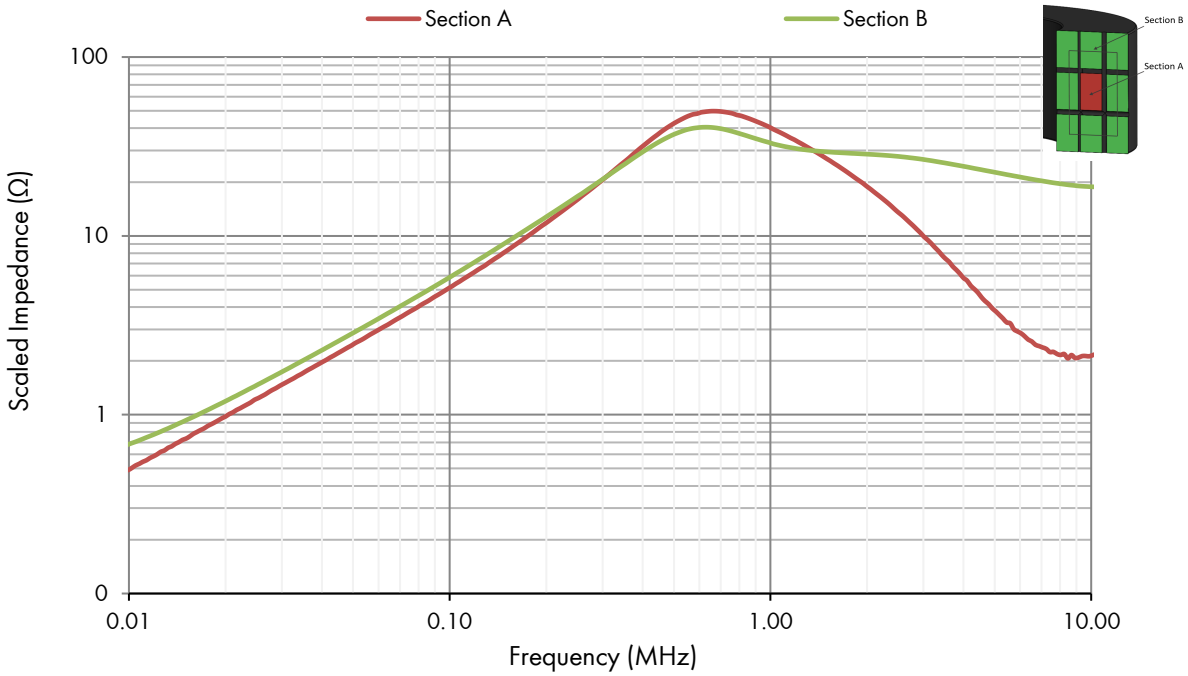

Figure 44. Section A and B scaled impedance vs. frequency for TX50 3E27 ring core.

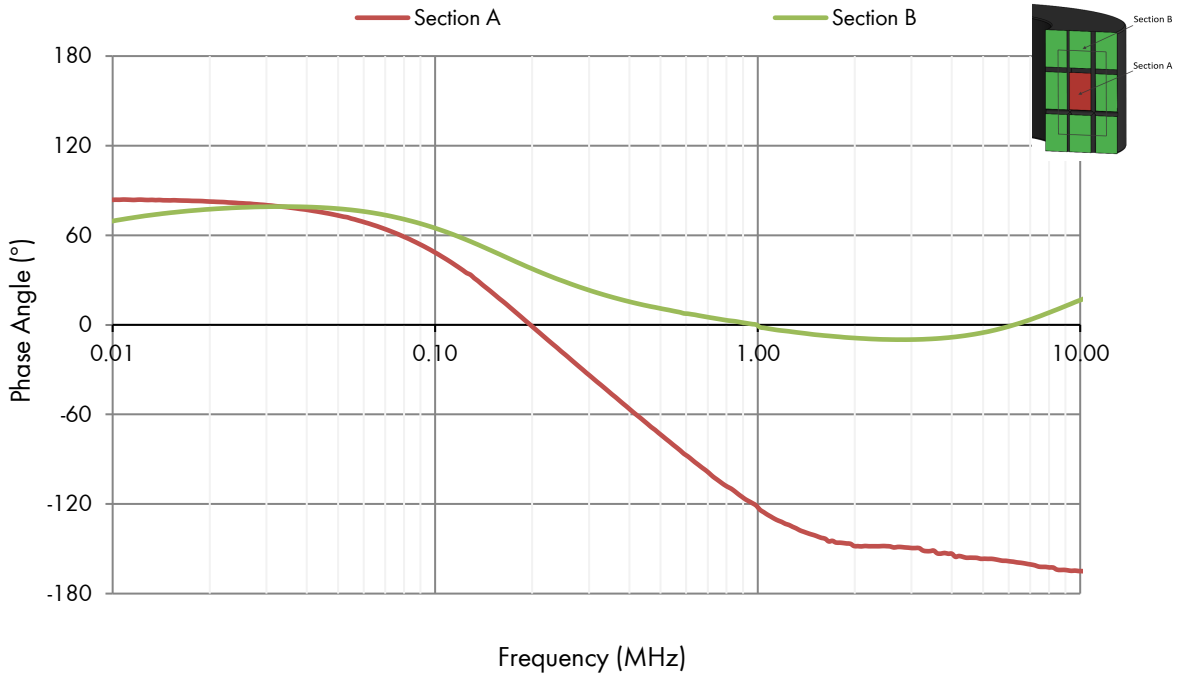

Figure 45. Section A and B phase vs. frequency for TX50 3E27 ring core.

8.2.5. TX50 core with 3C11 material

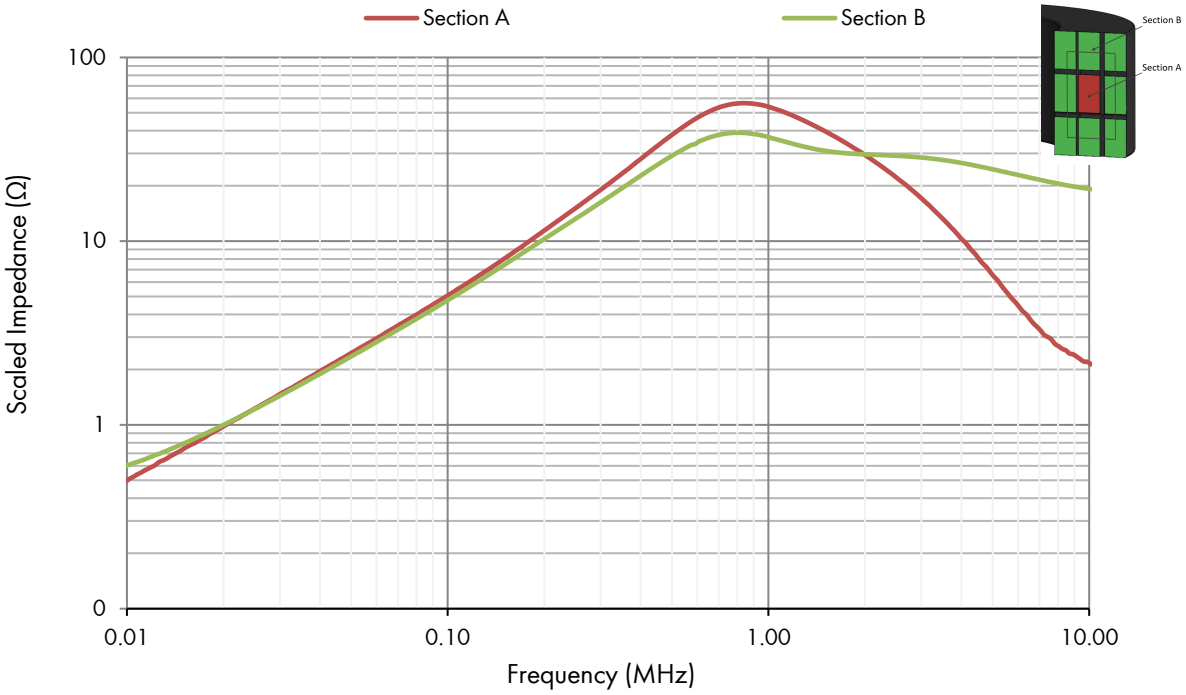

Figure 46. Section A and B scaled impedance vs. frequency for TX50 3C11 ring core.

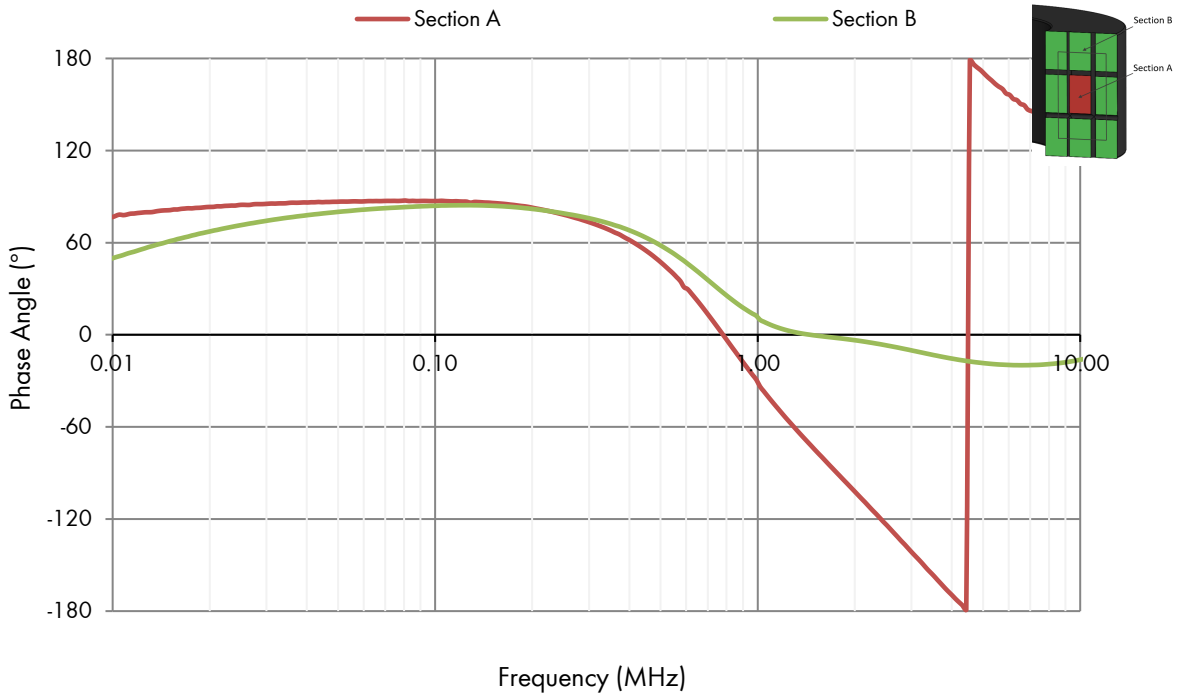

Figure 47. Section A and B phase vs. frequency for TX50 3C11 ring core.

8.2.6. TX50 core with 4S60 material

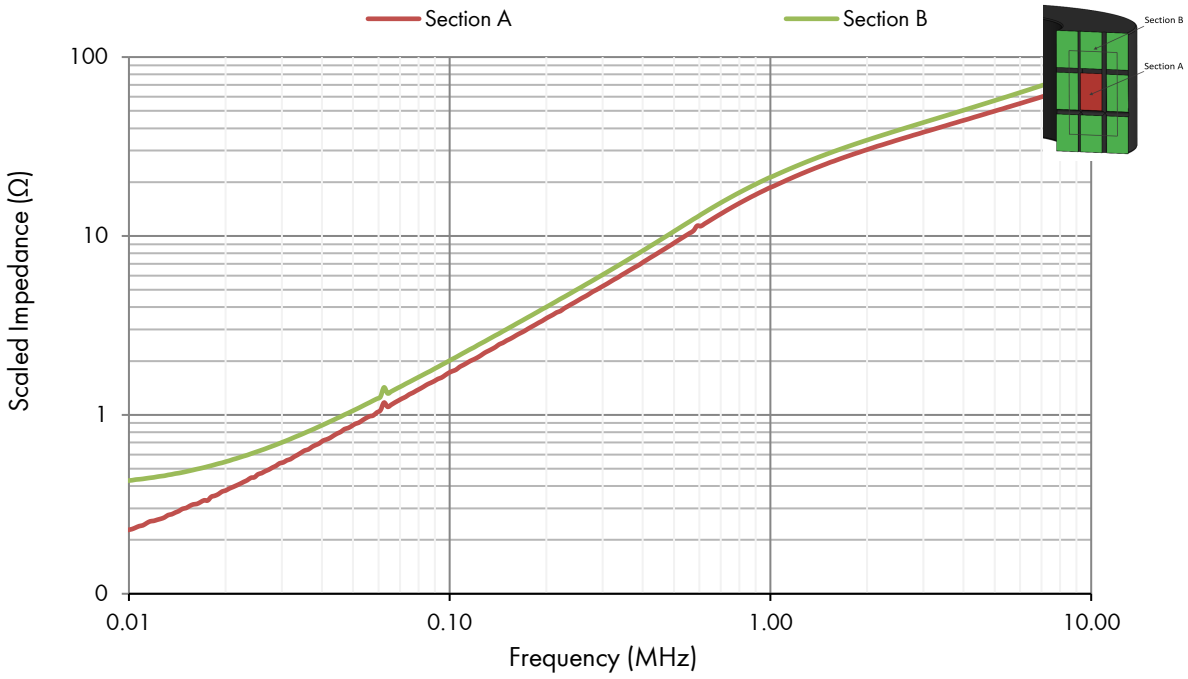

Figure 48. Section A and B scaled impedance vs. frequency for TX50 4S60 ring core.

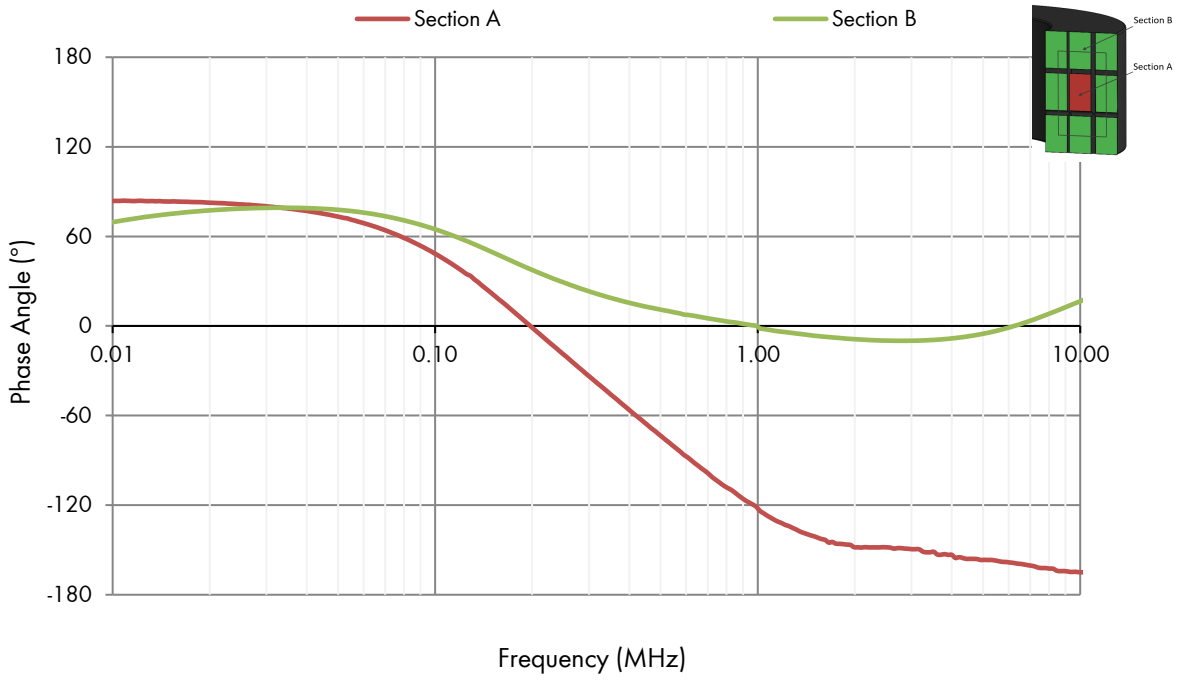

Figure 49. Section A and B phase vs. frequency for TX50 4S60 ring core.

8.2.7. TX50 core with 4A11 material

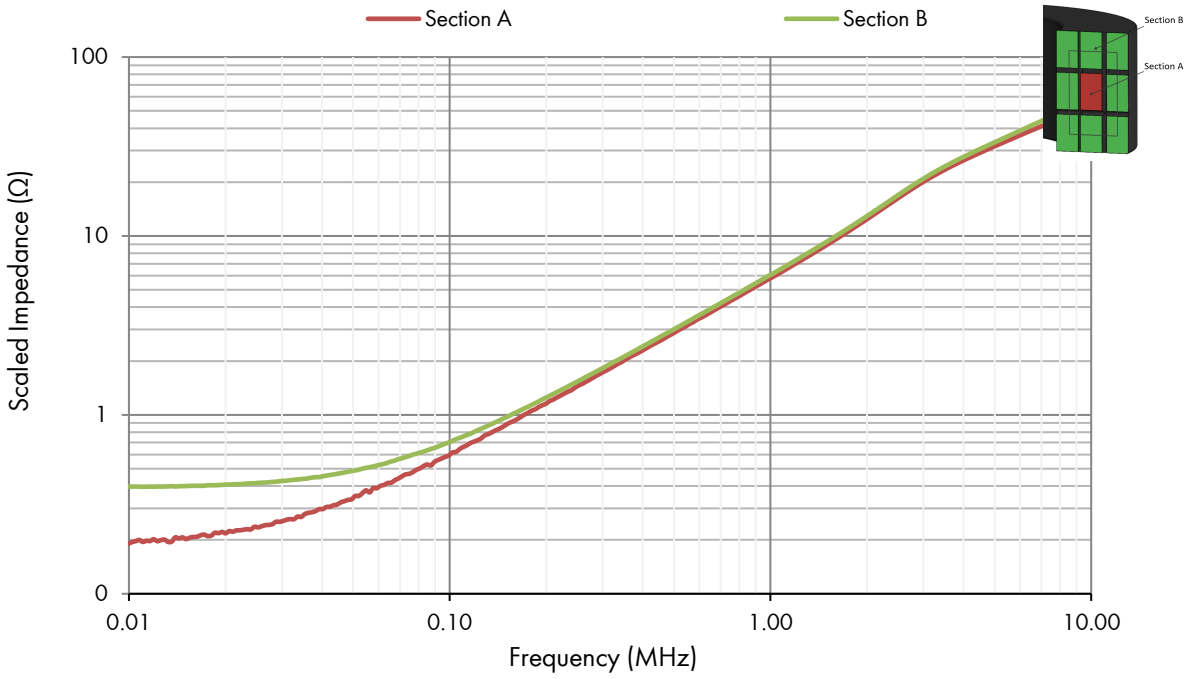

Figure 50. Section A and B scaled impedance vs. frequency for TX50 4A11 ring core.

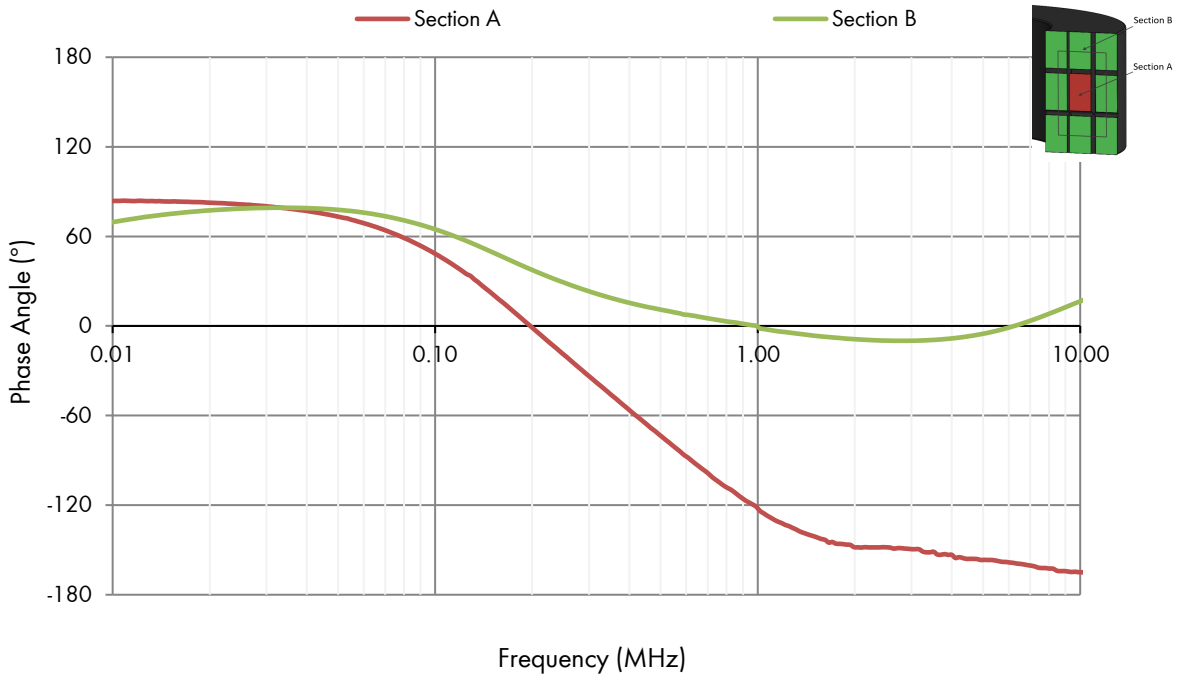

Figure 51. Section A and B phase vs. frequency for TX50 4A11 ring core.

8.2.8. TX105 core with FR78 material

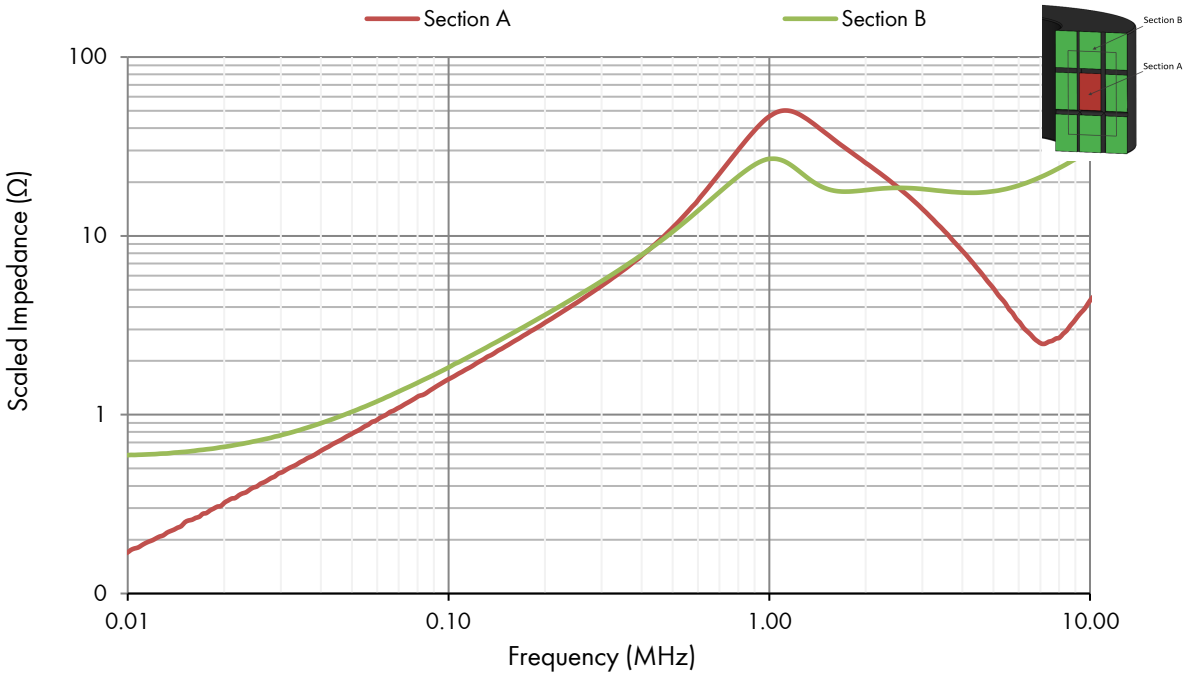

Figure 52. Section A and B scaled impedance vs. frequency for TX105 FR78 ring core.

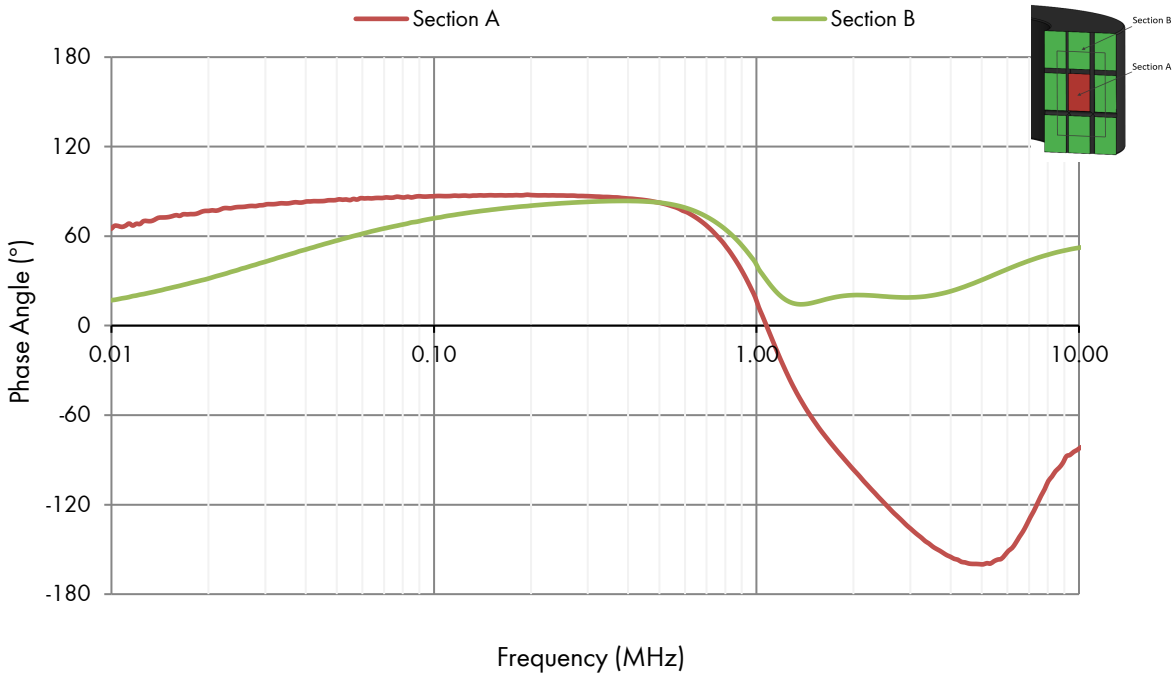

Figure 53. Section A and B phase vs. frequency for TX105 FR78 ring core.

8.2.9. TX105 core with FR79 material

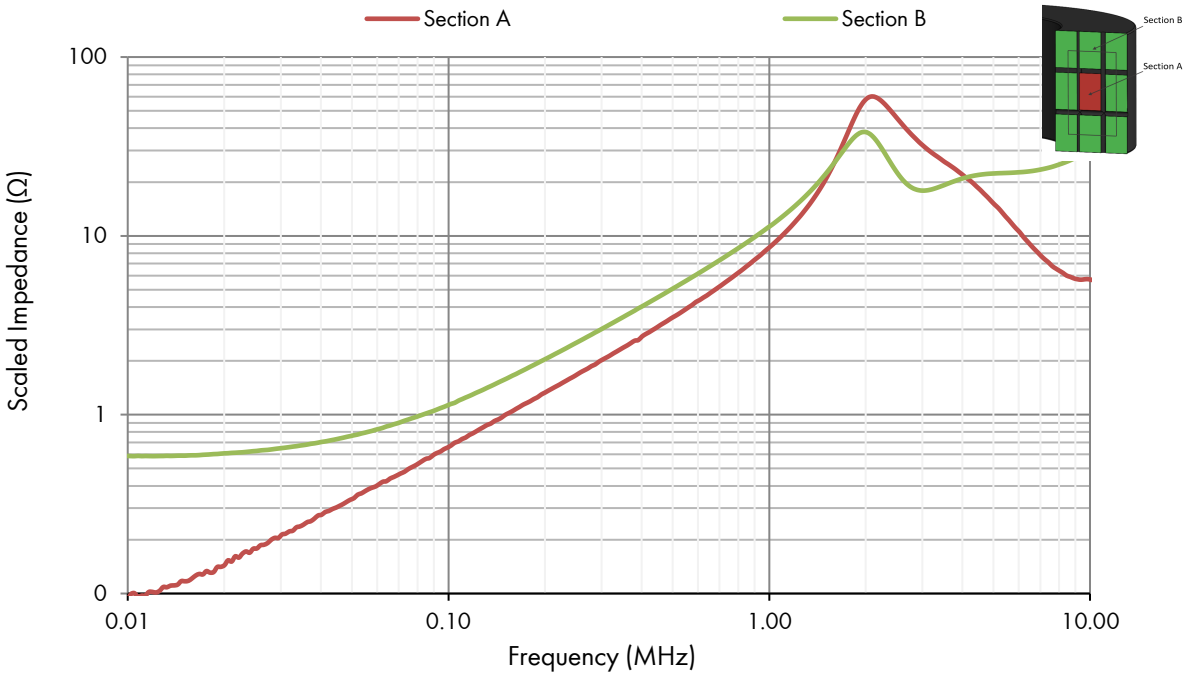

Figure 54. Section A and B scaled impedance vs. frequency for TX105 FR79 ring core.

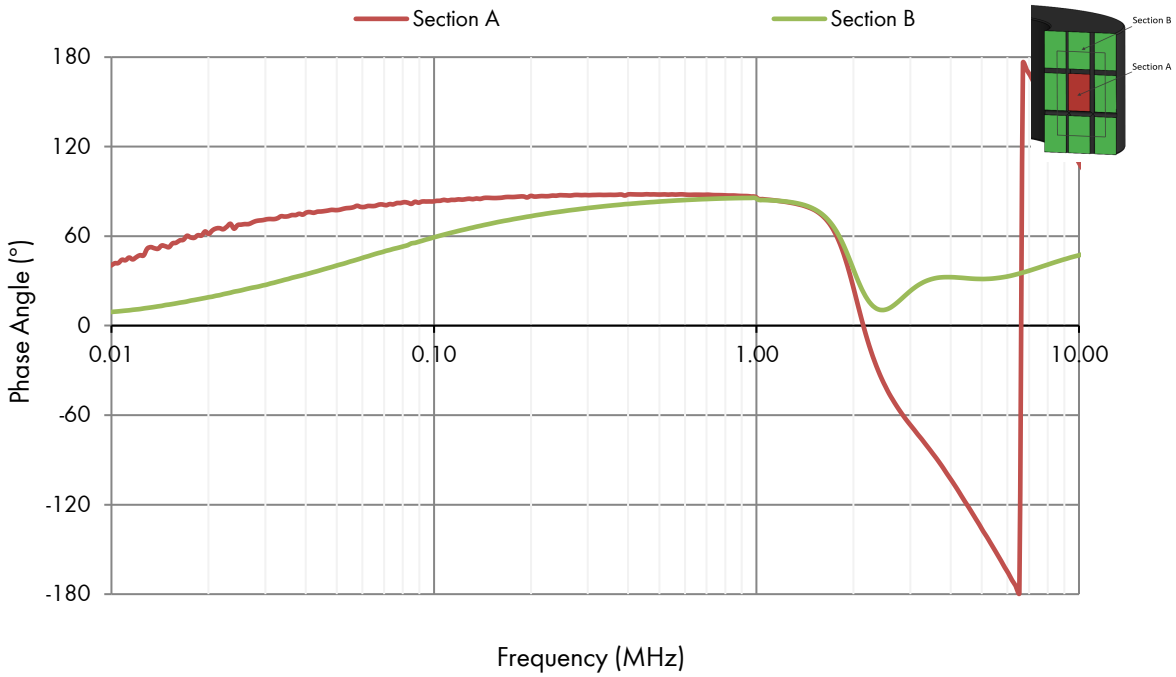

Figure 55. Section A and B phase vs. frequency for TX105 FR79 ring core.

8.2.10. TX105 core with FR61 material

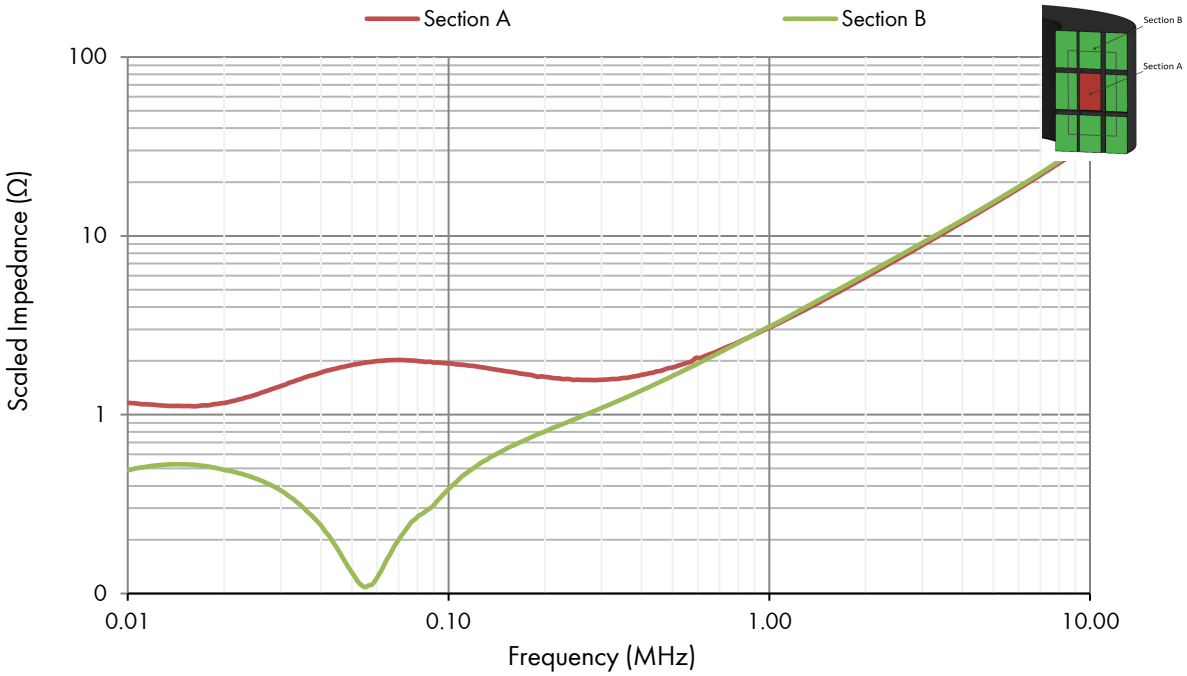

Figure 56. Section A and B scaled impedance vs. frequency for TX150 FR61 ring core.

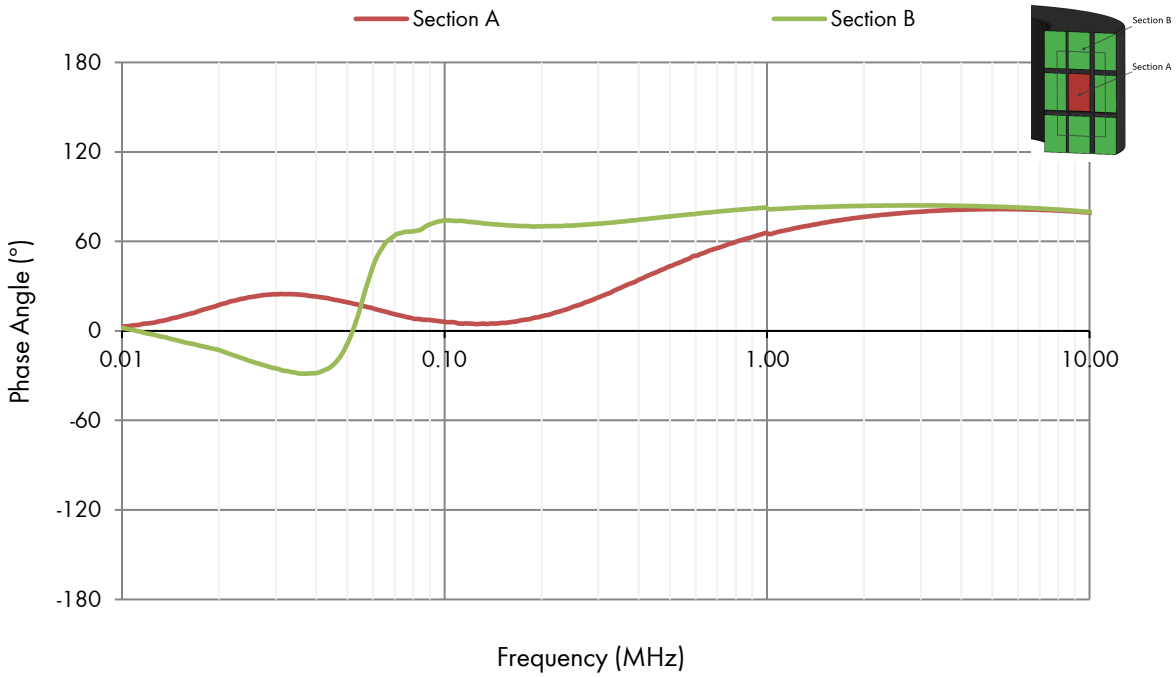

Figure 57. Section A and B phase vs. frequency for TX105 FR61 ring core.

8.2.11. TX105 core with FR67 material

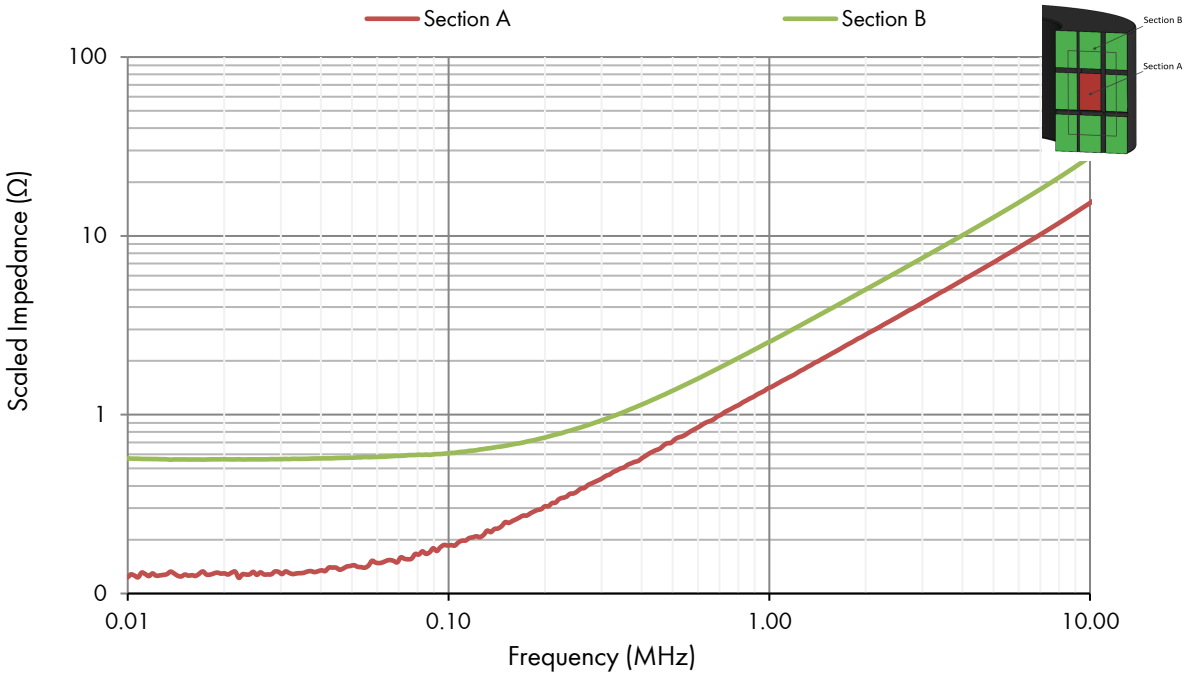

Figure 58. Section A and B scaled impedance vs. frequency for TX105 FR67 ring core.

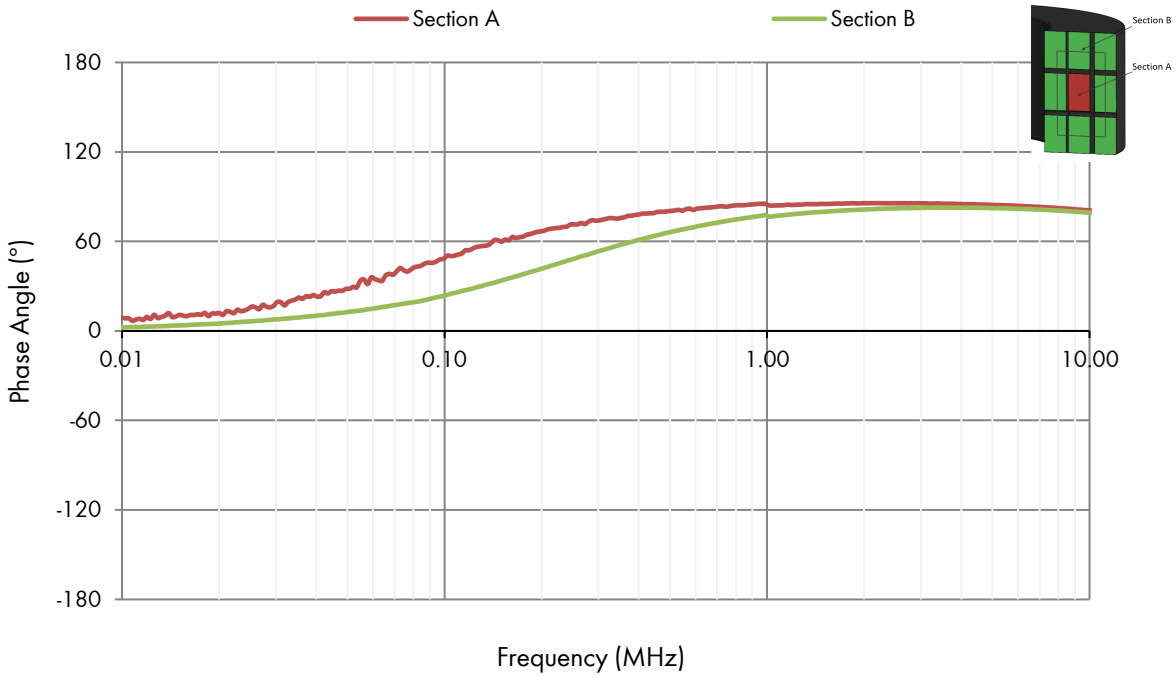

Figure 59. Section A and B phase vs. frequency for TX105 FR67 ring core.

8.2.12. Frame core with FR78 material

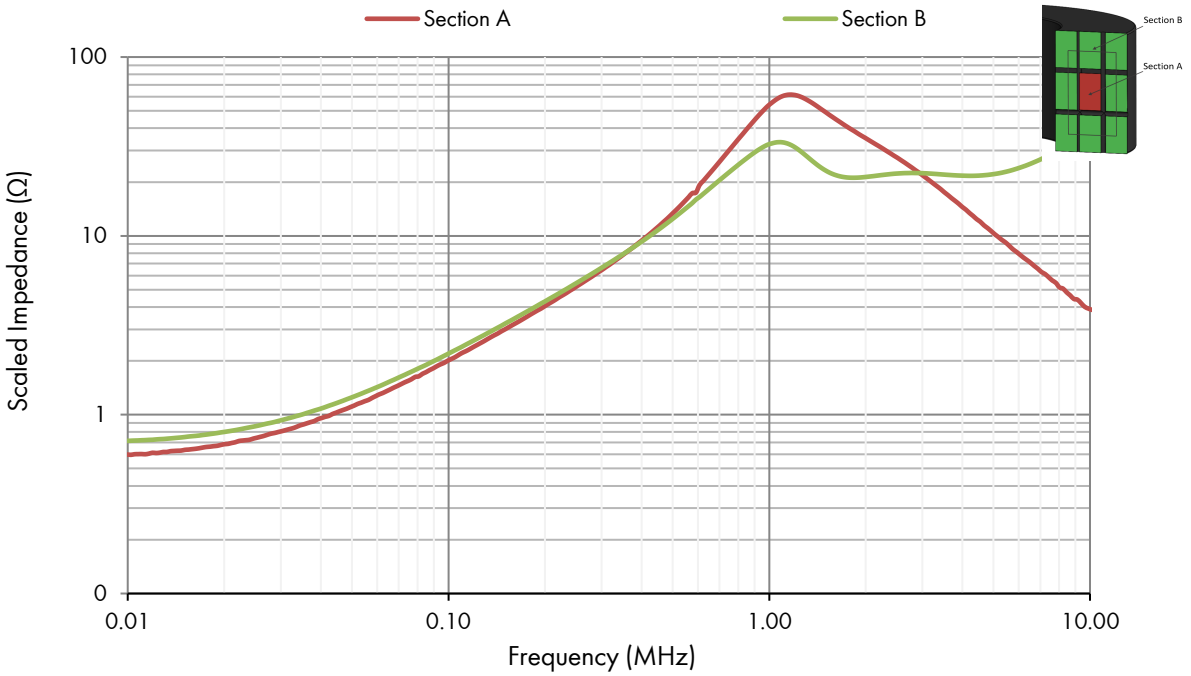

Figure 60. Section A and B scaled impedance vs. frequency for FR78 frame core.

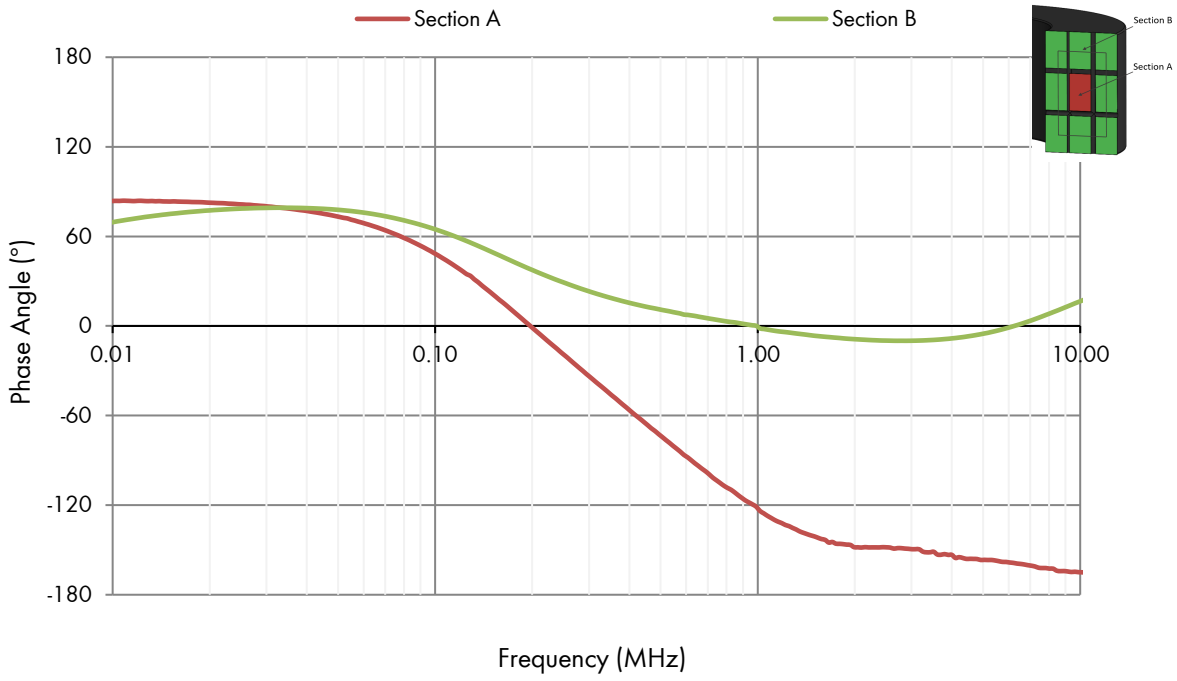

Figure 61. Section A and B phase vs. frequency for FR78 frame core.

8.2.13. Frame core with FR77 material

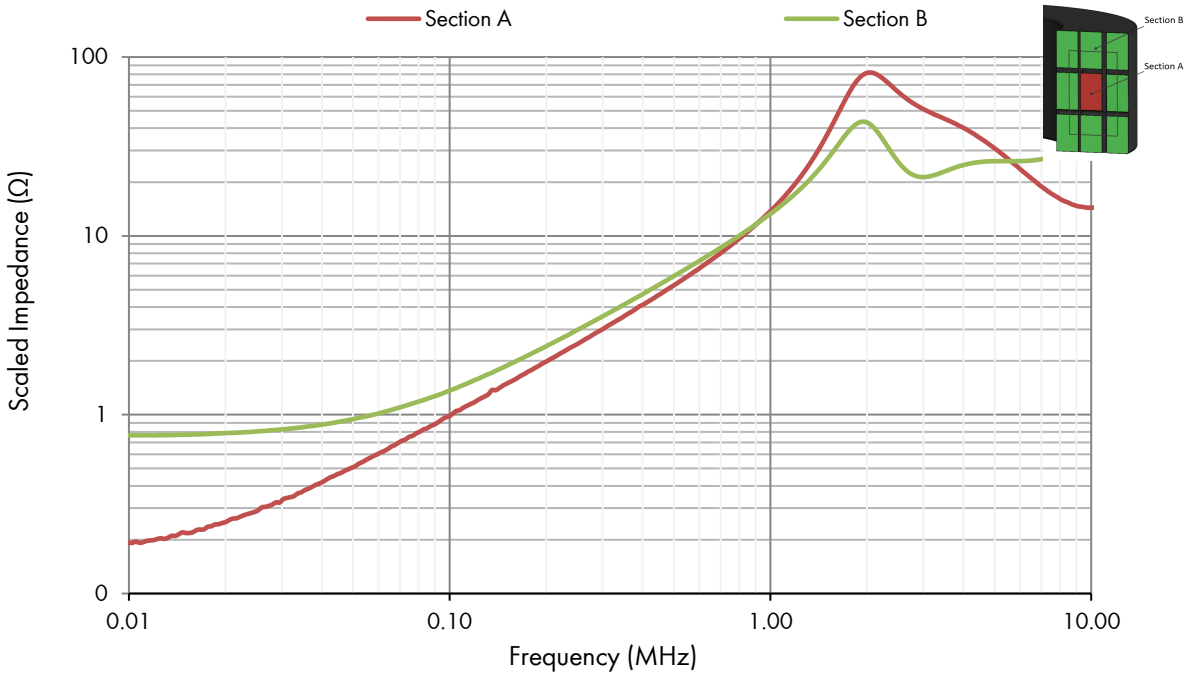

Figure 62. Section A and B scaled impedance vs. frequency for FR79 frame core.

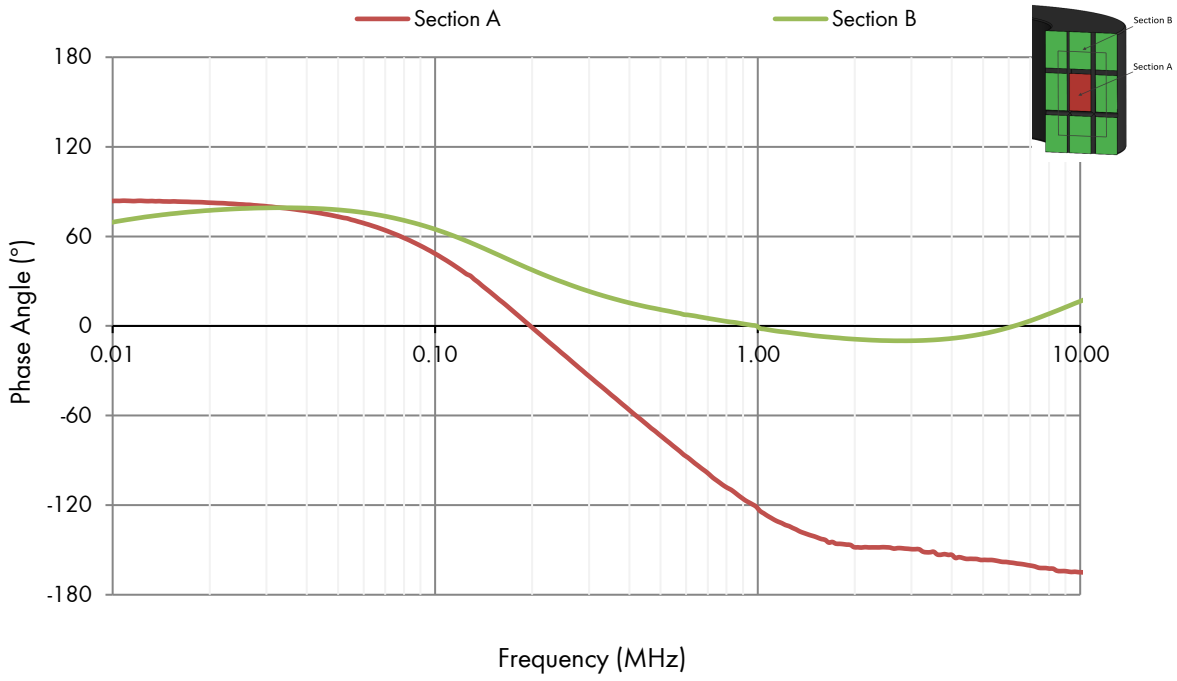

Figure 63. Section A and B phase vs. frequency for FR79 frame core.

8.2.14. Frame core with FR61 material

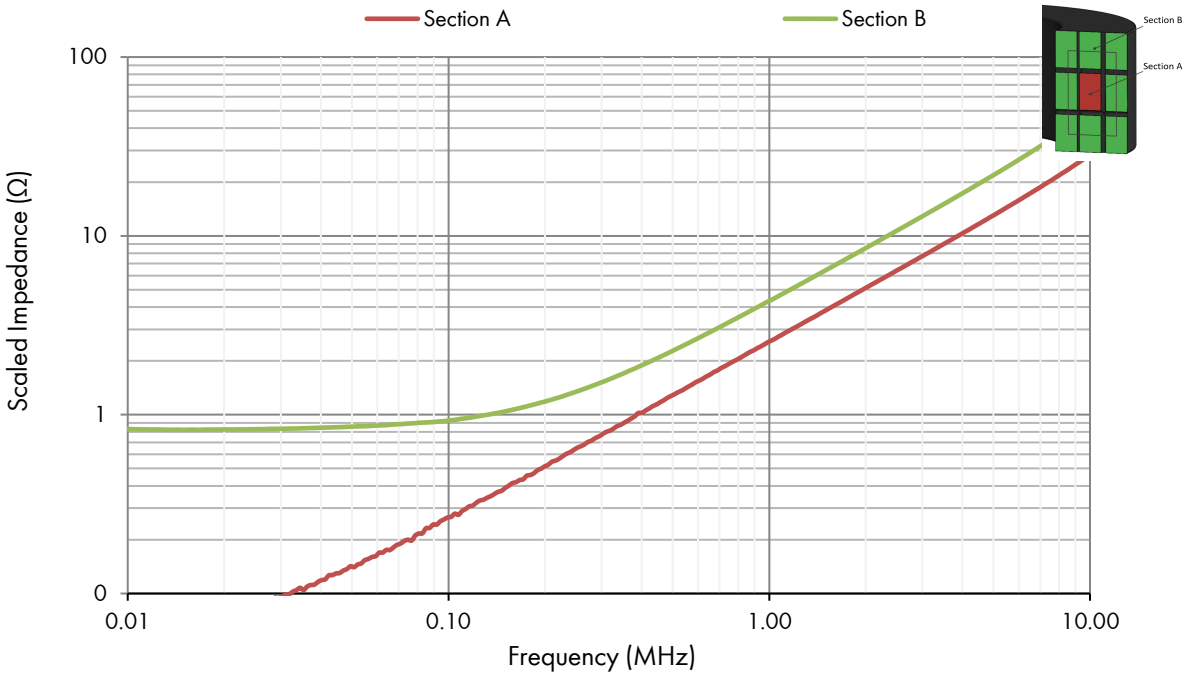

Figure 64. Section A and B scaled impedance vs. frequency for FR61 frame core.

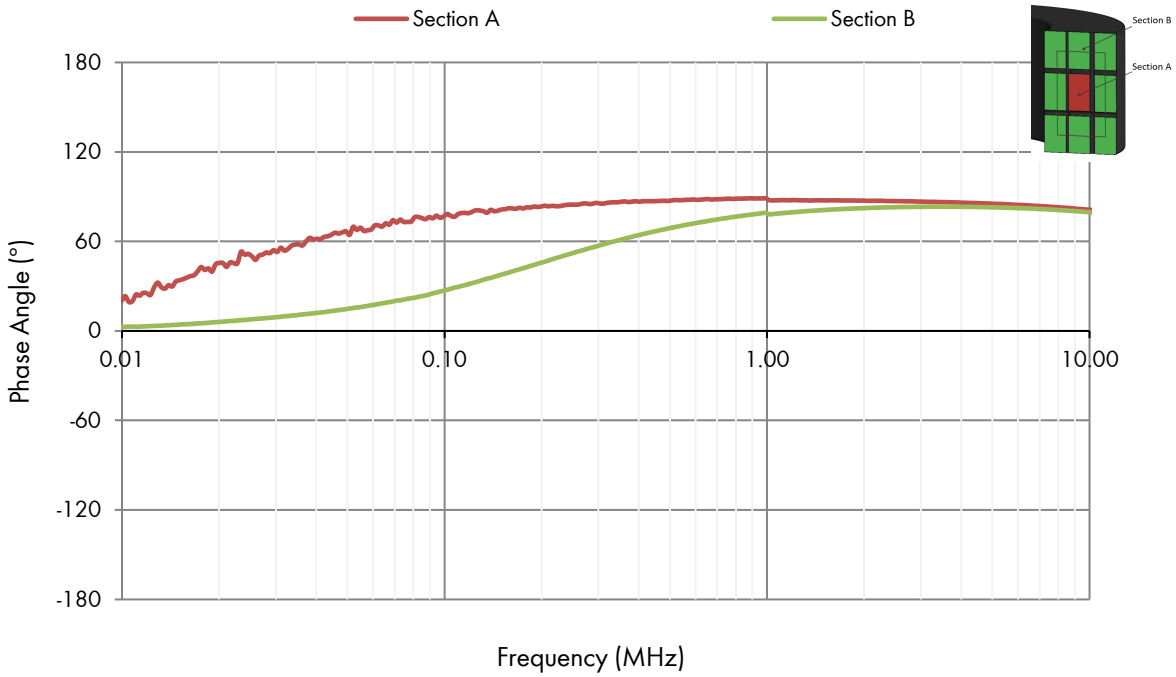

Figure 65. Section A and B phase vs. frequency for FR61 frame core.

8.2.15. TX105 core with FR67 material

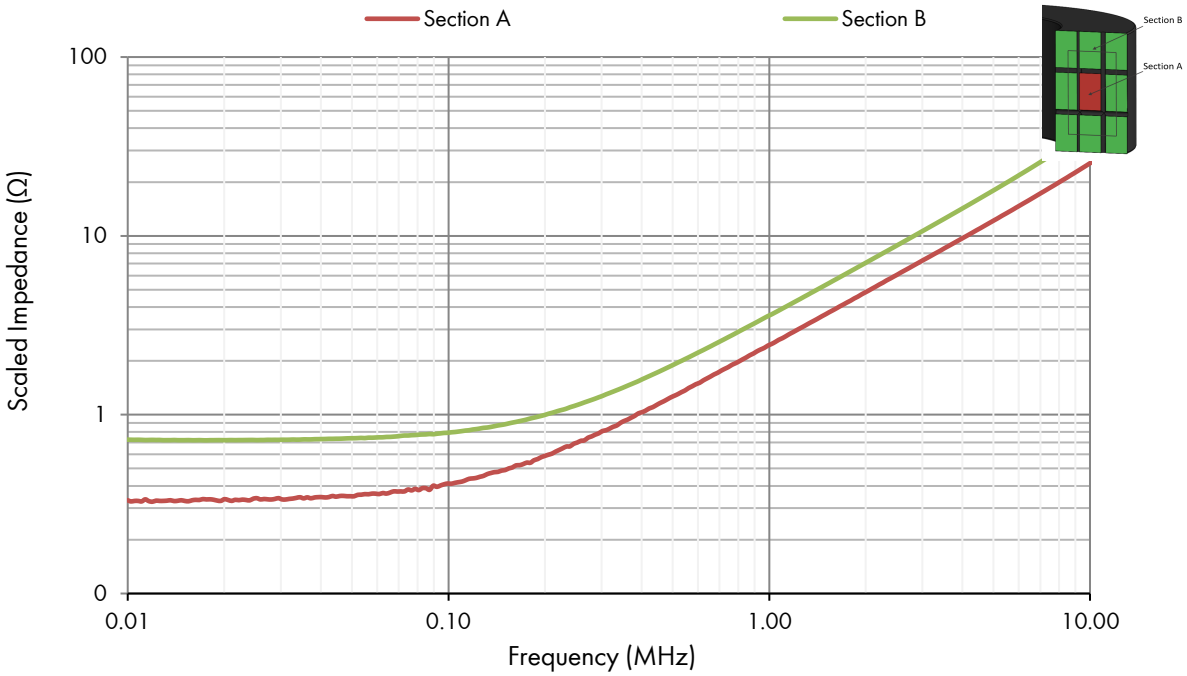

Figure 66. Section A and B scaled impedance vs. frequency for FR67 frame core.

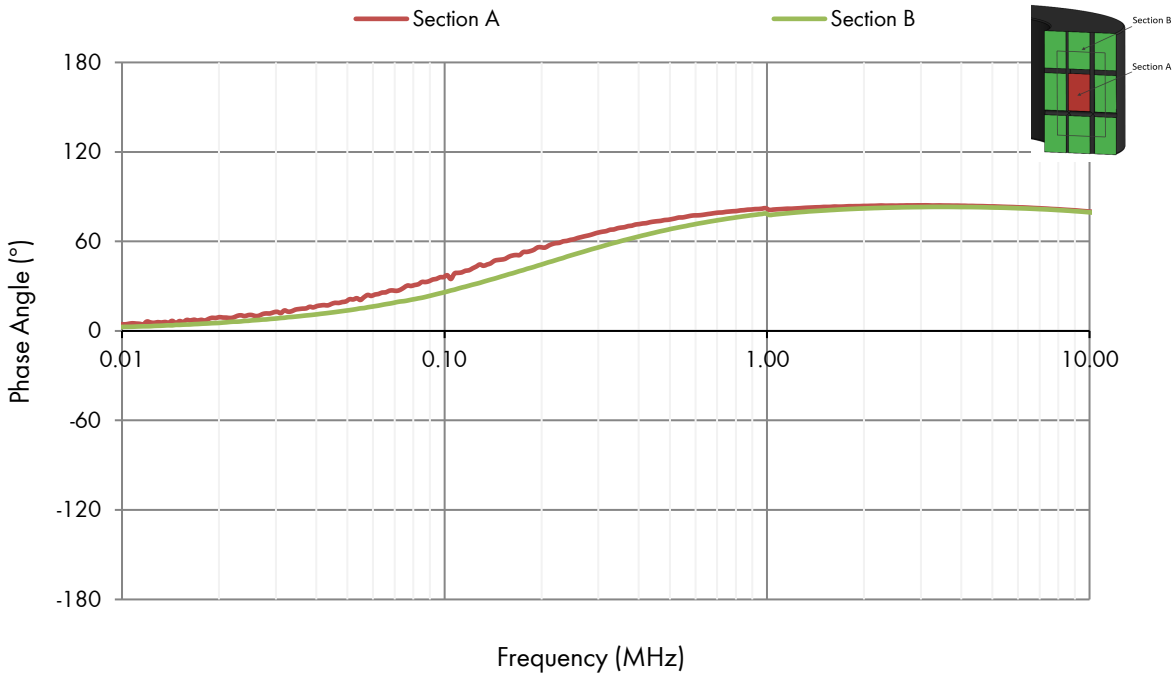

Figure 67. Section A and B phase vs. frequency for FR67 frame core.

9. Summary

9.1. TX50 Cores

Flux distribution in the inner segment of TX50 core made of MnZn ferrites are shown in Figure 68 while NiZn based materials are shown in Figure 69. Magnetic flux distribution depends on magnetic properties of the material. For high permeability MnZn materials the flux decreases as frequency increases. The magnetic flux reduction is seen from: 200 kHz for 3E6, 3E15 and 300 kHz for 3E10 material. In the low permeability MnZn materials flux increases with frequency at the first stage up to 1200 kHz and then starts decreasing. NiZn based materials show superior performance over the MnZn and thus, the frequency effects are not recorded in considered frequency range up to 4.5 MHz.

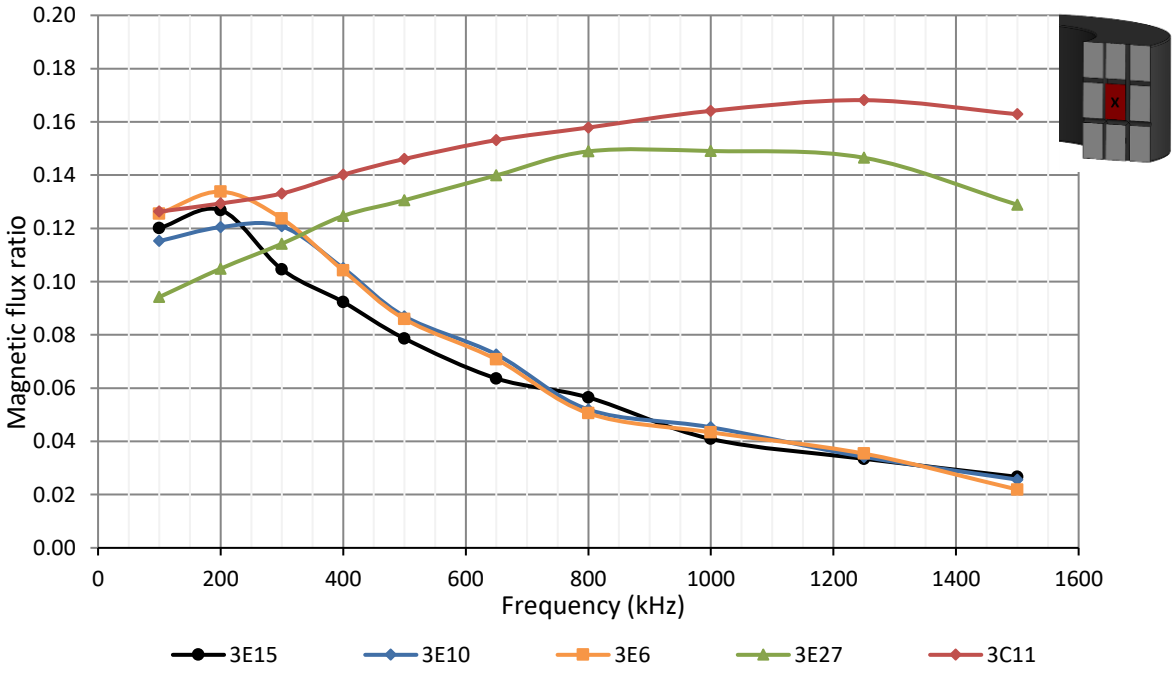

Figure 68. TX50 ring cores flux distribution in the inner segment for MnZn ferrite materials.

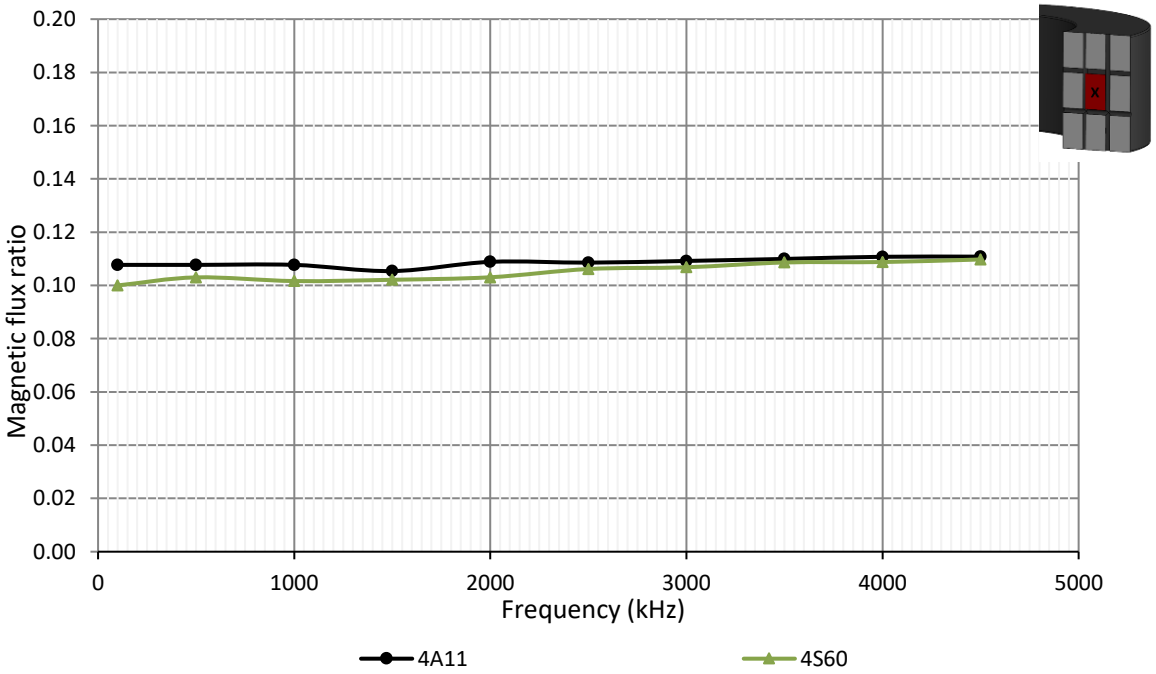

Figure 69. TX50 ring cores flux distribution in the inner segment for NiZn ferrite materials.

9.2. TX105 and Frame Core

Flux distribution in the inner segment of TX105 ring cores and frame core made of the MnZn and NiZn materials are shown in Figure 70 and Figure 71, respectively. In general, flux distribution in the ring and frame core have the same frequency behavior but different values. The NiZn show much better performance than MnZn, however onset for the frequency effects starts at 2.5 MHz for FR67 material.

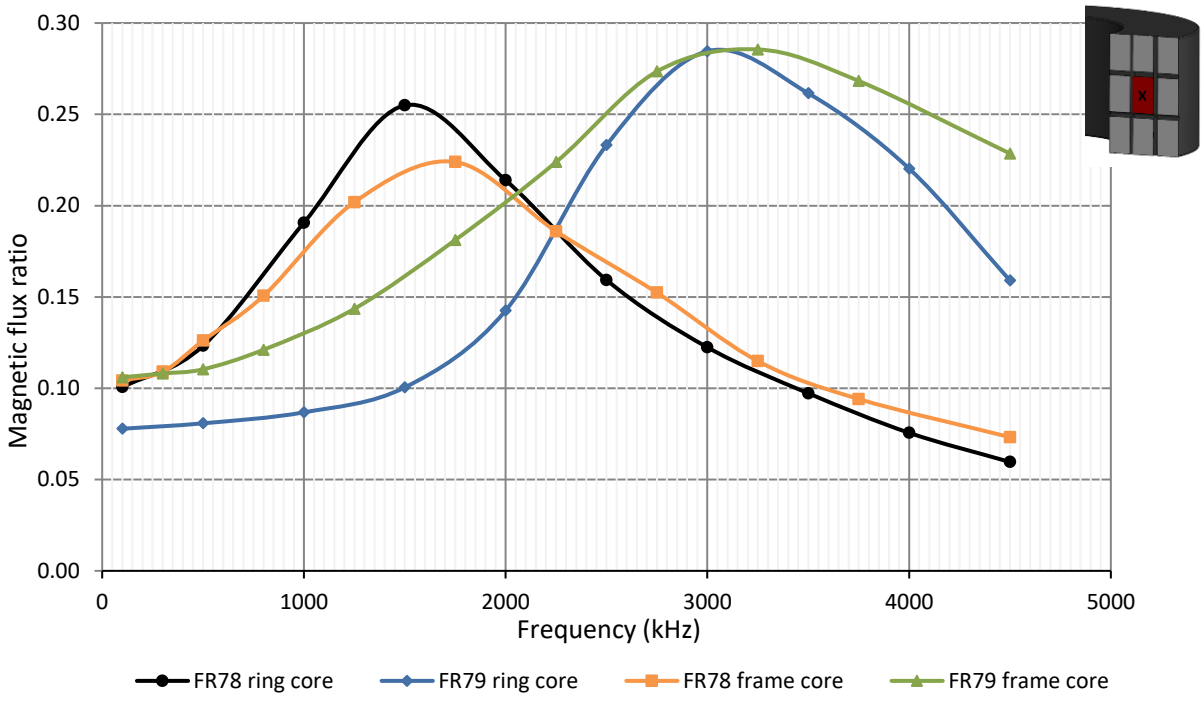

Figure 70. Frame and TX105 ring cores flux distribution in the inner segment for MnZn ferrite materials.

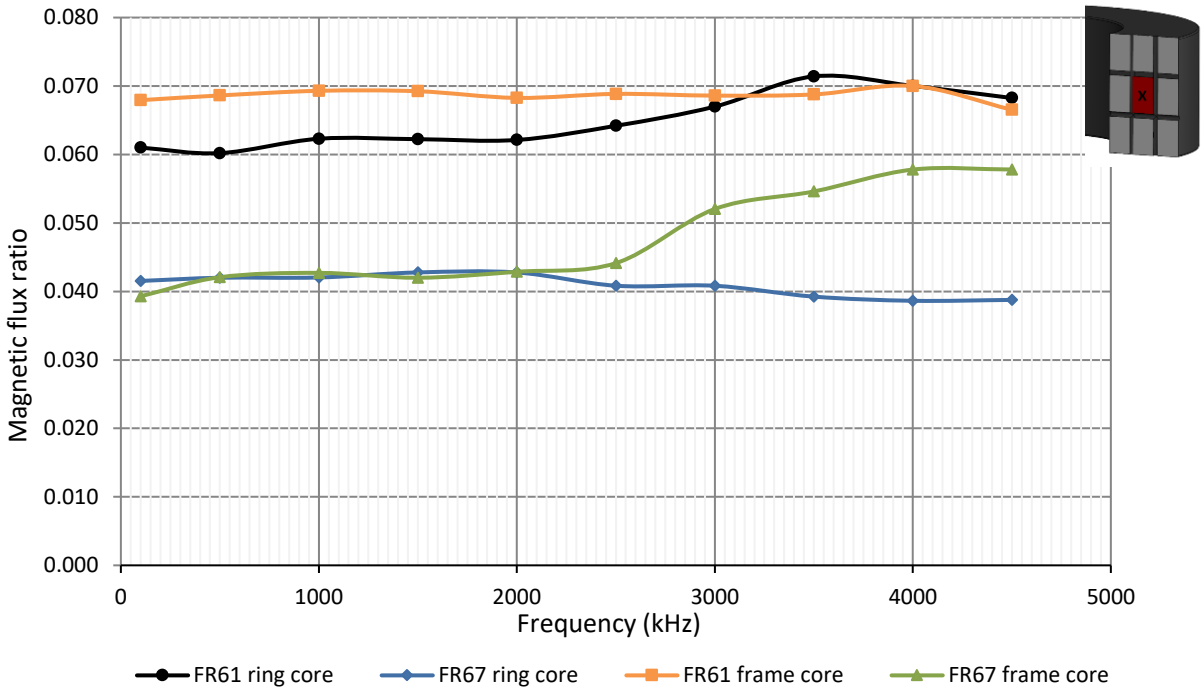

Figure 71. Frame and TX105 ring cores flux distribution in the inner segment for NiZn ferrite materials.

10. Conclusions

Eleven magnetic materials were tested. Flux distribution and impedance characteristic were measured for selected ring and frame cores.

It is observed that magnetic flux undergoes a skin effect analogous to conductors. In extreme case, magnetic flux in the core's middle section may flow in an opposite direction to the equivalent flux in the core. The magnetic flux skin effect results in core parameters deterioration as frequency increases. This effect was recorded by both experimental methods. It is a matter for further investigation what is the origin of the magnetic flux skin effect.

Magnetic materials permeability has direct impact on frequency where magnetic flux starts to drop in inner core segment. Lower permeability materials shows equal flux distribution to higher frequencies than high permeability materials. The flux skin depth is a function of material conductivity, permeability and permittivity. Therefore, the detail knowledge about magnetic material conductivity and permittivity characteristics is a key to understanding flux propagation in ferrite cores.

Actual test setup allows to test cores with frequencies up to 1.5 MHz. Dimensional resonance would develop where the physical dimension of the core is greater than half of the wavelength [1]. Therefore, TX50 low permeability cores would require testing at much higher frequency or alternatively, a bigger diameter core shall be used to develop dimensional resonance effect at the considered frequency range.

Presented drilling scheme divides core into two sections. Therefore, inner to outer core segments ratio is compared. This somewhat simplified approach allows to track flux changes with the limited extent to certain frequency where the magnetic flux skin depth effect is limited to the magnetic wire loop. Additional bores would allow to measure flux characteristics in 3 or 4 section and therefore would allow to verify flux distribution with frequency.

It is anticipated that magnetic flux concertation in the outer circumference of the core and weakening in the core center would affect core losses distribution. However, this effect was not investigated.

11. Future work

The range of presented work indicate areas for further investigation as many parameters are still missing, therefore as further action it is recommended:

- Verification of the flux distribution vs. frequency by increase the drilled holes mesh.
- Investigation of the effects in the magnetic materials with split between eddy current, dimensional resonance and other effects. Separation and measurement of the effects.
- Core shape effect on the core parameters.
- Accurate measurement of resistivity and permittivity characteristic for various materials and core sizes.
- Definition of simple tests that can be reproduced in industrial environment by ferrite manufacturers in order to add permittivity and resistivity characteristics to the datasheet.
- Application oriented investigation of the core parameters deterioration on the component efficiency and size.
- Approach to standardized approach for core manufacturers to provide on manufacturer's datasheet critical parameters to the designer.

12. References

[1] G.R. Skutt, "High-frequency dimensional effects in ferrite-core magnetic devices," PHD Virginia Polytechnic Institute, 1996

[2] G.R. Skutt, F.C. Lee, "Characterization of dimensional effects in ferrite-core magnetic devices, " *Power Electronics Specialist Conference,* 1996.

[3] M. Kącki, M.S. Ryłko, J.G Hayes, C.R. Sullivan, "Magnetic material selection for EMI filter," *IEEE Energy Conversion Congress and Exposition (ECCE)*, 2017.

[4] F.G. Brockman, P.H. Dowling, W.G. Steneck, "Dimensional effects resulting from a high dielectric constant found in a ferromagnetic ferrite," *Physical Review 77*, January 1950.

[5] F.P. Pengfei, Z. Ning, "Magnetodielectric effect of Mn-Zn ferrite at resonant frequency," *Journal of Magnetism and Magnetic Materials,* Vol. 416, 2016.

[6] B.D Cullity, C.D. Graham, "Introduction to magnetic materials," *John Wiley and Sons, 2009*.

[7] www.ferroxcube.com.

[8] www.fair-rite.com.